Catalysis Science & Technology

Applications of bimetallic PdCu catalysts

Journal:	*Catalysis Science & Technology*
Manuscript ID	Draft
Article Type:	Minireview
Date Submitted by the Author:	n/a
Complete List of Authors:	Gholinejad, Mohammad; Institue for Advanced Studies in Basic Sciences (IASBS), Chemistry Khosravi, Faezeh ; Institue for Advanced Studies in Basic Sciences (IASBS), Chemistry Afrasi, Mahmoud; Institute for Advanced Studies in Basic Sciences Najera, Carmen; Universidad de Alicante, Grupo de Procesos Cataliticos en Sintesis Organica. Departamento de Quimica Organica Sansano, José; University of Alicante, Organic Chemistry

REVIEW PROPOSAL

CHEMICAL SOCIETY REVIEWS

Please upload your completed form at https://mc.manuscriptcentral.com/csr

Chem Soc Rev Reviews provide an authoritative and in-depth understanding of important topics in the chemical sciences. They give a very high quality state-of-the-art account of the subject matter and a balanced assessment of the current primary literature. The implications of recent developments for the wider scientific community are emphasised and authors should aim to stimulate progress in the field.

Reviews must be:

- **Accessible:** Of general interest and enticing to the journal's wide, community-spanning readership.
- **Appealing:** A timely account which is needed and which genuinely adds to the existing literature.
- **Carefully referenced**: References should be selected to give a balanced view of the field.
- **Jargon free:** Specialist terms and symbols should be defined and fundamental ideas simply explained.

PROPOSED TITLE: Applications of bimetallic PdCu catalysts

AUTHOR(S): Mohammad Gholinejad,[a] Faezeh Khosravi,[a] Mahmoud Afrasi[a] and Carmen Nájera[b]
ADDRESS:
[a]Department of Chemistry, Institute for Advanced Studies in Basic Sciences (IASBS), P. O. Box 45195-1159, Gavazang, Zanjan 45137-6731, Iran
[b]Centro de Innovación en Química Avanzada (ORFEO-CINQA), Universidad de Alicante, Apdo. 99, E-03080 Alicante, Spain
EMAIL: cnajera@ua.es

PROPOSED SUBMISSION DATE: May 2020

PROPOSAL QUESTIONS:
Please complete all sections, ensuring your answers are succinct and within the word limit.

1) Please comment on the current importance of the field

The use of bimetallic PdCu nanoparticles (NPs) have shown in the last 30 years an important role in heterogeneous catalysis due not only to economic reasons, because less amount of Pd is used, and mainly due also to an improvement in the reactivity with respect to Pd NPs. The resulting synergic and cooperative intractions can be modulate depending on the stoichiometry between the two metals affording superior catalytic performance. In addition, these bimetallic NPs can be supported in different types of solid supports modulating also their reactivity retarding aggregation and allowing their recycling.

2) What are the implications for the wider scientific community?

The aim of this Review is to overview, for the first time, the characterization methods of these types of PdCu nanoparticles and their synthetic applications as sustainable catalysts in many chemical and electrochemical processes, including green transformations such as water purification and hydrodechlorination reactions and also to conversion of CO_2 in valuable chemicals and fuels.

3) To which communities will your article appeal?

The synthetic potential of PdCu bimetallic nanoparticles as catalysts has been demonstrated in the last 15 years in many fundamental reactions and industrial processes. This comprehensive information would be of interest for all the chemical community at the academia and specially at industrial level

4) Please comment on any other reviews published on a similar topic, justifying why there is room for another review

In the literature, the topic of bimetallic catalysis has been described in the following reviews. However, the use of PdCu catalysts has been only partially covered:

1. M. H. Pérez-Temprano, J. A. Casares and P. Espinet. Bimetallic catalysis using transition and group 11 metals: An emerging tool for C-C coupling and other reactions. *Chem. Eur. J.* 2012, **18**, 1864-1884.
2. W. Yu, M. D. Porosoff, J. G. Chen. Review of Pt-based bimetallic catalysis: from model surfaces to supported catalysts. *Chem. Rev*. 2012, **112**, 5780-5817.
3. M. Sankar, N. Dimitratos, P. J. Miedziak, P. P. Wells, C. J. Kielye, G. J. Hutchings. Designing bimetallic catalysts for a green and sustainable future. *Chem. Soc. Rev*. 2012, **41**, 8099-8139.
4. J. Shi, On the Synergetic catalytic effect in heterogeneous nanocomposite catalysts. *Chem. Rev*. 2013, **113**, 2139-2181.
5. E. Rivera-Chao, L. Fra, M. Fañanás-Mastral. Synergistic bimetallic catalysis for carboboration of unsaturated hydrocarbons. *Synthesis* 2018, **50**, 3825-3832.

5) *Chem Soc Rev* aims to publish only the very best review articles while avoiding repetition, and one way to achieve this is to have groups of authors to collaborate on writing the definitive review on a particular area. Are you willing to work together with other author group/s on the proposed review? If so, please identify some potential researchers with whom it might be suitable for you to collaborate. If not, please explain briefly why the proposed review would not benefit from being a collaborative effort.

The authors of this review have work already on the characterization and applications of Pd/Cu NPs as supported catalysts in carbon-carbon forming reactions.

6) Please provide section headings along with a brief discussion of each section and associated key references. List at least 10 of the main research articles you will use as core references in your proposed review.

1. **Carbon-Carbon Forming Reactions**: These Pd/Cu NPs have been used as catalysts in large variety of carbon-carbon bond forming reactions such as Suzuki, Sonogashira, Heck, cyclization processes, arylation and alkylation reactions, alkyne-alkene cross-coupling, decarboxylative cross-coupling, A^3-coupling of aldehydes, acetylenes and amines and other reactions such as reductive cross-coupling, carboboration and hydroarylation of alkenes.
Articles: (1) M. Nasrollahzadeh, M. Atarod, M. Alizadeh, A. Hatamifard and S. M. Sajadi, S. M. Recent advances in the application of heterogeneous nanocatalysts fo Sonogashira coupling reactions. *Curr. Org. Chem.,* 2017, **21**, 708-749; (2) M. H. Perez-Temprano, J. A. Casares and P. Espinet. Bimetallic catalysis using transition and group 11 metals: An emerging tool for C-C coupling and other reactions. *Chem.- Eur. J.,* 2012, **7**, 1864-1884.

2. **Hydrogenation Reactions**: In this section, hydrogenation methods to reduce nitrates and nitrites (important process for water purification), hydrogenation of CO_2 to methanol (to produce sustainable chemicals feedstock and fuels), semi-hydrogenation of alkynes and hydrogenation of several organic compounds such as furfural, glycerol, succinic acid, levulinic acid and nitro compounds will be considered.
Articles: (1) N. Barrabes and J. Sa. Catalytic nitrate removal from water, past, present and future perspectives. *Appl. Catal. B- Environmental,* 2011, **104**, 1-5; (2) T. Ye, D. P. Durkin, N. A. Banek, M. J. Wagner and D. Shuai. Graphitic carbon nitride supported ultrafine Pd and Pd−Cu catalysts: enhanced reactivity, selectivity, and longevity for nitrite and nitrate hydrogenation. *ACS Appl. Mater. Inter*. 2017, **9**, 27421-27426. (3) K. C. K. Swamy, A. S. Reddy, K. Sandeep and A. Kalyani. Advances in chemoselective and/or stereoselective semihydrogenation of alkynes. *Tetrahedron Lett.,* 2018, **59**, 419-429; (4) X. Jiang, X. Nie, X. Wang, H. Wang, N. Koizumi, Y. Chen, X. Guo and C. Song. Origin of Pd-Cu bimetallic effect for synergetic promotion of methanol formation from CO_2 hydrogenation. *J. Catal*., 2019, **369**, 21-32.

3. **Electrocatalytic Reduction Reactions**: electrocatalytic reduction of oxygen, CO_2 to CO, methanol, hydrocarbons, formate and hydrogen production can be also performed with Pd/Cu NPs.
Articles: (1) Y. Yang, C. Dai, D. Wu, Z. Liu and D. Cheng. The effect of size on oxygen reduction reaction activity of PdCu bimetallic nanoparticles. *ChemElectroChem*, 2018, **5**, 2571-2575. (2) L. Lu, X. Sun, J. Ma, D. Yang, H. Wu, B. Zhang, J. Zhang and B. Han. Highly efficient electroreduction of CO_2 to methanol on palladium-copper bimetallic aerogels. *Angew. Chem., Int. Ed*., 2018, **57**, 14149-14152. (3) S. Ma, M. Sadakiyo, M. Heima, R. Luo, R. T. Haasch, J. I. Gold, M. Yamauchi and P. J. A. Kenis. Electroreduction of carbon dioxide to hydrocarbons using bimetallic Cu-Pd catalysts with different mixing patterns. *J. Am. Chem. Soc.*, 2017, **139**, 47-51. (3) X. Zhang, D. Wu and D. Cheng. Component-dependent electrocatalytic activity of PdCu bimetallic nanoparticles for hydrogen evolution reaction. *Electrochimica Acta*, 2017, **246**. 572-579.

4. **Oxidation Reactions**: These types of catalysts can be employed in oxidation reactions using oxygen or hydrogen peroxide of CO, hydrocarbons to alcohols such as methane to methanol, and to carbonyl compounds, as well as of alcohols and other organic compounds, epoxidation of alkenes and in carbonylation reactions of alcohols and phenols.
Articles: (1) Z.-Q. Zhang, J. Huang, L. Zhang, M. Sun, Y.-C. Wang, Y. Li and J. Zeng. Facile synthesis of Cu-Pd bimetallic multipods for application in cyclohexane oxidation.

Nanotechnology, 2014, **25**, 435602. (2) J. Mao, Y. Liu, Z. Chen, D. Wang and Y. Li. Bimetallic Pd-Cu nanocrystals and their tunable catalytic properties. *Chem. Commun*. 2014, **50**, 4588-4591.

5. **Electrooxidation Reactions**: these NPs can be used as membranes for the oxidation of methanol, ethanol and polyols, formaldehyde and formic acid.
Articles: (1) Z. Yin, W. Zhou, Y. Gao, D. Ma, C. J. Kiely and X. Bao. Supported Pd-Cu bimetallic nanoparticles that have high activity for the electrochemical oxidation of methanol. *Chem. Eur. J*., 2012, **18**, 4887-4893. (2) L. Zhang, S.-I. Choi, J. Tao, H.-C. Peng, S. Xie, Y. Zhu, Z. Xie and Y. Xia. Pd-Cu bimetallic tripods: a mechanistic understanding of the synthesis and their enhanced electrocatalytic activity for formic acid oxidation. *Adv. Funct. Mater*., 2014, **24**, 7520-7529.

6. **Hydrodechlorination (HDC) Reactions**: hydrodechlorination reactions of chlorinated pollutants organic compounds such as carbon tetrachloride, 1,2-dichloroetane, $CF_3OCFClCF_2Cl$ and 4-chlorophenol are of high importance in industrial processes specially in water treatments.
Articles: (1) R. Hina, I. Arafa and F. Al-Khateeb. Gas phase hydrodechlorination of CCl_4 over Pd-Cu and Pd-Fe bimetallic catalysts supported on an AlF_3 matrix. *Prog. React. Kinet. Mech*., 2016, **41**, 29-38; (2) S. Lambert, B. Heinrichs, A. Brasseur, A. Rulmont and J.-P. Pirard. Determination of surface composition of alloy nanoparticles and relationships with catalytic activity in Pd-Cu/SiO_2 cogelled xerogel catalysts. *Appl. Catal. A-Gen*., 2004, **270**, 201-208.

7. **Oxygen-Assisted Water-Gas-Shift (OWGS) Reaction:** in order to reduce the CO in the water-gas-shift (WGS) reactor, oxygen and the PdCu bimetallic catalysts supported on CeO_2 has been successfully used.
Articles: J. Kugai, E. B. Fox and C. Song. Role of CeO_2 support for Pd-Cu bimetallic catalysts for oxygen-enhanced water gas shift. *Appl. Catal. A-Gen*., 2013, **456**, 204-214.

9. Hydrogen production
10. Antimicrobial activity
11. Cyanation reactions
12. Hydrosilylation
13. CO and NO elimination
14. Hydrogen evolution reaction (HER)
15. Other Reactions

Altogether, the proposed critical review will contain more than 300 references, most of them in the last 15 years.

AUTHOR CV

Please provide a brief CV of the leading author and a list of papers/reviews published in the last three years in the suggested topic area which qualify them for writing this review.

Carmen Nájera was graduated from the University of Zaragoza in 1973, obtaining her doctorate in chemistry from the University of Oviedo in 1979. She spent postdoctoral stays at the ETH (Zurich), the Dyson Perrins Laboratory (Oxford), Harvard University, and Uppsala University. She became Associate Professor in 1985 at the University of Oviedo and Full

Professor in 1993 at the University of Alicante. She is coauthor of more than 400 papers (h 64), 6 patents and 30 book chapters and has supervised more than 45 PhD students. She has been awarded with the 2006 Organic Chemistry Prize from the Spanish Royal Chemical Society of Chemistry, the 2006 Rosalind Franklin International Lectureship from the English Royal Society, the SCF 2010 French-Spanish Prize from the Société Chimique de France, the IUPAC 2015 Distinguished Women in Chemistry or Chemical Engineering Award and the 2018 Serratosa lectureship. In 2012 she was named full Member of the Royal Spanish Academy of Sciences and was appointed as Active Member of the European Academy of Sciences and Arts. In 2016-2017 was named ChemPubSoc Europe Fellow. Professor Najera has been in the Advisory Board of several international journals, among others, Tetrahedron, Tetrahedron Letters, Tetrahedron Asymmetry, Synthesis, European Journal of Organic Chemistry, Chemistry Letters and ChemCatChem. Professor Nájera has been during almost 20 years, Manager Director of the chemical company MEDALCHEMY S.L. for the development of APIs.

The authors have published the following papers related to this topic:

(1) M. Gholinejad, J. Ahmadi, C. Nájera, M. Seyedhamzeh, F. Zareh and M. Kompany-Zareh. Graphene quantum dot modified Fe_3O_4 nanoparticles stabilize PdCu nanoparticles for enhanced catalytic activity in the Sonogashira reaction. *ChemCatChem,* 2017, **9**, 1442.

(2) M. Gholinejad, Z. Naghshbandi and C. Nájera. Carbon-derived supports for palladium nanoparticles as catalysts for carbon-carbon bonds formation. *ChemCatChem,* 2019, **11**, 1792.

(3) M. Gholinejad, N. Jeddi and B. Pullithadathil. Agarose functionalized phosphorus ligand for stabilization of small-sized palladium and copper nanoparticles: efficient heterogeneous catalyst for Sonogashira reaction. *Tetrahedron,* 2016, **72**, 2491. (Highlighted in *Synfact,* 2016, **12**, 0766)

(4) M. Gholinejad, M. Bahrami, C. Nájera and B. Pullithadathil, B. Magnesium oxide supported bimetallic Pd/Cu nanoparticles as an efficient catalyst for Sonogashira reaction. *J. Catal*. 2018, **363**, 81.

Please note that pre-approval of a proposal does not guarantee final publication: the manuscript will be subject to full peer review in accordance with the journal's high standards.

Applications of bimetallic PdCu catalysts

Mohammad Gholinejad,*[a,b] Faezeh Khosravi,[a] Mahmoud Afrasi,[a] José M. Sansano[c] and Carmen Nájera*[c]

Bimetallic PdCu nanoparticles can be applied as catalyst in a wide range of chemical and electrochemical reactions. This review article overviews the preparation and synthetic applications of these bimetallic nanoparticles (BNPs) developed mainly along the last 20 years. They show better catalytic activity and selectivity than the monometallic counterparts due to their electronic and structural interactions. Simple preparation general methods include reduction of the corresponding salt precursors by different agents, solvothermal processes and galvanic replacement. In the case of supported catalysts mainly wet impregnation and in situ reduction processes are used. In addition, these nanomaterials are prepared with different Pd/Cu compositions and with different morphologies. In the case of supported materials, many solid supports specially alumina, silica, titania, ceria, magnetite, zeolites, active carbon, graphene, carbon nanotubes, resins and polymers are employed. Among several synthetic applications, C-C bond forming reactions such as Suzuki-Miyaura, Sonogashira-Hagihara, Heck-Mizoroki, Guerbert and A^3-coupling are efficiently performed with PdCu BNPs. Reduction reactions under PdCu catalysis such as nitrates for water purification, hydrodechlorination of organic pollutants, hydrogenation of CO_2 and CO to methanol, semihydrogenation of alkynes to alkenes, hydrogenation of C=C double bonds, furfural to furfuryl alcohol, polyols, levulinic and succinic acids to lactones, styrene oxide to 2-phenylethanol and nitroaromatics to aromatic amines can be successfully performed. In the case of electrocatalytic reductions, it can be highlighted oxygen reduction to water, CO_2 reductions to CO, to alcohols, to hydrocarbons and to formate as well as hydrogen generation from water splitting. In the field of oxidation reactions using oxygen, CO can be transformed into CO_2, alcohols into aldehydes, cyclopentene to cyclopentanone, ethylene and acetic acid to vinyl acetate and aromatic compounds can be hydroxylated to phenols. Electrooxidation reactions are useful process specially for direct alcohol and formic acid fuel cells. Oxygen-assisted water gas shift reaction can be efficiently performed under PdCu catalysis. In the field of chemical sensors, PdCu BNPs can detect hydrogen in low concentrations, liquefied petroleum gas, formaldehyde, glucose, thiocynate and phenols. Other applications such as catalysts in hydrosilylation of acetylenes to vinylsilanes and their use s antimicrobial agents has been also described.

[a] *Department of Chemistry, Institute for Advanced Studies in Basic Sciences (IASBS), P. O. Box 45195-1159, Gavazang, Zanjan 45137-6731, Iran. Email: gholinejad@iasbs.ac.ir*

[b] *Research Center for Basic Sciences & Modern Technologies (RBST), Institute for Advanced Studies in Basic Sciences (IASBS), Zanjan 45137-66731, Iran*

[c] *Centro de Innovación en Químia Avanzada (ORFEO-CINQA), Universidad de Alicante, Apdo. 99, E-03080 Alicante, Spain. Email: cnajera@ua.es; Fax: +34 965903549; Tel: +34 965950786*

1. Introduction

The use of bimetallic nanoparticles (BNPs) or nanoclusters derived from transition metals can exhibit enhanced physical and chemical properties compared to their monometallic counterparts due to the modification of their surface electrons. It has been often seen that metal interacting with other metal at the nano level can form nanocomposites with superior activities not seen in bulk alloys. They have attracted great interest specially in the field of metal catalysis.[1-7] Particularly, in the last 30 years PdCu BNPs have shown an important role in heterogeneous catalysis due not only to economic reasons (less amount of Pd is used) but mainly due also to an improvement in the reactivity with respect to Pd NPs. The resulting synergic and cooperative interactions can be modulate depending on the stoichiometry between the two metals affording superior catalytic performance. The excellent redox properties of the PdCu system are due to the electron-donor and -acceptor character of the Cu and Pd, respectively. In addition, these BNPs can be supported in different types of solid supports modulating also their reactivity by retarding aggregation and leaching, as well as allowing their recycling. These PdCu BNPs can be supported on different solid supports mainly by two-step sequential impregnation (TSI) or by co-impregnation (CI) and have been used in a broad number of catalytic and electrocatalytic processes.

The aim of this review is to consider a comprehensive coverage of bimetallic PdCu NPs catalysed transformations, such as carbon-carbon bond forming reactions, chemical reduction reactions such as hydrogenation of nitrates for water purification, hydrodechlorination reactions of chlorinated pollutants, hydrogenation of organic compounds and CO_2 and CO hydrogenation to MeOH. In the case of electrocatalytic reductions, oxygen reduction reaction, reduction of CO_2 to CO, to MeOH, to hydrocarbons and to formate, hydrogen generation from water splitting and other reductive dehalogenations are related. Chemical oxidations of CO, alcohols and other organic compounds such as cyclopentene, cyclohexane and benzene hydroxylation are considered. In the case of electroxidative reactions, alcohols and polyalcohols oxidation, formic acid oxidation and oxidation of formaldehyde and styrene epoxidation can be performed with these BNPs. They can be also used as catalyst in oxygen-assisted water gas shift (OWGS) reaction, in sensing electrodes and in other reactions such as hydrosilylation of alkynes and as antimicrobials. We expect that this comprehensive information will be of interest for catalytic processes both at the laboratory and at industrial scale.

2. Carbon-carbon bond forming reactions

In this section, classical cross-coupling processes such as Suzuki-Miyaura, Sonogashira-Hagihara and Mizoroki-Heck reactions will be considered. In addition, other reactions such as oxydative coupling reaction, cyclization of acetylenes with *N*-(2-iodobenzyl)triazoles and the A^3-coupling of aldehydes, amines and acetylenes will be considered.

2.1. Suzuki-Miyaura reaction

Cross-coupling of aryl or alkenyl halides or sulfonates with aryl or alkenyl boronic acids under Pd-catalysis allows the formation of Csp^2-Csp^2 bonds. Biphenyls, which are present in a large number of organic compounds, as well as conjugate polymers and valuable

materials are mainly prepared by Suzuki-Miyaura (S-M) reaction.[8-15] Several groups have demonstrated the advantage of using bimetallic PdCu catalysts in this cross-coupling reaction.

Rothenberg and co-workers[16] reported a comparative study of different nanocluster catalysts in the cross-coupling of phenyl iodide with phenylboronic acid using K_2CO_3 as base, and DMF as solvent at 110 ºC. From the bimetallic combinations PdCu (2 mol%) was the most active, similarly to pure Pd. Other aryl iodides and activated aryl bromides gave quantitative yields, and moderate results using aryl chlorides[17] (Table 1, entry 1). The nanocluster PdCu was prepared by mixing metal chlorides followed by reduction with tetraoctylammonium formate (TOAF), which also acted as stabilizer of the NPs, in DMF giving cluster cores around 2.5 nm in size.

Bimetallic PdCu supported on 4Å molecular sieves (MS) by TSI and CI procedures have been used by Fodor's group[18,19] as reusable catalysts for the S-M reaction. Inductively coupled plasma (ICP) analysis showed a Pd/Cu molar ratio was 0.2:1 in both cases and that the two metals were brought to close interaction on the surface of the support. They compared the activities of Cu@MS and Pd@MS and also bimetallic catalysts, PdCu@MS-TSI and PdCu@MS-CI in the S-M reaction of iodobenzene and phenylboronic acid. Results indicated that the bimetallic catalysts, PdCu@MS-TSI and PdCu@MS-CI, are more active than the monometallic ones and also that bimetallic catalyst PdCu@MS-TSI has better activity and selectivity than the CI's catalyst. PdCu@MS-TSI was reused for six times for the reaction of iodobenzene with phenylboronic acid without decrease in activity, while PdCu@MS-CI activity decreased to 80% yield after the sixth cycle. Aryl iodides and bromides were coupled with different arylboronic acids under EtOH reflux during 1 h to provide the corresponding biphenyls in excellent to good yields. The same group supported bimetallic PdCu catalysts on mixed oxides MgO-Al_2O_3, PdCu@MgAlO, by TSI and CI methods.[20] In this case also results showed that bimetallic catalysts were more active and stable than the monometallic ones. Recycling experiments for the reaction of iodobenzene with phenylboronic acid using CuPd@MgAlO-CI showed excellent activity during six runs without loss in activity. However, in the case of the TSI prepared catalyst after the fifth run yield decreased to 80% (Table 1, entry 3). Aryl iodides and bromides gave excellent yields using the previous described reaction conditions.

The use of the carbon supported CuPd BNPs as an effective catalyst in the Suzuki-Miyaura reaction of aryl iodides and bromides with phenylboronic acid and also in the reduction of nitroarenes with $NaBH_4$ under phosphine-free conditions has been reported by Nasrollahzadeh and co-workers.[21] This PdCu@C catalyst was prepared by deposition of Pd on the surface of Cu@C. Good to excellent yields were obtained in the reduction of nitroarenes and also in the synthesis of biphenyls (Table 1, entry 4). This catalyst was reused for four times in the Suzuki-Miyaura reaction of iodobenzene with phenylboronic acid without loss in activity.

Wang and co-workers[22] prepared PdCu in nanowires (NWs), which were stabilized by octylphenoxypolyethoxyethanol (NP-40). This PdCu-NWs were used as catalyst, using K_2CO_3 as base and a mixture 1:1 of DMF/H_2O at 80 ºC for 2 h, for the S-M reaction of aryl bromides amd chlorides with arylboronic acids in very good yields (Table 1, entry 5). This catalyst was reused during five consecutive cycles for the reaction of bromobenzene and phenylboronic acid.

In the case of $PdCu_3$ nanocrystals (NCs), C-Cl bonds could be also activated.[23] This $PdCu_3$-NCs were prepared by dissolving $Pd(acac)_2$ and $Cu(NO_3)_2 \cdot 3H_2O$ in EtOH and oleylamine-EtOH, respectively. After mixing these solutions a solution of oleylamine and 1-octadecene was added at 195 ºC and heated at 190 ºC. The S-M reactions were performed in water with NaOH as base and cetyltrimethylammonium bromide (CTAB) at 65 ºC for 30 min in good yields for iodo-, bromo- and chlorobenzene (Table 1, entry 6). The catalyst showed good catalytic efficiency during four cycles.

Synergistic catalysis has been observed by immobilization of PdCu BNPs on a metal organic framework (MOF) MIL-101. Singh and co-workers[24] compared the catalytic activity of PdNi@MIL-101, PdCu@MIL-101 and PdCo@MIL-101 in the S-M reaction. The most efficient catalyst was PdCu@MIL-101 for the cross-coupling of aryl iodides in aqueous EtOH (1:1) with NaOH as base at room temperature (rt) in the case of aryl iodides, and K_2CO_3 as base at 50 ºC for aryl bromides (Table 1, entry 7). The observed enhanced catalytic activity was explained by electronic charge transfer from Cu to the shell of Pd facilitating the oxidative addition. However, when the recovered catalyst was used in the cross-coupling of 4-bromoanisole with phenylboronic acid the lower activity was attributed to the aggregation of MIL-101 particles.

Lamei and co-workers[25] have prepared highly dispersed Cu NPs immobilized on core-shell Fe_3O_4@C (magnetite NPs) functionalized with arginine as a support with 92.8 ppm of Pd as impurity. This catalyst was used for the efficient cross-coupling of aryl iodides and bromides in water at rt using a mixture of metal hydroxides with only 0.1 mol% catalyst loading (Table 1, entry 8). This catalyst was reused during six runs for the reaction of 4-bromoanisole with phenylboronic acid. However, aryl chlorides gave low yields (up to 30%).

Table 1 Suzuki-Miyaura reactions catalyzed by supported bimetallic PdCu NPs

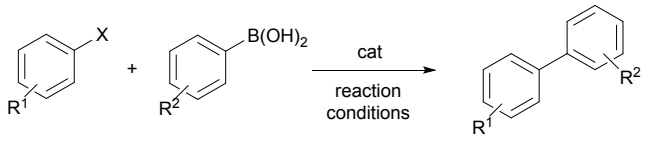

Entry	Cat. (loading)[lit.]	Reaction conditions	X, Yield (%)	Recycling
1	PdCu (1:1) nanocluster (2 mol%)[16,17]	K_2CO_3, DMF, 110 ºC, 0.5-24 h	X = I = Br = 100 X = Cl, 25-54	-
2	PdCu (0.2:1)@MS (12 mol%)[18,19]	K_2CO_3, EtOH, 78 ºC, 1-1.5 h	X = I, 30-98 X = Br, 45-99	6[a]
3	Pd Cu_5@MgAlO (10 mol%)[20]	K_2CO_3, EtOH, 78 ºC, 1 h	X = Br, 91-99	6[a]
4	PdCu@C[21]	K_2CO_3, EtOH, 78 ºC, 3-5 h	X = I, 86-93 X = Br, 88-91	5[a]
5	PdCu-NWs[22]	K_2CO_3, DMF/H_2O (1:1), 80 ºC, 2-6 h	X = Br, 72-96 X = Cl, 79-94	5[b]
6	$PdCu_3$-NCs (10 mol%)[23]	NaOH, H_2O, CTAB 65-100 ºC, 30 min	X = I, 100 X = Br, 98 X = Cl, 60	4[c]
7	PdCu@MIL-101[24]	X = I: NaOH, EtOH/H_2O (1:1), rt, 1 d, X = Br: K_2CO_3, EtOH/H_2O (1:1), 50 ºC	X = I, 65-95 X = Br, 87-97 X = Cl, 10	-
8	PdCu@Fe_3O_4@C-92.8 ppm Pd (0.1 mol%)[25]	KOH, $Ba(OH)_2$, $Ca(OH)_2$ $Mg(OH)_2$, H_2O, rt	X = I, 92-99 X = Br, 90-99	6[d]

[a] Iodobenzene and phenylboronic acid. [b] Bromobenzene and phenylboronic acid. [c] Chlorobenzene and phenyl-boronic acid. [d] 4-Bromoanisole and phenylboronic acid.

In conclusion, the last catalyst PdCu@Fe_3O_4@C with 92.8 ppm of Pd seems to be the best catalyst for the S-M reaction working with very low Pd loading and very mild reaction conditions for aryl iodides and bromides and good recyclability.[25] However, for aryl chlorides cross-coupling, PdCu-NWs are efficient for the S-M reaction.[22]

2.2. Sonogashira-Hagihara reaction

The formation of Csp^2-Csp bonds can be performed under metal-catalyzed alkynylation of aryl and alkenyl halides or triflates with terminal alkynes. This so-call Sonogashira-Hagihara (S-H) reaction, is a powerful method for the formation of arylalkynes and conjugated enynes, which are important building blocks in the synthesis of natural products, pharmaceuticals, conjugate polymers and materials.[26-28] In this process, typically a Pd source and CuI as catalysts using Et_3N as base and/or solvent are the most common reaction conditions, and also under Cu-free conditions.

Djakovitch and co-workers[29] described the preparation of different bimetallic PdCu catalysts for the direct preparation of 2-phenylindole from 2-iodoaniline and phenylacetylene. The best results were obtained by grafting bimetallic NPs with PdCu 2.5:1 molar ratio on zeolite NaY by a 'ship-in-a-bottle'procedure.[30] This supported catalyst PdCu@NaY showed better catalytic activity (100% yield) than silica gel (76%) or alumina (81%) as solid supports using 2 mol% loading, Et_3N as base and aqueous DMF at 100 ºC for 3 h (Scheme 1). This heterogeneous catalyst is sentitive to the extraction work-up, although it can be recycled during three runs when used in a continnous manner.

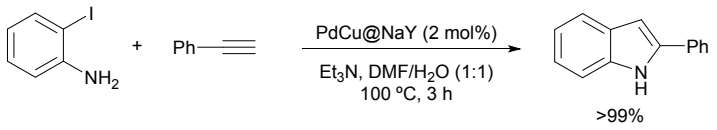

Scheme 1 Direct synthesis of 2-phenylindole catalyzed by PdCu@NaY.

Catalytic studies performed by Corma and co-workers[31] on the reaction of iodobenzene and phenylacetylene with different PdCu contents supported on MgO and mixed Mg–Al oxide derived from layered hydrotalcite (HT) as catalysts showed that a 3Pd/1.6Cu ratio gave the best results. In addition, MgO hydrotalcite supported catalyst had a higher activity than Mg–Al hydrotalcite. Indeed, the existence of copper on the calcinated HT enhanced the catalytic activity, but without the copper using sole Pd as transition metal the activity decreased. This reaction can be carried out in the absence of Et_3N due to the basic nature of the mixed oxides derived from layered HT but in low yield. Tolane was obtained in DMF/H_2O during 6 h at 100 ºC in 90% yield (Table 2, entry 1). This heterogeneous catalyst PdCu@HT, according to metal leaching determination and three-phase test experiments, can be reused only 3 runs and the PdCu BNPs of >20 nm size did not agglomerate during catalyst use and recycling.

In 2013, the use of a palladium coated tubular reactor in line with Cu tubing using a continuous flow platform (Cu-Pd dual reactor) for S-H reactions, has been reported by Lee and co-workers.[32] Using this Cu-Pd dual reactor, alkynes were obtained in moderate to good yields by reaction of a wide range of aryl iodides with 2,5-dimethylphenylacetylene in DMP with diisopropylethylamine (DIPEA) as base at 120 ºC (Scheme 2). The reactions took place in the Cu reactor catalyzed by the traces of leached Pd from the Pd reactor. Therefore, Pd reactor acts as a Pd source, and the catalytic amount could be decreased significantly without loss of reaction efficiency. Activity of this Pd-Cu dual reactor was preserved even after a continuous run of 10 times for reaction of 2-ethynyl-1,4-dimethylbenzene with iodobenzene. This continuous flow technology can be applied for large-scale synthesis.

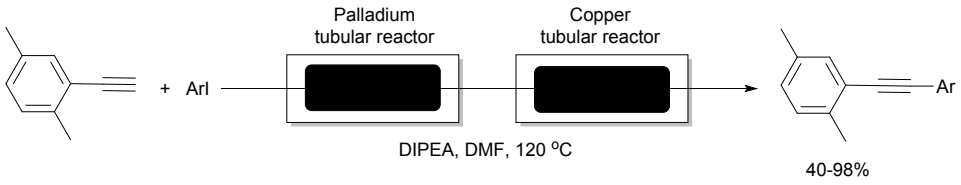

Scheme 2 S-H reactions using a PdCu continuous flow reactor.

According to Dkajovitch pionner results on alkynylation-cyclization sequence for the synthesis of indoles using PdCu@NaY,[29] Felpin's group[33] described the use of PdCu@C as catalyst for the synthesis of indoles and benzofurans. This heterogeneous catalyst allows the cascade reaction to give indoles, azaindoles and benzofurans in water using PPh_3 as cocatalyst and ethanolamine as base at 80 ºC with good yields (Scheme 3). The recyclability of this PdCu@C catalyst was evaluated for the preparation of 2-phenylindole. Unfortunately, the catalyst was inactive after the third run as in the case of PdCu@NaY.

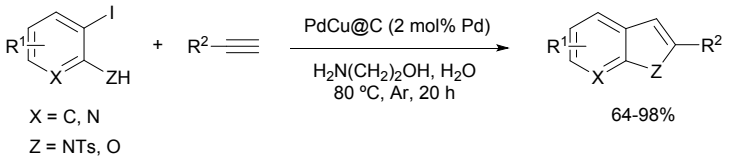

Scheme 3 Direct synthesis of indoles, azaindoles and benzofurans catalyzed by PdCu@C.

The same group developed a one-pot sequential Sonogashira-click and click-Heck reactions for the synthesis of heterocyclic compounds by using PdCu@charcoal (PdCu@C) as a heterogeneous multi-task catalyst.[34] This catalyst was used for tandem Sonogashira alkynylation and [3+2]-cycloaddition sequences for preparation of functionalized triazoles (Scheme 4). It has been characterized by XPS spectra, STEM-EDX elemental maps and HRTEM micrographs. TEM images of PdCu@C showed small PdCu BNPs with few larger colloids onto the charcoal support in an average size of 4-10 nm for the small BNPs, whereas the larger colloids were 20-30 nm size. Also, XPS spectra indicated two Pd spin-orbit peaks at 335.7 and 340.9 eV that related to mixture of Pd^0 and Pd^{+2}. This procedure allowed the preparation of various heterocyclic compound by using MeOH as solvent under MW irradiation.

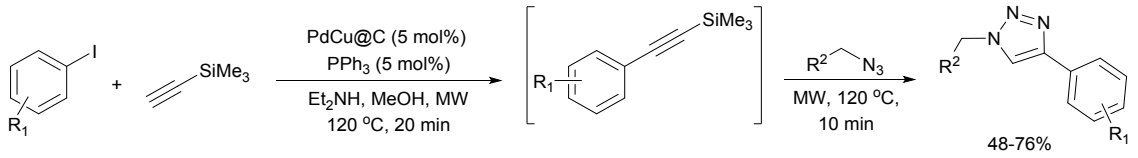

Scheme 4 Sequential synthesis of triazoles catalyzed by PdCu@C.

Bimetallic PdCu NPs embedded in microporous cationic amberlite resins with formate as counteranion (ARF) has been used by Basu and co-workers[35] in the S-H

reaction of aryl iodides and bromides with terminal alkynes. Transmission electron microscopy (TEM) images of PdCu@ARF showed relative uniform distributions of PdCu NPs in average size of 4.9 nm. The alkynyation took place in acetonitrile with K_2CO_3 as base at 80 ºC in good yileds (Table 2, entry 2). The heterogeneous nature of this catalyst was demonstrated by metal scavenger and hot filtration experiments. With respect to recycling tests for the reaction of 4-iodotoluene and propargyl acetate, the catalyst maintained the activity during five cycles.

Zhang and Gao group[36] has prepared PdCu and other bimetallic nanoalloys supported on montmorillonite (MMT). Among all, PdCu@MMT exhibited the highest activity in the S-H reaction of aryl iodides and terminal alkynes superior to the monometallic systems. The alkynylation was performed using 1 mol% loading of PdCu, 2 mol% of PPh_3, K_2CO_3 as base in EtOH at 65 ºC (Table 2, entry 3). TEM images showed diameters ranged from 10 to 11 nm. Recycling experiments were not reported.

In 2016, Gholinejad's group[37] has prepared PdCu BNPs supported on phosphinite functionalized agarose biopolymer PdCu@Phos-Agarose, which has been employed in the S-H reaction (Scheme 5). PdCu@Phos-Agarose catalyst was characterized by various techniques such as FT-IR and solid state UV-Vis, SEM, TGA, EDX, HRTEM, SAED and BET analyses. TEM images of PdCu@Phos. Agarose catalyst, revealed average sizes of nanoparticles in 5-7 nm. XRD studies of PdCu@Phos-Agarose confirmed the presence of Cu_3Pd and CuPd bimetallic species in the structure of the catalyst. This heterogeneous bimetallic catalyst showed high activity in Sonogashira coupling reaction of aryl iodides at room temperature and aryl bromides at 50 °C under low palladium loading conditions (containing 0.05 mol% Pd and 0.8 mol% Cu). PdCu@Phos-Agarose catalyst was recycled for three consecutive cycles without decrease of catalytic activity in the coupling of iodobenzene and phenylacetylene (Table 2, entry 4).

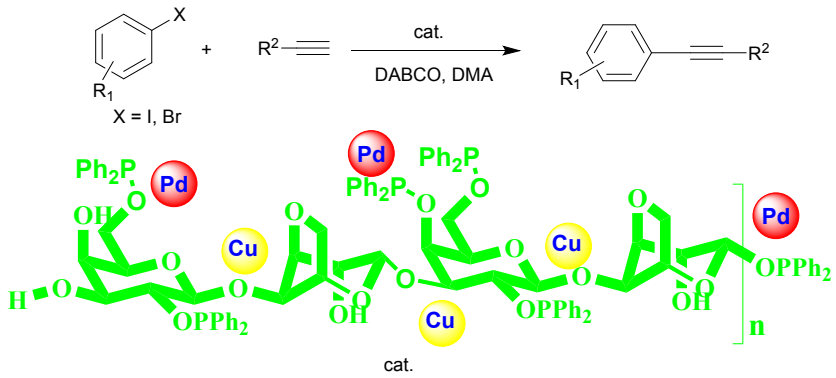

Scheme 5 S-H reaction catalyzed by PdCu@Phos-Agarose.

Bimetallic PdCu catalysts synthesized by metal vapor technique were supported on polyvinylpyridine crosslinked divinylbenzene (PVPy) by Evangelisti and co-workers and used in the S-H reaction.[38] HRTEM analysis of PdCu@PVPy revealed the existence of Pd NPs distributed in a slender range with 2.5 nm average diameter. XAFS analysis also showed the existence of Pd NPs and indicated alloying formation with Cu atoms. Alkynylation using PdCu@PVPy revealed that quantitative yield was obtained in the reaction of iodobenzene with phenylacetylene after 2.5 h, which showed higher activity than the Pd@PVPy monometallic catalyst. PdCu@PVPy catalyst was recycled and reused for three cycles with low decrease of catalytic activity (Table 2, entry 5).

In 2017, Gholinejad's group,[39] prepared Fe_3O_4 nanoparticles modified with graphene quantum dots (GQD) with a simple method and applied it for the stabilization of Pd-Cu BNPs. The new PdCu@GQD@Fe_3O_4 catalyst was characterized by different methods. This catalyst had good catalytic performance for the S-H reaction of aryl iodides at 60 ºC in toluene and aryl bromides in DMA at 60 to 80 ºC with various terminal acetylenes. However, in the case of activated aryl chlorides, higher temperature (110 ºC) and TBAB as stabilizer were required (Table 2, entry 6). Study of catalyst nature with various tests such as PVP, hot filtration, and kinetic measurements confirmed the heterogeneous nature of PdCu@GQD@Fe_3O_4 catalyst in S-H reaction. This catalyst was recovered easily by an external magnet and recycled for six times without loss in catalytic activity for the coupling of iodobenzene with phenylacetylene.

Zeng and co-workers[40] prepared a heterogeneous Pd^0/Cu^{2+} catalyst supported on montmorillonite-chitosan (MMT-CS) composite (Pd^0/Cu^{2+}@MMT-CS) with solution intercalation and complexion methods and used it in the S-H reaction. XPS analysis showed the valence states of Pd [both Pd(0) and Pd(II) coexisting] and Cu mainly Cu(II). Specific surface area (SBET) of Pd^0/Cu^{2+}@MMT-CS catalyst indicated that it had total pore volume (Vp) more than pure MMT. HRTEM images of the Pd^0/Cu^{2+}@MMT/CS catalyst illustrated that size of Pd^0 NPs was in about 3 nm on MMT layers. Catalytic experiments demonstrated that Pd^0/Cu^{2+}@MMT-CS had higher activity than the monometallics Pd^0@MMT-CS or Cu^{2+}@MMT-CS. This bimetallic catalyst was recycled for six runs with >70% yield for the alkynylation of iodobenzene and phenyl acetylene (Table 2, entry 7).

Magnesium oxide, with high concentration of reactive surface ions acting a Lewis acids, modified by a polymeric vinylimidazole (PVI) ligand has been used as solid support for PdCu NPs by Gholinejad and co-workers.[41] This catalyst PdCu@MgO-PVI was characterized by different analyses such as XRD, XPS, CHNS elemental analysis, TEM, SEM, and EDX-mapping. XRD of PdCu suspension before stabilization on MgO showed different species such $Cu(OH)_2$, Cu_3Pd, Cu_2O, CuO, and PdCu. TEM images revealed the presence of PdCu NPs before anchoring onto MgO nanosheet support. The HRTEM analysis indicated the existence of lattice fringes with a d-spacing value of 0.225 nm and 0.21 nm corresponding to the (111) plane of Pd and (111) plane of CuPd. Catalytic activity in the S-H reaction of PdCu@MgO-PVI of aryl iodides, bromides and chlorides with alkynes took place with low Pd loading (0.05–0.2 mol%) at 60–120 ºC (Table 2, entry 8). The reaction of iodobenzene with phenylacetylene using PdCu@MgO-PVI gave tolane in 97% yield, whereas 37% yield was obtained in the absence of copper indicating important role of Cu in this reaction. This supported catalyst was recovered and recycled for eight sequential times with low decline in catalytic activity in the coupling of iodobenzene with phenylacetylene. Heterogeneous behavior of this catalyst was confirmed by hot filtration and PVP poisoning tests.

Table 2 Sonogashira-Hagihara reactions catalyzed by supported bimetallic PdCu

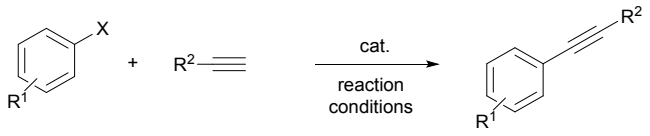

Entry	Cat. (loading)[lit.]	Reaction conditions	X, Yield (%)	Recycling
1	PdCu(3:1.6)@HT (3% wt)[31]	Et_3N, DMF/H_2O (1:1), 100 ºC, 6 h	X = I, 81	3[a]
2	PdCu@ARF[35]	K_2CO_3, CH_3CN, 80 ºC, 6-12 h	X = I, 77-95 X = Br, 77-93	5[b]
3	PdCu@MMT (1 mol%)[36]	PPh_3 (2 mol%), K_2CO_3, EtOH, 65 ºC, 16 h	X = I, 57-97	-
4	PdCu@Phos-Agarose (0.05 mol% Pd, 0.2 mol%Cu)[37]	DABCO, DMA, X = I, rt, 8 h X = Br, 50 ºC, 48 h	X = I, 75-99 X = Br, 72-97	3[a]
5	PdCu@PVPy (0.1 mol% Pd, 0.2 mol% Cu)[38]	H_2O, TBAB, 95 ºC, 2.5 h	X =I, <99	3[a]
6	PdCu@GQD@Fe_3O_4 (0.3 mol% Pd, 0.35 mol% Cu)[39]	X = I, DABCO, toluene, 50 ºC, 1d X = Br, Cl, DMA, 60-100 ºC, 1-2 d	X = I, 78-99 X = Br, 76-99 X = Cl, 86-91	9[a]
7	PdCu@MMT-CS (1 mol%)[40]	PPh_3 (2 mol%), Na_2CO_3, DME/H_2O (4:1), 80 ºC, 8 h	X = I, 58-96 X = Br, 48 X = Cl, 10	6[a]
8	PdCu@MgO-PVI (0.05-0.2 mol%)[41]	DABCO, DMF X = I (0.05 mol%), 60 ºC, 15-24 h X = Br (0.2 mol%), 60 0r 80 ºC, 1-2 d X = Cl (0.2 mol%), 100 or 120 ºC, 1 d	X = I, 75-99 X = Br, 25-95 X = Cl, 89-95	9[a]
9	PdCu@Al_2O_3 (3% wt)[42]	Pyrrolidine, DMF, 80 ºC, 6 h	X = I, 81	-

[a] Iodobenzene and phenylboronic acid. [b] 4-iodotoluene and phenylboronic acid.

Stakheev and co-workers[42] have investigated the influence of the Pd/Cu ratio on the activity of PdCu@Al_2O_3 as catalysts in the S-H reaction of phenyl iodide with phenylacetylene. In this report, a series of PdCu catalysts with a constant palladium loading (3 wt%) with different in Pd/Cu molar ratio from 1:0.5 ($Pd_1Cu_{0.5}$) to 1:4 (Pd_1Cu_4) were prepared. These catalysts were synthesized with incipient-wetness impregnation of α-Al_2O_3 with the solutions of Pd and Cu salts. Results indicated that Pd-Cu bimetallic catalyst with a Pd/Cu molar ratio of 1:2, had a maximum activity than the other ones and also, PdCu bimetallic catalyst with an optimal Pd/Cu ratio (Pd_1Cu_2) had higher activity

than the $Pd@Al_2O_3$ and $Cu@Al_2O_3$ monometallic catalysts in the S-H reaction of phenylacetylene with phenyl iodide (Table 2, entry 9). Recycling experiments were not reported.

In conclusion, $PdCu@GQD@Fe_3O_4$[39] and PdCu@MgO-PVI[41] have exhibit the highest catalytic activity in S-H reaction not only for aryl iodides but also for aryl bromides and chlorides as well as in recycling experiments.

2.3. Heck-Mizoroki reaction

Heck[43] and Mizoroki[44] described the alkenylation of aryl halides in the early 1970s. This H-M reaction has been an important process for the Csp^2-Csp^2 bond formation with a broad range of synthetic applications.[13, 45-47] The reaction is normally performed under palladium-catalysis in the presence of different types of ligands and bases.

In 1997, Sudalai and co-workers[48] reported PdCu exchanged montmorillonite K10 clay, PdCu@MMT-K10, as efficient and reusable catalyst for the arylation of acrylates and styrene. Several supported mono and bimetallic catalysts were prepared by exchanging the clay with aqueous $PdCl_2$ and/or $Cu(NO_3)_2$. The best results were obtained with 0.29%wt% of Pd and 0.36 wt% of Cu exchanged MMT-K10. Aryl iodides reacted with acrylates in good yields using K_2CO_3 as base under DMF reflux for 2 h. However, bromobenzene gave metyl cinnamte in low 32% yield. In the arylation of styrene both aryl iodides and bromides afforded stilbenes in good yileds, but the reaction with chlorobenzene failed (Scheme 6a). This catalyst was recovered by filtration and reused three times in the alkenylation of 4-iodoanisole with methyl acrylate. The same heterogeneous catalyst was used in the H-M reaction of anilines with methyl acrylate by Rigo and co-workers.[49] This alkenylation takes place by C-N bond cleavage of anilines by Pd catalysts to give Ar-Pd-N species.[50] The corresponding cinnamates were prepared under AcOH reflux in 4-7 h and 63-76% yields (Scheme 6b). The catalyst was reused once in the alkenylation of 2,5-dimethoxy-1-(4'-aminobenzyl)benzene.

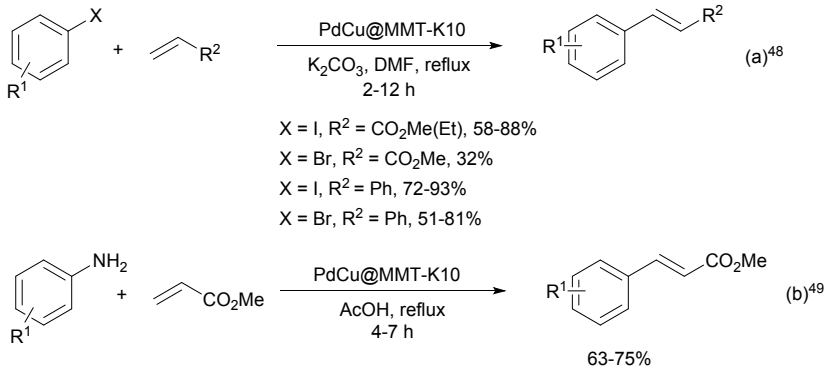

Scheme 6 Heck-Mizoroki reaction of aryl halides and anilines catalyzed by PdCu@MMT-K10.

A reverse micelle technique[51] has been used for the preparation of spherical metal NPs (Pd, Ag, PdAg, PdNi and PdCu) by Heshmatpour and co-workers.[52] Bimetallic PdCu NPs in 4:1 ratio showed the highest catalytic activity in alkenylation of iodobenzene with styrene and was reused for six runs using Et_3N as base in MeOH as solvent at 100 ºC with $4.5 \cdot 10^{-2}$ mol% catalyst loading for 18 h with yields in the range of 91 to 80%.

2.4. Other reactions

Guerbert reaction[53] and aldol condensation processes of alcohols allow C-C bond formation to give higher oxygenated molecules for producing fuels and chemicals. Grabow, Toste and co-workers[54] reported that PdCu BNPs in a 3:1 ratio supported on hydrotalcite Pd_3Cu@HT[31] is an active catalyst for oxygenative coupling reaction. In addition, these BNPs decreased decarbonylation, which is an important side recation using monometallic Pd catalysts. In the case of using 1-octanol, the solution phase Guerbert condensation gave 50% conversion of a 7:1 mixture of 2-hexyl-1-decanol and octyl octanoate (Scheme 7). Starting from a mixture of ethanol/acetone/butanol (1:2.3:3.7 molar ratio) 68.3% of a mixture of 2-pentanone, 2-heptanone, 4-nonanone, 6-undecanone and the corresponding alcohols were obtained. DFT calculations suggested that the surface segregation of Cu atoms produced Cu sites with increased reactivity, while the Pd sites, responsible for the unselective decarbonylation pathway, were selectively poisoned by CO. A combination of XRD, XAS, TEM and CO chemisorption and TDP techniques revealed the formation of PdCu BNPs with a Cu-enriched surface.

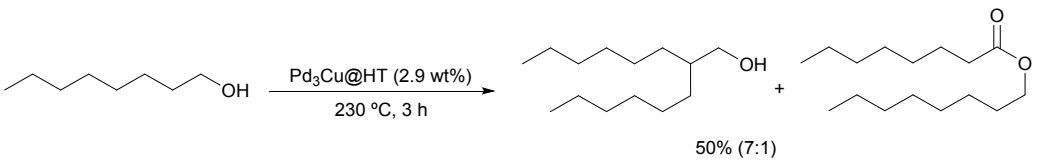

Scheme 7 Guerbert reaction of 1-octanol catalyzed by Pd_3Cu@HT.

Sekar and co-workers[55] have prepared surface enriched Pd on PdCu BNPs using binaphthyl moiety as a stabilizer, for the synthesis of polycyclic triazoles. For the preparation of these PdCu BNPs a two-step procedure was used. The starting 1,1´-binaphthyl-2,2´-diamine (BINAM) was transformed into 2,2´-binaphthalene-bisdiazonium tetrafluoroborate by treatment with $NaNO_2$ and HBF_4 at 0 ºC and then simultaneous reduction of $Pd(OAc)_2$ and $Cu(OAc)_2$ (1:1) with $NaBH_4$ in the presence of the diazonium salt occurred (Scheme 8). The reaction of *N*-(2-iodobenzyl)triazoles with internal alkynes using 2.5 mol% of PdCu BNPs in the presence of Et_3N and AcOH in DMF at 110 ºC during 20 to 48 h afforded the corresponding fused triazoles in good yields (Scheme 8). This reaction was performed at gram scale using as model reaction the triazole compound with R^1 = H and diphenylacetylene to gave the polycyclic triazole in 88% yield. According to hot centrifugation and mercury poisoning tests no Pd or Cu leaching was detected. This heterogeneous catalyst was recycled during four runs for the same model reaction with yields in the range of 92% to 86%. The mechanism of this reaction was proposed by Lautens and co-workers.[56]

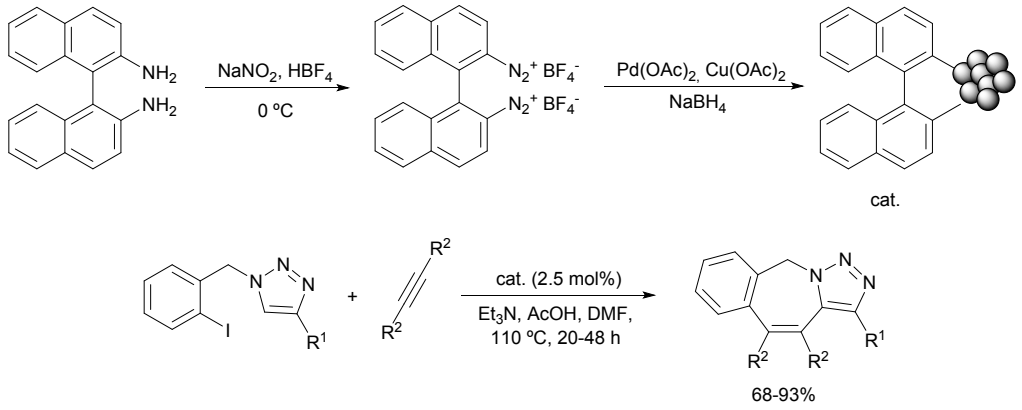

Scheme 8 Polycyclic triazoles synthesis catalyzed by PdCu BNPs.

The three-component coupling of an aldehyde, an amine and an acetylene, named A^3-coupling, is a direct method for the synthesis of propargylamines.[57] Liang, Xu and co-workers[58] have recently used PdCu-NWs[22] for the A^3-coupling of aromatic and aliphatic aldehydes, secondary amines and terminal acetylenes under solvent-free conditions at 110 ºC for 10 min to provide propargylic amines in good yields (Scheme 9). The reaction between benzaldehyde, piperidine and phenylacetylene was used as model reaction to scaled-up to 10 mmol and to study the recyclability of this BNPs during five runs (yields in the range of 97 to 92%). In the proposed mechanism, the reaction is initiated by coordination of the catalyst to the terminal alkyne to activate the C-H bond. Then, the formed acetylide on the surface of the BNPs gave addition to the iminium intermediate to afford the propargylamine.

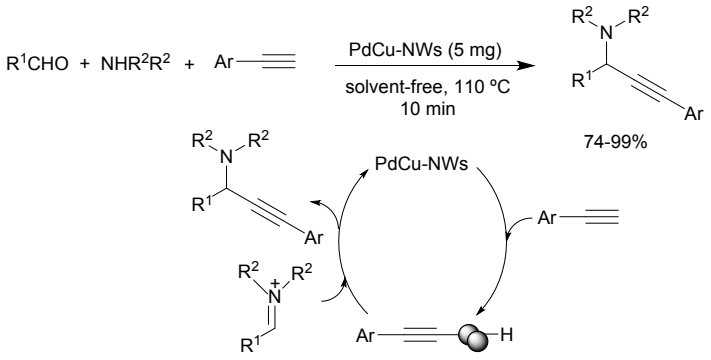

Scheme 9 A^3-Coupling reaction catalyzed by PdCu-NWs.

3. Reduction reactions

In this section, reduction methods of nitrates for water purification, hydrodechlorination of organochlorinated compounds, hydrogenation of CO_2 and CO to methanol and hydrogenation of different types of organic compounds such as semihydrogenation of alkynes, hydrogenation of C-C double bonds, hydrogenation of furfural and polyols and other reductions like levulinic acid, succinic acid, styrene oxide and nitroaromatics will be considered.

3.1. Nitrate reduction

Increase in nitrate pollution of groundwater, which is the main source of drinking water, is mainly due to agricultural activities, especially mineral fertilization, waste efluents from certain industries and as well as from nitrogen oxides release from combustion processes. High concentration of nitrates in drinking water can be damaging due to their reduction to nitrites, which combine with haemoglobin in the blood form methaemoglobin. Furthermore, cancer and hypertension are created with nitrites via nitrosamine formation. For these reasons, a lot of attention has been paid to the development of catalytic reductive processes for water purification. Among them, one of the most efficient methods for removal of nitrates from polluted water is the catalytic hydrogenation using PdCu BNPs as catalyst because nitrate is transformed into nitrogen gas. However, the NH_4^+ production as a main byproduct of the hydrogenation of nitrates in water media and it is considered as major problem. A revision of Barrabés and Sá has covered research on this field until 2010.[59]

Vorlop and Tacke[60] described for the first time in 1989 how to transform nitrates into nitrogen by hydrogenation using bimetallic catalysts. Since then, from the several combinations of a noble metal (Pt or Pd) and a promoter (Cu, Ni, Fe, Sn, In and Ag) used, PdCu BNPs is the most efficient catalyst. The metals ratio Cu/Pd can be 0.5[61,62] to 1-1.7.[63-65] The decrease on Pd content improves metal dispersion leading to an increase of exposed active phase. In addition, the preparation method and the solid support also plays an important role in the optimal ratio because adsorption effects depend from the material employed. Several supports have been used such as pumice,[66] γ-alumina,[67-70] titania,[71-74] zirconia,[75] niobia,[76] active carbon,[63,77-80] carbon nanotubes,[65] zeolites,[81-83] hydrotalcites[84-86] and resins.[87,88] From all of them, active carbon exhibits higher selectivity to nitrogen due to a high BNPs dispersion and surface chemistry of this support.[63,77-80,89,90] The ability of hydrotalcites (HT) to concentrate anions between layers decreases ammonia formation and improve diffusion of reactive species.[85,86] As a summary, a good support should be able to adsorb nitrates, exhibit high metal dispersion and be slightly acidic to control hydroxide anion concentration on the active sites.[59]

In 2012, Sá, Barrabés and coworkers[91] have investigated the oxidation state of copper in PtCu@Al_2O_3 and PdCu@Al_2O_3 catalysts during the hydrogenation of nitrates in water. *In situ* determination of copper oxidation state in the denitration of water was performed using high-energy resolution fluorescence detection (HERFD) and X-ray absorption spectroscopy (XAS) measurements revealed that the initial state of the catalyst were a PtCu and PdCu alloys. There were two important differences between the PdCu and PtCu catalyst. First, in the PtCu@Al_2O_3 catalyst, the copper alloy phase was rapidly transformed into metallic Cu and its oxide. Another important difference was in the nitrate conversion, because PdCu@Al_2O_3 afforded a higher conversion than the PtCu@Al_2O_3 system. Results indicated that during the denitration of water, active oxidation states of copper were metallic and alloy. In this work the hydrogen concentration showed an important role in the catalyst activity. Indeed, the enhancement of hydrogen flow did not affect the oxidation state of copper but changed extremely the catalytic conversion from 70% to 20% due to reactive surface poisoning with hydrogen. TEM image of PdCu@Al_2O_3 and PtCu@Al_2O_3 after reduction indicated extremely disperse metal particles with a mean size of 5.0 and 4.0 nm, respectively. Recently, Costa and co-workers[92] have investigated the catalytic activity and selectivity of PdCu@TiO_2-Al_2O_3

and PdCu@Al_2O_3 catalysts in the NO_3^-/H_2 and $NO_3^-/H_2/O_2$ reactions in order to elucidate the promoting role of TiO_2 and O_2 in suppressing the unwanted NH_4^+. state steady Using Fourier infrared reflectance diffuse and (SSITKA) analysis kinetic transient isotopic (DRIFTS) spectra transform, this group has shown that the mechanism of N_2 production depends on the nature of the support and the presence of O_2 (air) in the reaction. In addition, an alternative route has been proposed for the reduction of NO_2^- to NO and then to N_2 on the support or metal-support interface instead of Pd metal surface. Results indicated that the bimetallic catalyst, PdCu@TiO_2-Al_2O_3, has higher catalytic activity for nitrate conversion than PdCu@Al_2O_3. Importantly, support containing TiO_2 has Bronsted and Lewis acid sites for the formation of adsorbed nitrogen-species which are known as active intermediates in the reaction. Thus, less observed reactivity and selectivity in the case of support containing pure Al_2O_3, is due to absence of TiO_2. The effect of the activity of PdCu catalysts supported on various metal oxides such as TiO_2, CeO_2, ZrO_2, SiO_2, and Al_2O_3 in the reduction of nitrate and nitrite ions at constant pH, ranging from 4 to 10, was investigated by Inoue and co-workers.[93] Among the compared supports, titania xerogel revealed the highest catalytic activity in nitrates reduction. Different factors such as the type of preparation method, crystal structure, and calcination temperature of titania have influence on the activity of the catalyst. Generally, a titania xerogel catalyst, synthesized by the glycothermal method and calcinated at 800 °C, (TiO_2(XG)-800), had the highest catalytic performance as a support of the PdCu BNPs for nitrate reduction. Also, for the reduction of nitrite ions, Pd or PdCu@CeO_2 catalyst showed the highest catalytic activity, while the Pd catalyst supported on TiO_2(XG)-800 showed a good activity in reduction of nitrite ions. For these catalysts the selectivity to nitrogen product significantly improved by lowering the partial pressure of H_2.

Denitration of a highly concentrated $NaNO_3$ aqueous solution via a catalytic reduction with bimetallic PdCu immobilized on carbon powder (PdCu@C) and hydrazine monohydrate ($N_2H_4 \cdot H_2O$) as a reductant at 333 ºK was performed by Kadowaki and Meguro.[94] In this work, PdCu@C with different molar ratio of Pd/Cu compositions were prepared and various reductants such as hydrogen or N_2H_4 were examined. Results showed that the catalyst with a molar ratio of Pd/Cu 1:0.66 has the highest reaction rates for NO_3^- and NO_2^- reduction with N_2H_4 as reductant. These results indicate that N_2H_4 is more active and suitable than the H_2 in the reduction of nitrates. Also, results indicated that reduction of NO_3^- using $N_2H_4 \cdot H_2O$ in the absence of the catalyst at 333 ºK failed. Calvo and co-workers[95] studied as BNPs, PdCu, PdSn and PdIn, supported on different activated carbons (GS). The first PdCu BNPs, prepared by chemical activation of grape seeds with phosphoric acid, gave the highest nitrate removal activity. Thus, the catalyst PdCu@GS with 2.5% Cu and 5% Pd allowed achieving the European standards for drinking water when a 100 mg/L nitrate starting solution was treated. In 2017, Shuai and coworkers[96] reported the use of the ultrafine Pd and PdCu NPs supported on graphitic carbon nitride (g-C_3N_4) for nitrite and nitrate hydrogenation. Catalysts prepared by ethylene glycol reduction gave ultrafine NPs (2 nm) with high Pd and PdCu NPs loadings on the support and improved the catalytic activity and sustainability for catalyst synthesis. Generally, these types of catalysts revealed high reactivity, high selectivity towards nitrogen production over byproduct ammonium and excellent stability over multiple reaction cycles. Also, the bimetallic PdCu BNPs supported on graphitic carbon nitride catalyst have higher selectivity towards nitrogen production than the monometallic catalyst. In addition, the g-C_3N_4 supports have unique nitrogen-abundant surface, porous

structure, and hydrophilic nature which facilitated metal NPs dispersion, mass transfer of reactants, and improvement of catalytic activity towards nitrogen production.

Concerning zeolites, in 2011 Gao and Li[97] prepared PdCu BNPs supported on ZSM-5, this PdCu@ZSM-5 catalyst was prepared using a chemical reduction method and applied in the hydrogenation of nitrate ions in drinking water under mild reaction conditions. The catalytic activity of this catalyst was compared with β and γ-Al_2O_3 supported PdCu BNPs in this reaction. Better results were achieved with PdCu@ZSM-5 than with the monometallic catalysts, Pd@ZSM-5 and Cu@ZSM-5. Generally, in this work the effect of different factors such as total metal content, metals molar ratio and the addition of CO_2 were investigated. Results demonstrated that bubbling CO_2 increased the selectivity, with small changes in NO_3^- conversion. Also, the optimum Pd:Cu molar ratio for the highest catalytic activity found is 3:1 (nitrate conversion: 25.82%) with the optimum total metal content of 3 wt%.

Lee and coworkers[98,99] used four iron-bearing soil minerals, hematite (H), goethite (G), maghemite (M), and lepidocrocite (L), which were transformed to hematite with calcination, for stabilization of bimetallic PdCu. These materials were applied as catalyst in selective reduction of nitrate to nitrogen gas (Figure 1). The synthesized PdCu@hematite catalysts were characterized by BET surface area, XRD, TPR, ICP-AES, TEM-EDX, H_2 pulse chemisorption, zetapotential, and XPS. The results of TPR and TEM-EDX analysis indicated that PdCu@hematite-H have the closest contact distance between the Cu and Pd sites on the hematite surface in comparison with the other catalysts that led to the high nitrate removal. TEM image of various PdCu@hematite showed the amorphous shape of the hematite particles from 40−500 nm. Catalytic activity studies indicated that PdCu@hematite-H have the highest NO_3^- removal (96.4%) after 90 min and N_2 selectivity (72.4%). However, a lower removal of 90.9%, 51.1%, and 30.5% was obtained by using PdCu@hematite-G, M, and L, respectively. The same group used nanoscale zerovalent iron (NZVI) supported PdCu BNPs in a continuous reactor system.[100] This PdCu@NZVI maintain the catalytic activity during 200 h with excellent nitrate removal and 42-60% nitrogen selectivity. XRD, TEM and XPS analyses revealed that both the support and Cu(0) oxidized after continuous denitrification.

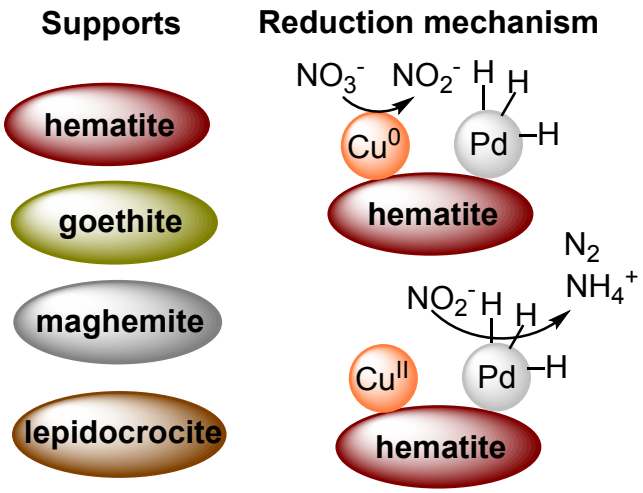

Figure 1 Representation of the nitrate reduction by catalytic hydrogenation with PdCu@hematite.

The reduction of nitrate in secondary effluent of waste water treatment plants by using PdCu supported on graphene, PdCu@GR, with Fe^0 as reductant was investigated by Li and co-workers.[101] The SEM images of PdCu@GR indicated that the supported active metal clusters were visible and homogeneously dispersed on graphene. In this work, the effect of various factors such as mass ratio of Pd:Cu, catalyst loading, reaction time, and pH of the solution were examined. Results demonstrated that 5 g/L Fe^0, 3:1 mass ratio Pd/Cu, 4 g/L catalyst, 2 h reaction time, and pH 5.1 are the optimal reaction conditions with 82% of nitrate removal and 66% of N_2 selectivity (Figure 2). The same group[102] have used Fe^0 as reductant and PdCu@Al_2O_3 as catalyst for water denitrification. The best catalytic performance, 74% of nitrate removal and 62% of nitrogen selectivity, was obtained with 5 g/L of Fe^0, a 3:1 Pd/Cu ratio, 4 g/L catalyst and 2 h reaction time at pH = 5.1.

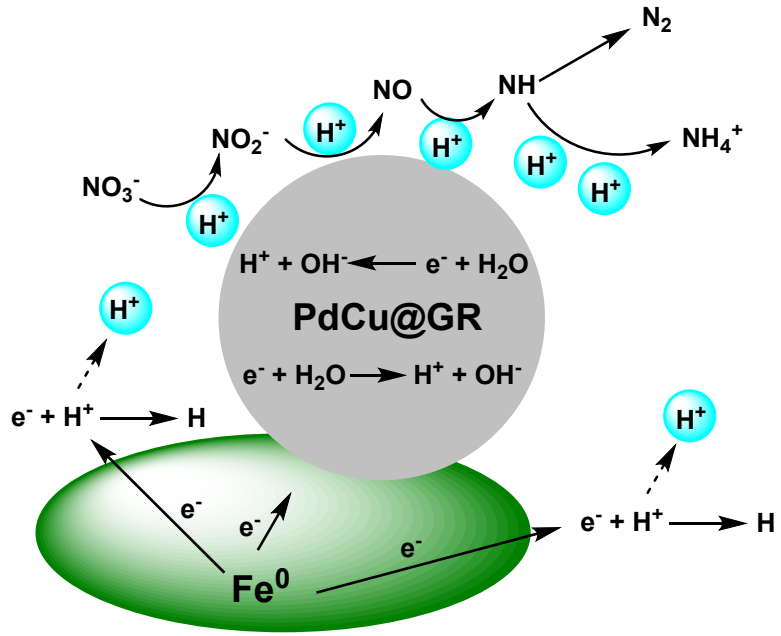

Figure 2 Representation of the nitrate reduction by Fe^0 catalyzed by PdCu@GR.

In the case of using resins as supports, Querini and coworkers[103] have designed a novel two processes in the nitrate reduction in water by using PdCu BNPs supported on a macroporous anion exchange resin WA30 as catalyst. The process, called reaction ion exchange – regeneration (RIE-R), is performed in a continuous fixed bed reactor. The two mechanisms of ion exchange and chemical reduction for nitrates elimination occurred simultaneously and the regeneration step was performed by bubbling hydrogen through the catalyst. By this way, 100% of nitrates present in the resin at the end of the RIE-R cycle was eliminated. The other process called ion exchange – regeneration (IE-R) in which in a first step only ion exchange of nitrates occurred and in the second step the catalyst is regenerated only 36.7% of the nitrates present in the resin at the beginning of the regeneration was eliminated. Indeed, results indicated that using the RIE-R process and ratio of Pd (2%)-Cu (0.5%) excellent activity for the removal of nitrates of water was obtained with respect to the IE-R process. The catalyst PdCu@WA30, was characterized by CO chemisorption, SEM, electron probe microanalysis (EPMA), TEM and XRD. Pd

migration towardss the external surface and also a decrease in dispersion takes place during the process, leading to a small decrease in activity in consecutive reaction-regeneration cycles. In 2019, Bradu and co-workers[104] prepared a PdCu BNPs catalyst with a mass ratio Pd/Cu of 4:1 supported on a microporous strong base anionic resin [A-520E Purolite, having polystyrene divinyl benzene matrix (S-DVB)] by different methods. This catalyst was applied in simultaneous removal of nitrate and 4-chlorophenol in aqueous solution. PdCu@A-520E catalysts were characterized by XPS, XRD, AAS, SEM-EDX and H_2 chemisorption and tested in a continuous flow system. It exhibits the highest catalytic activity in the simultaneous reduction of nitrate and hydrodechlorination of 4-chlorophenol. $PdCu_3$ catalyst indicated high nitrate removal degree and high selectivity in the reduction of NO_3^- to gaseous nitrogen at a conversion of 95% and a selectivity to N_2 of 92% and complete hydrodechlorination of 4-chlorophenol. The preparation of the selected catalyst included two-step method, firstly the deposition of palladium by ion exchange and the subsequent deposition of copper by controlled reaction on the surface of the pre-reduced palladium were performed. This group found that the activity of the bimetallic PdCu catalyst in the selective reduction of nitrate strongly depends on the second metal deposition procedure. Experimental results showed that this bimetallic catalyst was relatively stable after 100 h of running. Indeed, the conversion of nitrate declined slightly from 95% to 90%, however, the conversion of 4-chlorophenol to phenol did not change.

It can be concluded that important advances have been achieved in the last decade. In the case of hydrogenation methods the use of a flow reactor with PdCu BNPs supported on a macroporous anion exchange resin is an excellent methodology for the total elimination of nitrates in water allowing the regeneration of the catalyst.[103] On the other hand, for safety reasons, the use of Fe^0 as reducing agent could be a competitive alternative safe technology avoiding the use of hydrogen.[101,102]

3.2. Hydrodechlorination reaction

An important field of environmental catalysis focused on the treatment of pollutants is the catalytic hydrodechlorination (HDC) reaction. This HDC involves hydrogenolysis of C-Cl bonds catalyzed by a metal[105] or by a supported transition metal.[106] In this section, HDC processes catalyzed by supported PdCu BNPs would be considered (Figure 3).

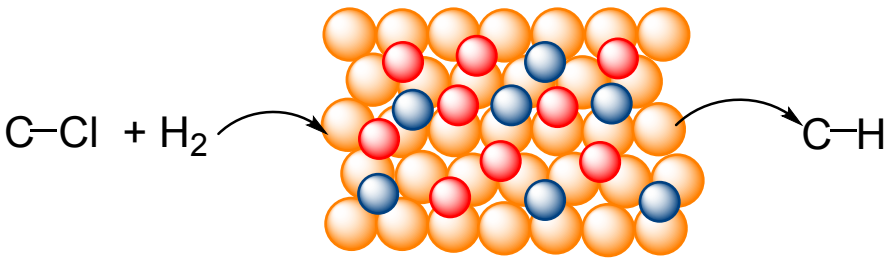

Figure 3 Representation of the hydrodechlorination reaction catalyzed by PdCu BNPs.

Hydrogen-promoted dechlorination of 1,2-dichloroethane to ethylene was performed by Heinrichs and co-workers[107,108] using PdCu BNPs supported on silica cogelled xerogel as catalyst. When they used $Pd@SiO_2$ mainly ethane was produced, while with

PdCu@SiO_2 an increment in ethylene selectivity was observed using 1.4% wt Pd and 3.0% wt of Cu at temperatures in the range of 250 ºC to 350 ºC. In 2011, Karpiński and co-workers[109] performed the same HDC of 1,2-dichloroethane to ethylene with PdCu@C at lower temperatures of 210 ºC to 230 ºC.

In the case of HDC of trichloroethene to ethylene also in gas phase, Föttinger and co-workers[110] used Pd containing Cu@HT as catalyst. High activity (>90% conversion) and excellent selectivity (more than >90% of ethylene) was observed at 300 ºC using stoichiometric concentrations of hydrogen and trichloroethene. The catalyst PdCu@HT prepared by co-precipitation without the previous reduction step exhibits higher activity (and not alloy formation) than the method used a reduction step. However, decreasing rate of ethylene formation with time was attributed to increasing Cu areas blocked by Cl. The authors proposed that the reaction proceeds via cleavage of the C-Cl bond on Cu, which is regenerated by spillover of hydrogen from the Pd. Further studies by the same group[111] using PdCu@Al_2O_3, prepared by impregnation of PdCu BNPs onto γ-alumina support, gave high values (up to 90%) of ethylene with a Pd/Cu ratio of 1.6:1 at 300 ºC. The preparation of the catalyst has an important influence in its activity, thus by the BNPs polyol synthesis, a PdCu alloy is formed, according to HRTEM and TPR analyses, leading to very high selectivity for ethylene.

Carbon tetrachloride has been subjected to HDC to give longer hydrocarbons than methane (C_2-C_5) by Karpiński and co-workers[112] using PdCu BNPs supported on active carbon under hydrogen atmosphere at 90 ºC. PdCu@C catalyst was obtained by incipient wetness co-impregnation of Sibunit carbon method[113] and results were compared with Pd@C. Results showed good metal dispersion and significant extent of PdCu alloying in PdCu/C catalyst papered. In this case, the addition of Cu to Pd in the co-impregnate catalyst led to enhancement of synergistic effect between two metals which caused the increasing of the selectivity towards longer than methane hydrocarbons. Hina and co-workers[114-116] have reported the use of the bimetallic PdCu and PdFe NPs, supported on AlF_3, as catalysts for the gas phase HDC of CCl_4. A pore-controlled version of the PdFe@AlF_3 bimetallic catalyst, called PdFe*@AlF_3 was prepared using ethylenediamine as a pore-control agent and used it for (HDC) of CCl_4. The effect of temperature, time, rate of reaction and product distribution with bimetallic PdCu@AlF_3, PdFe@AlF_3 and PdFe*@AlF_3 catalysts was studied. HDC conversion rates enhance rapidly with increasing of temperature for the PdFe*@AlF_3 and PdCu@AlF_3 catalysts. Comparison of catalytic activity showed that PdFe*@AlF_3 has higher activity than PdFe@AlF_3 due to the higher BET surface area. According to catalytic experiments, PdFe*@AlF_3 showed a greater efficiency favouring the formation of $CHCl_3$ and CH_2Cl_2, compared to PdFe@AlF_3, CH_3Cl of formation the favoured predominantly which. However, the monometallic Pd@AlF_3 has a greater tendency for the formation of the C_2–C_5 products and the bimetallic PdCu@AlF_3 for C_1-products ($CHCl_3$, CH_2Cl_2 and CH_3Cl).

In 2018, Fang and co-workers[117] reported the synthesis of a series of PdCu@C as a catalyst, through sequential incipient wetness impregnation method and also the synthesis of nonsupported PdCu bimetallic catalysts series through the reversed-phase microemulsion method and applied both of them in the HDC of 4-chlorophenol. Results indicated that the use of the PdCu@C as catalyst led to a quick conversion of 4-chlorophenol and selective formation of phenol. They proposed that Pd played a major role in the HDC reaction of 4-chlorophenol. Due to the prevention of the growth of palladium NPs, the content of copper in PdCu@C was low. Furthermore, catalytic activity

was lower when Cu content is high. In addition, PdCu alloy formed in the nonsupported PdCu catalysts has lower catalytic activity than the supported PdCu@C bimetallic catalysts in the HDC of 4-chlorophenol. As mentioned previously in Section 3.1, Bradu and co-workers[104] performed HDC of 4-chlorophenol to phenol using the resin supported catalyst PdCu@A520E. This resin was able to retain 4-chlorophenol accompanied by chloride release from the resin with complete conversion to phenol under the same reaction conditions than nitrate reduction in aqueous solutions.

3.3. Carbon dioxide hydrogenation to methanol

The atmospheric CO_2 concentration is enhanced by 20% in the past 50 years due to burning of fossil fuels. In order to mitigate the concentration of CO_2 in the atmosphere several strategies have been implemented, such as separation, storage and utilization of CO_2 as a carbon source for synthesis of chemical feedstocks and transportation fuels in worldwide. The incorporation of renewable energy to produce hydrogen via electrolysis will make CO_2 conversion more effective and environmentally friendly. The CO_2 conversion is energy demanding because CO_2 is a highly stable molecule. By introducing another substance with higher Gibbs energy as co-reactant, such as hydrogen, the conversion will become thermodynamically easier. Methanol is a primary liquid petrochemical and is also used for the production of valuable chemicals. Therefore, to develop efficient catalyst for selective CO_2 hydrogenation to methanol is an important objective.[118]

In 2015 Song and co-workers[119] described for the first time that PdCu BNPs supported on amorphous silica are selective catalysts for CO_2 hydrogenation to methanol. This group studied the strong synergistic effect on promoting methanol formation by using PdCu BNPs with the Pd/(Pd+Cu) atomic ratios in the range of 0.25-0.34. The Pd(0.34)Cu@SiO_2 catalyst had the maximum CH_3OH formation rate at 573 K and under high pressure (4.1 MPa) among all bimetallic prepared catalysts. Also, other catalysts supported on uniform mesoporous silica such as SBA-15, MCM-41 and MSU-F have similar promotional effects in methanol synthesis like the amorphous silica supported catalyst. The methanol formation rate by using Pd(0.25)Cu@SiO2 was compared to monometallic Cu and Pd catalysts showing that methanol formation rate over PdCu bimetallic catalyst was two times higher than the monometallic ones. Characterization results of PdCu@SiO_2 catalyst from quantitative analyses revealed the importance of two well-dispersed PdCu alloy particles (PdCu and $PdCu_3$) for the observed methanol production.

Fang and coworkers[120] have carried out mechanistic studies of Pd-Cu bimetallic catalysts for methanol formation from CO_2 hydrogenation. DFT calculations systematically examined the effect of the surface composition of pure Cu(111) catalysts and the role of metal dopants in the catalytic activity for the CH_3OH synthesis from CO_2 hydrogenation on Cu(111), Pd_3Cu_6(111), Pd_6Cu_3(111) and Pd ML (monolayer) surfaces (Figure 4). This group found that the addition of Pd atoms on the Cu(111) surface has not only influenced on the adsorption configuration but also altered the interactions between the adsorbed species and the metal surfaces. The rate-limiting step was showed to be the formation of trans-COOH* from CO_2 hydrogenation on Pd_3Cu_6(111) and Pd_6Cu_3(111) surfaces which is the same as that on pure Cu(111) surface changed to cis-COOH* decomposition forming CO* and OH* on Pd ML surface. More importantly, the highest

activation barriers for the overall reaction pathway were reduced in the following order: Cu(111) > Pd_6Cu_3(111) > Pd_3Cu6(111) > Pd ML. Therefore, results demonstrated that the complete reaction pathways for CH_3OH synthesis on PdCu(111) surfaces, especially on Pd ML is faster than the reaction on pure Cu(111) surface and the yield of the by-products, CO and CH_4, was suppressed.

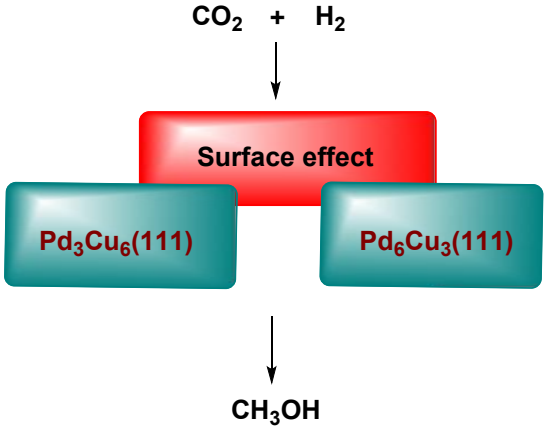

Figure 4 Representation of the CO_2 hydrogenation to methanol catalyzed by PdCu.

Song and coworkers[121] found a strong bimetallic promoting effect on supported PdCu bimetallic catalysts on silica gel for methanol formation from CO_2 hydrogenation (Figure 5). The effect of different H_2/CO_2 ratios and Pd/(Pd+Cu) atomic ratios on catalyst were examined. Maximum MeOH STY (space-time yields) were obtained within the range of Pd/(Pd+Cu) = 0.25~0.34 at H_2/CO_2 = 3/1 ratio from CO_2 hydrogenation. However, at H_2/CO_2 = 1 ratio, both the activity and CH_3OH selectivity was decreased. Hydrogen-TPR analysis showed a strong interaction between Pd and Cu which had an outstanding impact on the alloy structure. DRIFTS analysis demonstrated the dominance of formate and carbonyl species on the bimetallic surface during CO_2 hydrogenation, and their surface concentrations increased greatly on bimetallic surface than for the monometallic catalysts.

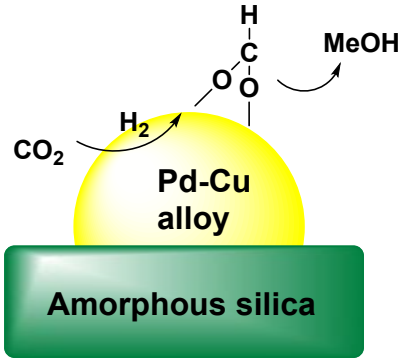

Figure 5 Representation of the CO_2 hydrogenation to methanol catalyzed by PdCu@SiO_2.

The same group[122] has investigated the alloy effect and water promotion in the PdCu@SiO_2 catalyzed CO_2 hydrogenation to methanol. For the examination of PdCu alloy structure effects on MeOH formation, the impact factors such as the structural properties and energetics for adsorption, activation, and dissociation of the reactant CO_2 and H_2, as well as the energy profiles associated with CO_2 hydrogenation on $PdCu_3$(111) and PdCu(111) surfaces, were investigated. DFT calculations showed that the structures of Pd-Cu alloys significantly influenced on the surface chemistry in CO_2 reactions. The PdCu(111) surface with low-coordinated Pd atoms exposed on top of the surface demonstrated better capability for adsorption and activation of CO_2 and H_2, and also showed superior activity for initial CO_2 hydrogenation than the Cu-rich flat $PdCu_3$(111) surface. Also, the effect of water on surface chemistry and elementary energetics in CO_2 hydrogenation to MeOH was more important over PdCu(111). Indeed, this path is preferred energetically for MeOH production. DFT calculations revealed that the presence of small amount of water can reduce the kinetic barriers through changing the "H-transfer" mechanism in hydrogenation process as well as altering the rate-limiting step. CO_2 conversion and selectivity to MeOH production was significantly promoted in the presence of a small amount of H_2O in which TOF is approximately 3000 times higher than the case without H_2O water. The same group has studied the process of methanol formation with lower metal loadings.[123] A series of Pd-Cu bimetallic catalysts supported on amorphous silica with a range total metal loadings (2.4-18.7 wt%) and optimal Pd/(Pd+Cu) atomic ratio = (0.34 at^{-1}) were prepared. These PdCu@SiO_2 catalysts were applied in CO_2 hydrogenation to methanol at 523 K and 4.1 MPa. TEM images of these catalysts showed that difference in total metal loadings hardly altered the alloy particle size. Also, PXRD analysis indicated the appearance of single Pd^0 phase with PdCu alloy phases, at relatively lower metal loadings. $PdCu_{2.4}$@SiO_2 catalyst, which has the lowest metal loading, gave the highest CO_2 conversion for MeOH production. Also, experimental results indicated that $PdCu_{2.4}$@SiO_2 catalyst has higher MeOH product formation than the commercial Cu-ZnO-Al_2O_3 catalyst. In 2019, the influence of different materials such as ZrO_2, TiO_2, Al_2O_3, CeO_2 and SiO_2 as supports for stabilization of PdCu BNPs in the CO_2 hydrogenation to methanol were investigated.[124] Methanol formation using supported PdCu catalysts decreased in the following order: TiO_2-P1 ~ ZrO_2 > Al_2O_3 > CeO_2-D ~ SiO_2. Indeed, SiO_2 support have too weak MSI (metal-support interaction) and adsorption capacity and also, TiO_2-P1~ZrO_2 have moderate MSI and best of all, CeO_2-D/Pd-Cu have the strongest MSI and extremely strong CO_2 adsorption due to abundant oxygen vacancy. Among the TiO_2 supports for PdCu, commercial TiO_2 P25 (TiO_2-P1) has higher CO_2 hydrogenation activity than SiO_2. Characterization of various PdCu supports showed that methanol formation was mainly related to $PdCu_3$ alloy phase and H_2/CO_2 adsorption on surface (Figure 6).

Further studies of Song's group[125] about the importance of PdCu alloy of PdCu@SiO_2 catalyst in selective methanol promotion by means of XRD, STEM/EDS, H_2-O_2 and N_2O titrations as well as surface chemical properties of PdCu combinations including DFT calculations were reported. The alloy formation is crucial for methanol formation and the initial adsorption of CO_2 as carbonate and bicarbonate species on the surface was higher in the bimetallic than in the monometallic catalysts.

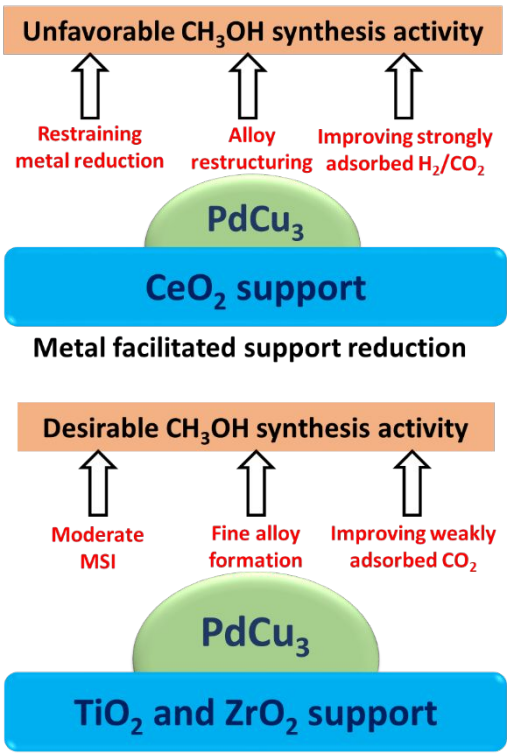

Figure 6 Representation of the CO_2 hydrogenation to methanol catalyzed by PdCu@different suppports.

Mierczynski and coworkers[126] have prepared the bimetallic (PdCu) and monometallic Cu catalysts supported on ZnO-Al_2O_3 and ZrO_2-Al_2O_3 with wet and other impregnation methods and examined them in methanol synthesis reaction from CO_2 and hydrogen under elevated pressure (3.5 MPa) at 220 ºC. The physicochemical properties of synthesized catalysts were investigated using X-ray, BET, TPD-NH_3 and TPR-H_2 techniques. The acidity measurements indicated that the addition of palladium into copper catalysts enhanced the total acidity, catalytic activity and selectivity in methanol synthesis. From the characterization techniques it can be deduced that PdCu system were in alloy form.

Selective hydrogenation of CO_2 to ethanol has been performed by Huang and co-workers[127] using Pd_2Cu BNPs supported on P25 an inorganic support mainly formed by TiO_2 instead of Pt as catalyst. This Pd_2Cu@P25 exhibits high selectivity to EtOH up to 92% with the highest TOF 350 h^{-1}. DRIFTS revealed that the EtOH production and selectivity is due to *CO (adsorption CO) hydrogenation to *HCO.

3.4. Carbon monoxide hydrogenation to methanol

Mierczynski and coworkers[128] have prepared monometallic Cu and bimetallic PdCu catalysts supported on $ZnAl_2O_4$ or $ZnAl_2O_4$–ZrO_2 using impregnation method for CO hydrogenation to methanol. The experimental studies of CO reduction showed that presence of both ZrO_2 and Pd increased the reduction of CuO species and methanol yield. The high activity of PdCu catalysts is related to the synergistic effect between Pd and Cu. The physicochemical properties of PdCu@$ZnAl_2O_4$-ZrO_2 catalyst were examined using SEM–energy dispersive spectrometry, BET, XRD, temperature programmed reduction-

H_2, and Fourier transform infrared techniques (FTIR). XRD analysis showed the alloy PdCu formation during reduction process and FTIR revealed the existence of additional surface species b-HCOO-Zr, b-HCO_3-Zr, m-CO_3-Zr adsorbed on ZrO_2 catalyst surface after methanol exposure. Generally, the activity of bimetallic and monometallic systems in methanol synthesis were by following order: Pd(2%)Cu(20%)@$ZnAl_2O_4$-ZrO_2(5%) >Cu(20%)@$ZnAl_2O_4$–ZrO_2(5%)>Cu(20%)@$ZnAl_2O_4$. The same group[129] used monometallic Pd and Cu as well as bimetallic PdCu supported on $ZnAl_2O_4$-ZrO_2 and CeO_2 in methanol production. The catalytic activity on CO hydrogenation was studied under elevated pressure (4.8 MPa) in a fixed bed reactor. Tha highest activity and selectivity was found with PdCu@$ZnAl_2O_4$-5%CeO_2. By FTIR it could be detected the presence of of several adsorption species such as b-HCO_3-Ce and b-HCOO-Ce on the surface of CeO_2 promoted catalyst.

3.5. Hydrogenation of organic compounds

In order to increase selectivity in hydrogenation reactions of unsaturated compounds under Pd catalysis is important the addition of a second metal (Au, Ag, Sn, Ni and Cu) unable to effectively dissociate hydrogen. For this reason, the use of PdCu catalysts has been studied in different hydrogenation reactions. In this section, semihydrogenation of alkynes to alkenes, hydrogenation of dienes to alkenes, nitroalkenes to amines, polyols, furfural and other organic compounds, such as diacids and epoxides are considered.

3.5.1. Semihydrogenation of alkynes

Selective partial hydrogenation of alkynes is an important transformation for the synthesis of alkenes at the laboratory and industrial scale. Monometallic Pd and Cu supported catalysts have been used for semi-hydrogenation of the C-C triple bond. In order to enhance the selectivity of Pd several bimetallic PdNi, PdZn, PdAg and PdCu have been used as catalysts. Pumice-supported PdCu catalysts[130] were employed for the semi-hydrogenation of phenylacetylene to styrene. Bimetallic catalysts were prepared by *in situ* reduction under hydrogen flow for 1 h at 298 K and at 623 K. XPS analysis of catalyst reduced at 298 K indicated that most of the copper is in the form of CuO but for catalysts reduced at 623 K, complete reduction of copper occurred to provide metallic copper. Catalyst reduced at 298 K, exhibit lower hydrogenation activity than the monometallic Pd catalyst, while the catalyst reduced at 623 K has higher selectivity than the monometallic Pd catalyst. In the case of the catalyst reduced at 623 K, the rate and the turnover frequencies declined with higher enhancement of copper content than the bimetallic catalyst reduced at 298 K. However, both gave total conversion of 95% to styrene. Indeed, in the presence of CuO the conversion rate unchanged while the selectivity to styrene increased. On the other hand, the existence of metallic Cu declined the conversion with enhancement of the selectivity.

Bimetallic PdCu catalyst supported on silica, PdCu@SiO_2, reported by van Koten and co-workers[131] has shown high selectivity in the liquid phase semihydrogenation of terminal and internal alkynes. The catalysts with different metal loadings were synthesized via reaction of lithium di(4-tolyl)cuprate with palladium acetate in the presence of silica particles under mild conditions. Characterization methods of PdCu@SiO_2 catalysts by EXAFS and TEM-EDAX revealed the existence of moderately

abundant palladium-rich particles. Catalyst containing 4 wt% Pd and 2.4 wt% Cu showed high selectivity to *Z*-alkenes. The addition of quinoline or potassium hydroxide to the reaction mixture or air exposure of the catalyst before use enhanced the selectivity towards the alkene formation. The $PdCu@SiO_2$ catalyst had better activity in comparison with Lindlar catalyst giving the corresponding alkenes in general in moderate to high yields (28% to 99%, 35 examples). Generally, semihydrogenation was performed at atmospheric hydrogen pressure in ethanol at room temperature.

Moon and co-workers[132] studied the hydrogenation of acetylene to ethylene, process used to obtain pure ethylene as monomer for polyethylene synthesis, using $PdCu@Al_2O_3$ prepared by adding Cu by a surface redox method to $Pd@Al_2O_3$. This catalyst exhibits higher ethylene selectivity than the one prepared by impregnation conventional method and than the Ag-promoted catalyst. In the case of Cu-promoted catalyst, the metal was deposited preferentially onto the low-coordination sites of Pd. The group of Sykes[133] examined the surface alloy created when Pd atoms are absorbed on a Cu surface by desorption measurements in combination with high resolution scanning microscopy. They found out a lower energy barrier to both hydrogen uptake on and subsequent desorption from the Cu metal surface. The facile hydrogen dissociation at Pd atom site and weak binding to the Cu allow for very selective hydrogenation of acetylene as compared with pure Cu or Pd metal surface. Fu and Luo[134] have performed first-principles calculations supporting the impact of Pd atoms in the Cu surface by reducing the energy barrier of hydrogen dissociation. The same group[135] have used scale atom alloy (SAA) surfaces and have prepared heterogeneous PdCu bimetallic alloy. The synthetic procedure consists in deposition of small amounts of Pd exclusively onto the surface of already performed Cu NPs supported on Al_2O_3 by galvanic replacement reaction. The catalytic performance of these $Pd_{0.18}Cu_{15}$ BNPs for the semihydrogenation of phenylacetylene at rt under a head pressure of hydrogen (6.9 bar). Greater than 94% selectivity to styrene was observed being better than monometallic Pd catalyst. PdCu BNPs prepared on native SiO_2/Si(100) support under ultrahigh vacuum, are active with respect to benzene formation from acetylene.[136]

Stakheev and coworkers[137] have reported the preparation of $PdCu@Al_2O_3$ catalyst by using the incipient wetness impregnation of the support with a $PdCu(CH_3CO_2)_4$ complex solution in dilute acetic acid (pH = 2.8) and applied in the liquid-phase diphenylacetylene semihydrogenation. This $PdCu@Al_2O_3$ catalyst with 1% Pd and 0.6% of Cu showed more selectivity and activity than the commercial Lindlar catalyst (5% $Pd/PbO@CaCO_3$) in the reaction and also, the maximum selectivity of diphenylacetylene semihydrogenation was obtained with the catalyst reduced in a hydrogen atmosphere without any intermediate calcination. McCue, Anderson and co-workers[138] have doped $Cu@Al_2O_3$ with Pd by three methos, CI, TSI and colloidal approach. The most active catalyst for acetylene semihydrogenation to ethylene prepared by TSI has a 50:1 Cu/Pd ratio giving 80% of selectivity at 98% conversion working at 353 K. Jang and co-workers[139] have reported the use of the bimetallic PdCu single atom alloys supported on alumina catalysts with less than 1 wt-% Cu and 0.03 wt-% Pd for selective hydrogenation of acetylene to ethylene. These catalysts were prepared with 3 different methods such as galvanic replacement, CI and TSI. Results of high angle annular dark field-scanning transmission electron microscopy (HAADF-STEM) and H_2 chemisorption of catalysts indicated that the three bimetallic $PdCu@Al_2O_3$ catalysts have the PdCu single atom alloy (SAA) structures. Working at 150 °C, the conversion of acetylene and the selectivity of

ethylene for three single atom alloy catalysts were above 99% and 73.0%, respectively. Generally, the PdCu single atom alloy catalyst prepared by TSI showed the best stability among the three procedures used.

Stakheev and coworkers[140] have reported the use of the PdCu catalyst prepared from heterobimetallic $PdCu_2(OAc)_6$ in the liquid-phase semihydrogenation of internal and terminal alkynes (Figure 7). This group studied the 1%Pd–1.2%Cu_2@Al_2O_3 catalysts by XRD and EXAFS techniques and the activity and selectivity of $PdCu_2$@Al_2O_3 catalyst in the hydrogenation of various internal and terminal alkynes were examined. XRD and EXAFS analysis of $PdCu_2$@Al_2O_3 catalyst indicated that presence of PdCu alloy with a faced-centered cubic (fcc) structure. The results of reaction products showed a significantly improvement in the selectivity to alkene formation in the reduction of structurally different diarylacetylenes. Therefore, by using this catalyst, diphenylacetylene conversion of 95% and selectivity of 93% was achieved at rt under H_2 pressure of 10 bar, which are close to the selectivity of the commercial Lindlar catalyst (~95%) and significantly higher than that for monometallic Pd@Al_2O_3 (~83%). Generally, for all substrates the selectivity of $PdCu_2$@Al_2O_3 catalyst in olefin formation is higher than that of monometallic Pd@Al_2O_3. It should be noted that the selectivity of $PdCu_2$@Al_2O_3 are closer or even higher (for 1-phenylprop-1-yne) than the selectivity of the commercial Lindlar catalyst but there was only exception in case of 1-phenylbut-1-yne substrate, in which selectivity to olefin formation was in order of Pd@Al_2O_3 > Lindlar catalyst > $PdCu_2$@Al_2O_3. The same group[141] has studied the catalytic activity of PdCu BNPs supported on SiO_2 and Al_2O_3 in the hydrogenation of diphenylacetylene to *cis*-stilbene. The best catalyst PdCu@Al_2O_3 with *ca*. 1:1 Pd/Cu ratio showed the highest selectivity having smaller BNPs size than in SiO_2.

Zhou and co-workers[142] have compared the catalytic selectivity in the semihydrogenation of phenylacetylene to styrene of PdCu@Al_2O_3, PdZn@Al_2O_3 and Pd@Al_2O_3. Among all prepared catalysts, $PdZn_6$@Al_2O_3 displayed the best selectivity with 86% selectivity at 99.5% phenylacetylene conversion in ethanol at 313 K and 0.1 MPa.

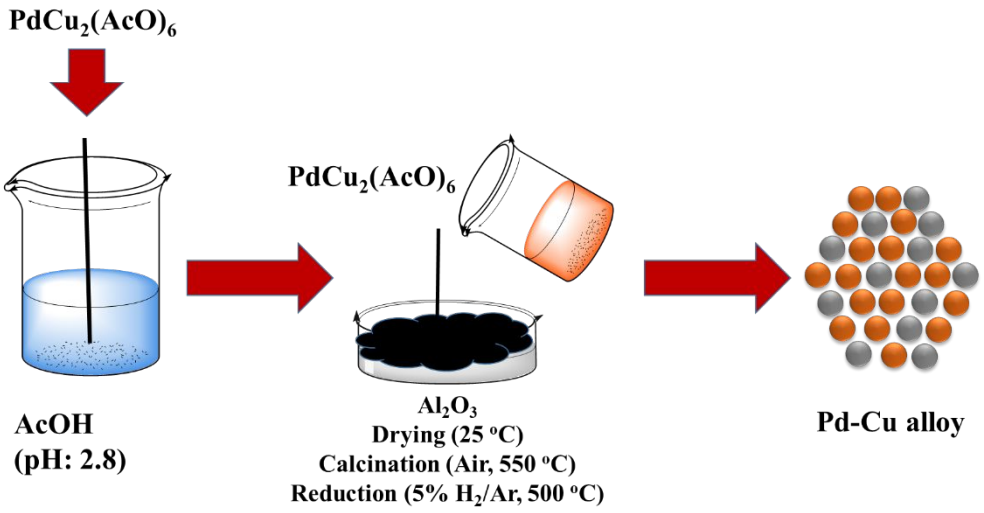

Figure 7 Representation of the preparation of $PdCu_2$@Al_2O_3 catalyst for semihydrogenation of alkynes.

Selective semihydrogenation of concentrated vinyl acetylene in mixed C4, generated from the butadiene extraction process, is carried out due to safety reasons. Insorn and Kitiyanan[143] have compared the selectivity of this reaction using $Pd@Al_2O_3$ and different $PdCu@Al_2O_3$ catalysts prepared by incipient wetness impregnation. The 1,3-butadiene selectivity was not significantly changed by adding Cu to $Pd@Al_2O_3$. However, compared to monometallic catalyst $Pd_3Cu_2@Al_2O_3$ with a 3:2 ratio improved the activity and selectivity for long-term application retarding the carbon deposition on the catalyst during the hydrogenation.

Highly dispersed PdCu alloy with a 1:40 Pd/Cu ratio supported on hydrotalcite was prepared by CI method by Feng and co-workers.[144] Partial hydrogenation of acetylene to ethylene was achieved with 100% conversion and 82% selectivity at 100 ºC under 0.4 MPa during 48 h of continuous reaction.

In 2018, Stakheev and coworkers[145] have investigated the effect of Pd/Cu ratio in the range of 2:1 to 1:4 on the performance of $PdCu@Al_2O_3$ catalysts in the liquid-phase hydrogenation of diphenylacetylene. The XRD analysis and TEM data of $PdCu@Al_2O_3$ catalysts showed the formation of uniform bimetallic PdCu BNPs (d = 20-60 nm) without the presence of monometallic Pd^0 and Cu^0 NPs on the surface. This group found that the activity of the catalyst and the yield of a desired alkene product increased with the Cu content enhancement. In addition, the selectivity of alkene formation by using $PdCu@Al_2O_3$ as catalyst with Pd/Cu = 1:3 and 1:4 ratios had higher selectivity than the commercial Lindlar catalyst in the semihydrogenation of diphenylacetylene.

Wang, Fan and co-workers[146] have recently studied the activity and selectivity of Pd-doped Cu catalyst towards the efficient removal of acetylene from ethylene using DFT calculations. The ensemble composed of a surface and a joint sublayer Pd atoms over a Cu surface enhaced the catalytic activity and selectivity in acetylene semihydrogenation to ethylene.

An efficient and easy accessible catalyst for the semihydrogenation of terminal alkynes has been developed by Radivoy and co-workers.[147] Bimetallic PdCu (1:5 ratio) supported on mesostructurated silica (MCM-48) allowed the partial hydrogenation with a 4.7 mol% C and 0.5 mol% Pd loadings in toluene at 110 ºC under a hydrogen balloon in good yields (Scheme 10). In the case of 1-phenyl-1-propyne, doble catalyst loading was necessary to provide (*Z*)-1-phenyl propene in 97% conversion. TEM data of this catalyst showed spherical BNPs with an average size of 2 to 6 nm and XPS spectrum showed that metallic Pd and Cu coexist with the corresponding counterparts on the surface of the support. This catalyst could be recovered and reused upon thermal treatment (150 ºC) followed by reduction under H_2 atmosphere.

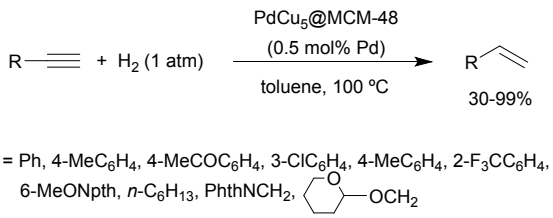

Scheme 10 Semihydrogenation of terminal alkynes with $PdCu_5@MCM-48$ as catalyst.

Domingos and co-workers[148] have recently supported different NPs in amberlite resin. These supported catalysts were prepared by immobilization of different metal ions

(Pd, Ag, Cu and Ni) on the surface of the resin by ion exchange followed by reduction with $NaBH_4$. Hydrogenation of phenylacetylene in ethanol with 0.27% of total metal loading revealed that the monometallic Pd@R and bimetallic NiPd@R and PdNi@R gave 93-99% conversion of ethylbenzene. However, CuPd@R or PdCu@R were able to produce semihydrogenation to styrene as the major product (>90%).

Carbon nanotubes (CNTs) have been used as efficient support for mono (Cu, Pd) and bimetallic (NiCu, PdCu) NPs by Delgado, Godard and co-workers.[149] The preparation of these NPs and BNPs was carried out by decomposition of the metallic precursors Cu_5Mes_5, $Pd(dba)_2$ and mixtures of $Ni(COD)_2/Cu_5Mes_5$ or $Pd(dba)_2/Cu_5Mes_5$ under 3 bar of hydrogen in the presence of N-heterocyclic carbene (NHC) ligand resulting from the decarboxylation of 1,3-dimethylimidazolium-2-carboxylate. Catalytic evaluation in the selective hydrogenation of alkynes and alkynols revealed that PdCu@CNTs with Pd/Cu 1:1 ratio is a selective catalyst for semihydrogenation of terminal and internal alkynes and also in the industrially relevant acetylene/ethylene-rich model gas feeds with excellent stability after 40 h of reaction. The process is carried out in THF at 30 ºC under 3 to 6 bar hydrogen pressure giving the alkenes in general with good yields and *Z*-selectivity (Scheme 11).

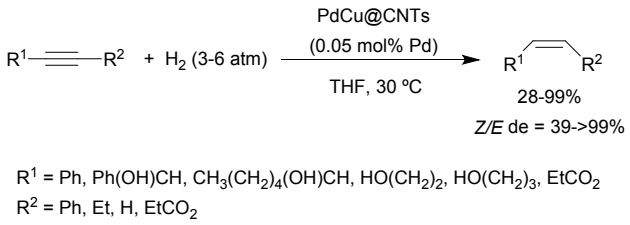

Scheme 11 Semihydrogenation of alkynes with PdCu@CNTs as catalyst.

3.5.2. Hydrogenation of C-C double bonds

Only some special cases of hydrogenation of C-C double bonds have been studied using PdCu bimetallic catalysts. For instance, chemoselective hydrogenation of *o*-xylene and carvone has been performed by Mélendrez and co-workers.[150] A series of Pd and PdCu bimetallic supported on silica catalysts was prepared by using surface redox reaction and co-impregnation methods. In the case of the bimetallic catalyst prepared by surface redox method higher selectivity to *trans*-1,2-dimethylcyclohexane was observed with $Pd@SiO_2$ due to a preferential deposition of Cu on the surface of Pd. However, when the catalyst was prepared by CI method higher selectivity for *trans*-1,2-dimethylcyclohexane with $PdCu@SiO_2$ than $Pd@SiO_2$ catalyst was obtained (Scheme 12). Also, in the selective hydrogenation of carvone by using redox catalyst higher selectivity was obtained for the formation of carvotanacetone. However, by using CI prepared catalyst higher selectivity was observed for the formation of carvomenthone product (Scheme 12).

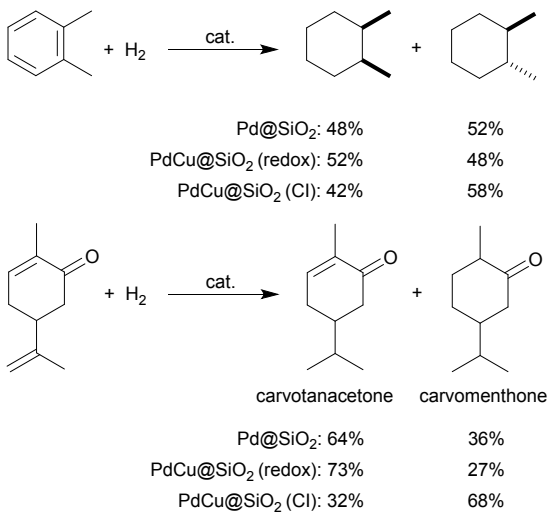

Scheme 12 Hydrogenation of *o*-xylene and carvone with $Pd@SiO_2$ and $PdCu@SiO_2$ catalysts.

Another chemoselective hydrogenation example is the reduction of 3-nitrostyrene to 3-nitrophenylethane with PdCu alloy nanocrystals described by Zeng and co-workers.[151] This group used decylamine as coordinating ligand to control the co-reduction of Pd and Cu species by affecting their reduction potential. From all different morphologies obtained, 48 nm PdCu concave tetrahedral nanocrystals were highly active for the hydrogenation of 3-nitrostyrene with >99.9% chemoselectivity to C-C double bond instead for the nitro group working at 76 ºC in dodecane as solvent.

Hydrogenation of 1,3-butadiene to purify butene streams is used in the oil and gas industry. Pd is highly active for this reaction but shows a strong selectivity to butane due to double C-C bond and geometry isomerization. In 1993, Schmal and co-workers[152] reported the use of niobia PdCu supported catalysts for 1,3-butadiene hydrogenation.The catalyst $PdCu_5@Nb_2O_5$ prepared by reduction at 573 K decreased the hydrogen adsorption capacity and the TOF but increased the selectivity for 1-butene and *trans*/*cis*-2-butene ratio. This hydrogenation was carried out in a flow system at atmospheric pressure at 343 K. Addition of Cu to Pd NPs supported on graphite increased the selectivity to partial hydrogenation of 1,3-butadiene as it has been described by Bachiller-Baeza and co-workers.[153] However, the selectivity to 1- and 2-butenes including trans/cis ratio diminished with the PdCu@G catalyst as compared to monometallic Pd@G.

In 2019, Huang, Li and co-workers[154] reported that PdCu supported on Mn_2O_3 catalysts with different weight amounts of Cu and Pd were prepared by two biogenic methods, sol-immobilization (SI) and adsorption-reduction (AR). These catalysts were compared with synthesized catalysts through three conventional methods, impregnation (CI), deposition of colloids stabilized with poly(vinylpyrrolidone) (DCPVP) and deposition−precipitation with urea (DPU), in the gas-phase selective hydrogenation of 1,3-butadiene. Characterizations of DRIFTS, CO adsorption, TPR, XPS and XRD proved the alloy nature of catalysts. Selectivity of these prepared catalysts directly correlated with increasing Cu content and butadiene conversion depended to Pd content. Indeed, catalysts with more Cu content and Pd-to-butadiene conversion. The prepared catalysts by SI method with a Pd/Cu atomic ratio of 0.9:1.4 afforded a high conversion to butadiene (99.1%) and selectivity towards butene (>92%). However, the prepared catalysts by IPC

had the worst activity in butadiene conversion but they had high selectivity towards butenes. In addition, the prepared catalysts by DCPVP and DPU methods had 100% butadiene conversion, but they had less selectivity to 1-butene. Generally, the order of selectivity of prepared catalysts were as follows: the IPC (97.3%) > AR (93.8%) > SI (91.9%) > DUP (44.4%), and DCPVP (26.4%) methods, whereas the opposite behavior was observed for butadiene conversion.

3.5.3. Hydrogenation of furfural

Furfural, commercially produced from agriculture and forestry waste, is an important raw material for a variety of chemicals and products for biofuels. By catalytic hydrogenation, furfuryl alcohol, tetrahydrofurfuryl alcohol, 2-methylfuran and cyclopentanone are obtained. In the case of Cu-catalyzed hydrogenation of furfural, furfuryl alcohol is isolated and 2-methylfuran in low yield as well. On the other hand, under Pd catalysis decarbonylation to furan is mainly observed.

Resasco and co-workers[155] reported the hydrogenation of furfural using silica-gel supported Pd and PdCu catalysts. The monometallic catalyst Pd@SiO_2 (0.5 mol%) only produced furan by the corresponding decarbonylation, while PdCu@SiO_2 gave mainly furfuryl alcohol working at 200 ºC. They also studied the hydrogenation of 2-methylpentanal with both catalysts. In the case of Pd@SiO_2 (5 mol%) *n*-pentane and 2-methylpentanol (derived from decarbonylation and hydrogenation of the carbonyl group, respectively) were isolated. Moreover, using PdCu@SiO_2 as catalyst, decarbonylation decreased and hydrogenation and etherification reactions increased.

The effect of copper on the activity and selectivity of supported palladium catalyst in the hydrogenation of furfural in water solution was investigated by Witońska and co-workers.[156] Bimetallic PdCu@Al_2O_3 catalysts containing 5 wt% Pd and 1.5-6 wt% Cu revealed high activity in this reaction. The formation of the catalysts at 300 °C in a hydrogen atmosphere led to the preparation of PdCu alloys which were characterized by analysis of XRD, SIMS-ToF (time of flight secondary ion mass spectrometry), SEM-EDS, FTIR-CO and TPR-H2. Generally, by using the pure 5% Pd@Al_2O_3 catalyst, furfuryl alcohol was obtained and then reduced to tetrahydrofurfuryl alcohol. However, the addition of copper influences the activity of palladium catalysts which led to significantly enhancement of selectivity towardss furfuryl alcohol. Indeed, the incorporation of Cu limited the formation of tetrahydrofurfuryl alcohol than the monometallic Pd@Al_2O_3 catalysts.

Hronec and co-workers[157] have prepared a series of Pd, Cu and bimetallic PdCu catalysts with different metal loadings supported on different supports by various methods and applied them for the selective hydrogenation of furfural to furfuryl alcohol in water. Among the various prepared catalysts, bimetallic PdCu catalysts supported on MgO and $Mg(OH)_2$, prepared by electroless plating method, gave the highest conversion and selectivity to furfuryl alcohol than the Pd@C, PdCu@C, Pd@HT, Pd@MgO and Cu@MgO catalysts. By using 5% Pd/5% Cu supported on MgO or $Mg(OH)_2$ at 110°C and 0.6 MPa of hydrogen, complete conversion of furfural and higher than 98% selectivity to furfuryl alcohol was achieved during 80 min. Also, the complete conversion of furfural and the same amount of selectivity were obtained after five catalytic cycles for hydrogenation of furfural to furfuryl alcohol without extra catalyst treatment or reactivation. Furthermore, in this work the role of Cu loading on the activity and

selectivity of bimetallic PdCu catalysts for aqueous phase hydrogenation of furfural to furfuryl alcohol determined by using physico-chemical characterization. The main differences among catalysts with different Cu loadings were attributed to changes between monometallic Pd^0 sites and closely interacting bimetallic Pd^0–Cu_2O catalytic sites over the surface and the Cu^+ sites participating on activation of the carbonyl group in furfural. TEM image of PdCu@MgO catalysts revealed homogeneous distribution of metallic particles and fornatiom of very small particles.

Extremely selective rearrangement of furfural to cyclopentanone by using 5%Pd-10%Cu@C bimetallic catalyst and also, the effect of the amount of copper on the catalytic activity aqueous media were investigated by Hronec and co-workers.[158] A very active and selective PdCu@C catalyst was prepared using electroless plating procedure to deposite copper nanoparticles on pre-reduced Pd@C in the presence of tartrate carboxylate ligands. Results indicated that use of the Cu species in the prepared catalyst led to enhance selectivity in the hydrogenation of the C=O bond. XRD analysis indicated that in these catalysts the copper existed in Cu^+ oxidation state as Cu_2O. Besides, metallic palladium with the particle sizes 6.8 nm were formed and there was also not metallic copper in these catalysts. Furfural conversion was 98% and cyclopentanone was obtained in 92% yield at 160 °C, 3 MPa of hydrogen and 1 wt% of catalyst during 1 h. Importantly, the concentration of hydrogen in the aqueous phase and also selective conversion of furfuryl alcohol from furfural influenced on the production of cyclopentanone. In Scheme 13 has been depicted the proposed mechanism to explain the formation of cyclopentanone, by rearrangement of furfuryl alcohol to cyclopentanone by formation of an oxycation.

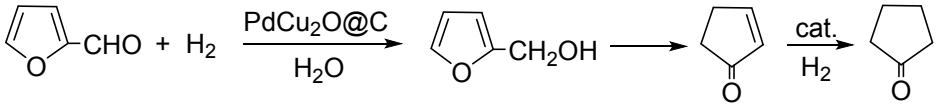

Scheme 13 Hydrogenation of furfural to cyclopentanone catalyzed by $PdCu_2O$@C.

Recently, Zhang and co-workers[159] have prepared a series of Cu-MOFs catalysts as supports for Pd NPs, Pd@Cu-BTC and Pd@FeCu-DMC, with different Lewis acidity for hydrogenative ring-rearrangement reaction of furanic aldehydes such as furfural and 5-hydroxymethyl furfural to cyclopentanone and 3-(hydroxymethyl)cyclopentanone, respectively. Hydrogenation rate of Pd@Cu-BTC catalyst with a strong Lewis acidity was six times faster than Pd@FeCu-DMC catalyst as well as higher selectivity towards cyclopentanone products (more than 90% yield) from both of furfural and 5-(hydroxymethyl)furfural. However, Pd@FeCu-DMC catalyst with weak Lewis acidity had a low conversion of furanic aldehydes and high selectivity for alcohols furfuryl alcohol or 2,5-bis(hydroxymethyl)furan.

In 2019, Zhang, Li and co-workers[160] reported furfural hydrogenation using $Pd@SiO_2$, $PdCo@SiO_2$ and $PdCu@SiO_2$ as catalysts. The bimetallic catalysts, prepared using direct deposition techniques, exhibited higher selectivity than $Pd@SiO_2$ for furfuryl alcohol. In the case of $PdCu@SiO_2$, furfuryl alcohol was almost exclusively formed at 200 ºC under 10 bar hydrogen pressure.

Catalytic transfer hydrogenation of furfural has been performed by Huang and co-workers[161] using isopropanol as hydrogen source and different bimetallic catalysts such as, NiCu, RuCu and PdCu supported on ZrO_2. The supported catalyst $Pd_3Cu_{10}@ZrO_2$

showed the highest selectivity towards the formation of 2-methylfuran and 2-methyltetrahydrofuran (3:1 ratio) in 84% total yield working at 220 ºC in 4 h (Scheme 14). Mechanistic studies revealed that the reaction proceeded mainly through the hydrogenation of furfural to furfuryl alcohol, which was deoxygenated to 2-metylfuran or experimented subsequent hydrogenation to 2-methyltetrahydrofuran. This catalyst preserved the activity during five cycles giving 82% yield of both products.

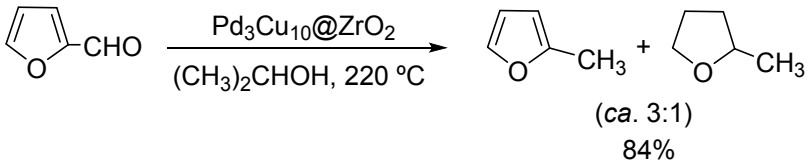

Scheme 14 Transfer hydrogenation of furfural catalyzed by $Pd_3Cu_{10}@ZrO_2$.

3.5.4. Hydrogenation of polyols

The production of biodiesel has increased the production of glycerol as side-product. For this reason, several industrially relevant chemicals have been prepared from glycerol such as acrolein, glyceric acid, lactic acid and propanediols. Namely, propanediols are used for the preparation of polyester resins, pharmaceuticals, cosmetics, fragances, paints and other products. 1,2-Propanediol is produced mainly by hydrolysis of propylene oxide but the hydrogenation of glycerol is another synthetic alternative.

Hou and co-workers[162] have employed PdCu bimetallic catalysts supported on basic solids for the hydrodeoxygenation of glycerol to 1,2-propanediol. A series of bimetallic PdCu catalysts through thermal decomposition of $Pd_xCu_{0.4}@Mg_{5.6-x}Al_2(OH)_{16}CO_3$ layered double hydroxides precursors have been prepared and applied in the hydrogenolysis of glycerol to 1,2-propanediol (Figure 8). Structured layered double hydroxides $Pd_xCu_{0.}4@Mg5_{.6-x}Al_2(OH)_{16}CO_3$ crystals characterized by XRD, SEM and N_2O oxidation and followed by H_2 titration, were prepared with amount of Pd less than x < 0.04 Pd. PdCu@solid-base catalysts have higher activity than the Pd and Cu monometallic ones in hydrogenolysis of glycerol. Generally, high conversion of glycerol and selectivity of 1,2-propanediol were obtained (88% and 99.6%) by using, $Pd_{0.04}Cu_{0.4}@Mg_{5.56}Al_2O_{8.56}$, at 2.0 MPa H_2, 180 °C, 10 h in ethanol solution. Also, this catalyst was recyclable and stable for five runs. It was concluded that hydrogen spillover from Pd to Cu increased the activity of this catalyst in the hydrogenolysis of glycerol (Figure 8).

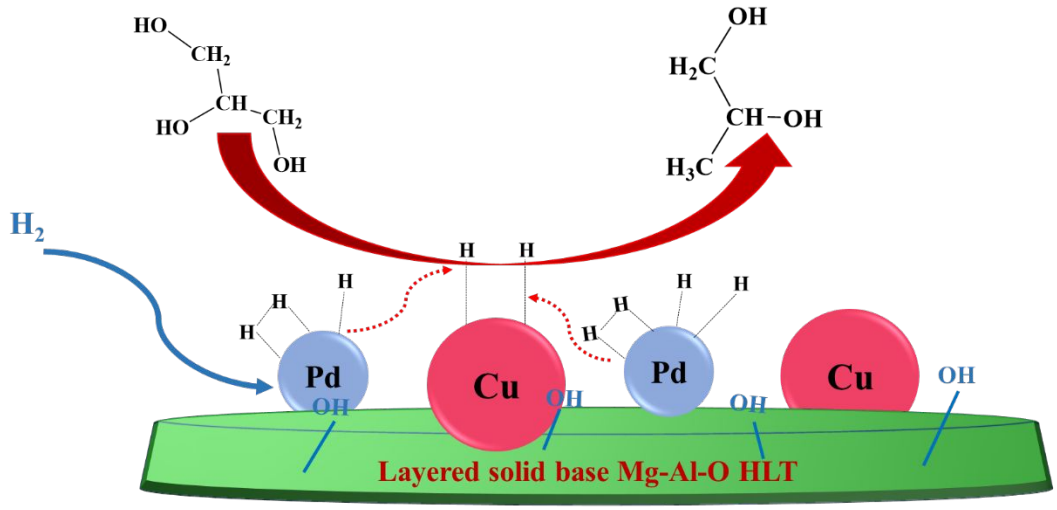

Figure 8 Representation of the hydrogenolysis of glycerol to 1,2-propanediol catalyzed by $Pd_{0.04}Cu_{0.4}@Mg_{5.56}Al_2O_{8.56}$.

Glycerol hydrodeoxygenation to 1.2-propanediol has been studied by Ardila and co-workers[163] using $PdCu@TiO_2$-Na. This catalyst was prepared by sequential wet-impregnation of TiO_2, previously treated with NaOH in MeOH followed by drying and calcination. An aqueous solution of glycerol and the catalyst was heated in the presence of hydrogen in a batch reactor at 220 ºC. Bimetallic catalyst gave higher activity than the monometallic ones and can be reused maintaining high stable activity and 1,2-propandiol selectivity.

Selective hydrogenolysis of sorbitol to ethylene glycol and propylene glycol has been reported by Jia and Liu.[164] Bimetallic PdCu supported on ZrO_2 catalysts with a wide range of Cu/Pd atomic ratios in the presence of $La(OH)_3$ were studied. Nearly 100% sorbitol conversion, with combined selectivity of 61.7% to ethylene glycol, propylene glycol, and glycerol was obtained by using $PdCu_5@ZrO_2$ at 493 K under 5.0 MPa H_2 (Figure 9). Also, the activity and selectivity of bimetallic $PdCu@ZrO_2$ catalysts were compared with $PtCu@ZrO_2$, $RuCu_3@ZrO_2$, $Pd@ZrO_2$ and $Cu@ZrO_2$ catalysts in sorbitol hydrogenolysis. These studies indicated that bimetallic $PdCu@ZrO_2$ catalysts have higher activities and selectivity than the other catalysts and higher stability and recyclability than the $Cu@ZrO_2$ catalyst.

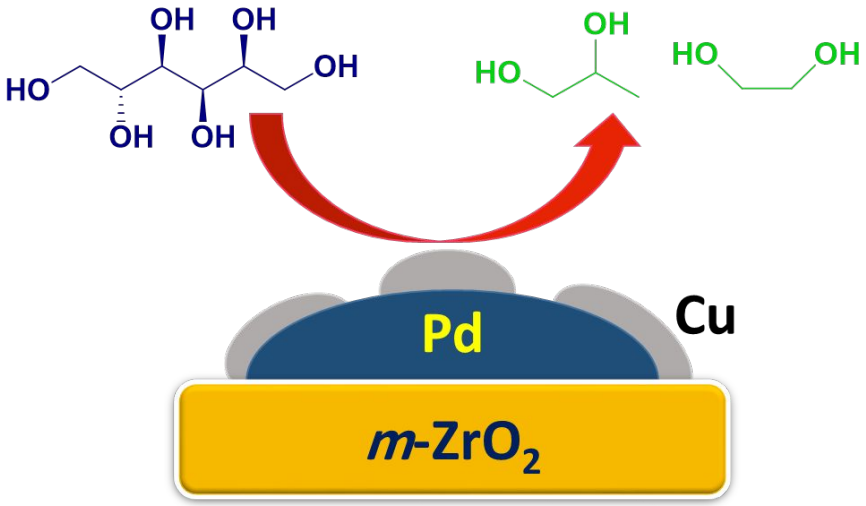

Figure 9 Representation of the hydrogenolysis of sorbitol to ethylene glycol and propylene glycol catalyzed by PdCu@ZrO_2.

3.5.5. Other reductions

Levulinic acid (4-oxopentanoic acid) derived from natural sources as glucose or fructose and is produced at industrial scale from cellulosic feedstock. Hydrogenation of levulinic acid under a suitable catalyst produced several chemicals such as γ-valerolactone, 1,4-pentanediol and 2-methyltetrahydrofuran. Patankar and Yadav[165] used PdCu@ZrO_2 as heterogeneeous catalyst for levulinic acid hydrogenation using water as solvent. The catalyst contains 1% of Pd and 29% of Cu and the reaction was performed at 200 ºC under 60 atm hydrogen pressure to provide 70% of γ-valerolactone, 25% of 1,4-pentanediol and 5% of 2-methyltetrahydrofuran (Scheme 15). The presence of Pd avoided the leaching of Cu from Cu@ZrO_2 catalyst by forming the corresponding alloy. Zirconia was a much better support than HT, alumina or hexagonal mesoporous silica.

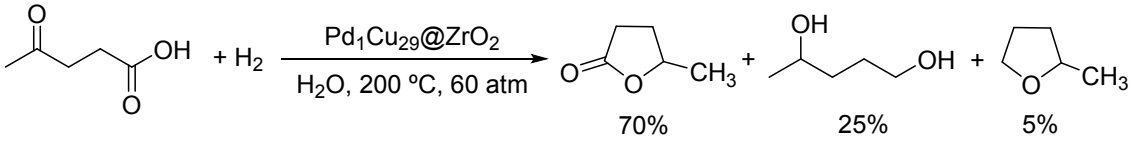

Scheme 15 Hydrogenation of levulinic acid catalyzed by Pd_1Cu_{29}@ZrO_2.

The same group has studied the hydrogenation of succinic acid by means of PdCu (1:1) BNPs supported on alumina xerogel (AX).[166] In this case, PdCu@AX was able to catalyze the formation of γ-butyrolactone, an important building block molecule for use in agrochemicals, pharmaceuticals, dyes, textile processing and epoxides preparation.The catalytic experiments were carried out in a batch reactor at 190 ºC under 70 atm hydrogen pressure in isopropanol as solvent to furnish 90% of γ-butyrolactone and 10% of tetrahydrofuran (Scheme 16). In this case, the loading was reduced to 2.5% with respect to 5% of monometallic Pd@AX to lead to an enhancement in the selectivity of γ-butyrolactone. Reusability studies of the catalyst PdCu@AX showed no significant loss of hydrogenation activity during at least five cycles.

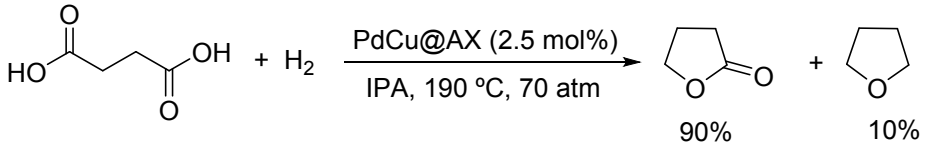

Scheme 16 Hydrogenation of succinic acid catalyzed by PdCu@AX.

Selective hydrogenation of styrene oxide to 2-phenylethanol is a direct synthetic method to produce this important fragrance to roses used in perfums, deodorants, soaps and detergents, which also possesses bacteriostatic and antifungicidal properties. The group of Yadav[167] reported the use of bimetallic PdCu catalyst encapsulated (EnCat) with polyurea in the preparation of 2-phenylethanol by using hydrogenation of styrene in methanol and supercritical carbon dioxide ($scCO_2$). The catalytic performance of PdCu@EnCat was compared with monometallic Pd@EnCat and bimetallic PdRu@EnCat. Using these catalysts, 100% conversion of styrene oxide to 2-phenylethanol, 1-phenylethanol, methoxymethylbenzene and phenylacetaldehyde products were obtained with higher selectivity to 2-phenylethanol. However, among them bimetallic PdCu@EnCat gave the best results with 65% selectivity to 2-phenylethanol. Also, the effect of $scCO_2$ was examined systematically in the hydrogenation of styrene. Results indicated that in the presence of $scCO_2$, the PdCu@EnCat catalyst revealed 100% yield and 100% selectivity to 2-phenylethanol without formation of any isomerization or deoxygenated products. Also, the effect of different parameters such as hydrogen pressure and temperature were investigated in hydrogenation of styrene oxide. It was found that using higher temperatures (343 K) and higher pressure of hydrogen (4.560 MPa) afforded higher conversion (94%) and selectivity (100%) to 2-phenylethanol in $scCO_2$ (Scheme 17). The PdCu@EnCat catalyst was stable and recycled for three times without decrease of activity or selectivity.

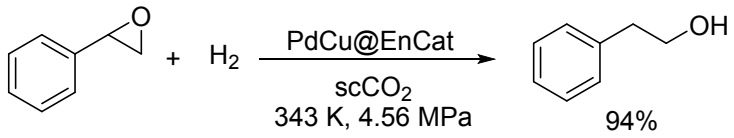

Scheme 17 Hydrogenation of styrene oxide on $scCO_2$ catalyzed by PdCu@EnCat.

Catalytic hydrogenation of nitroaromatics allows the production of large quantities of aromatic amines in the pharmaceutical, dyestuff, plastic and perfumery industry. Liao and co-workers[168,169] have performed this hydrogenation using different bimetallic Pd-based catalysts (Ni, Co, Cu, Fe, Ru) in ethanol under 1 atm of hydrogen. However, this reduction has been performed with PdCu BNPs mainly using $NaBH_4$ instead of hydrogen. Mingqing and co-workers[170] used PdCu or PdAg BNPs stabilized by poly(*N*,*N*-diethylacrylamide) grafted poly(acrylonitrile-styrene) (PDEAm-g-PAN-PS) polymeric microspheres. These catalysts exhibit superior activity than the monometallic NPs. Moreover, the catalytic properties can be regulated by increasing the temperature and can be recycled and reused for five times without loss of activity. Bimetallic Cu-M (M = Au, Pt or Pd) nanorods have been applied as catalyst in the same reduction by Chen and co-workers.[171] Ultra small PdCu BNPs have been prepared by Mallikarjuna and Kim[172] using a hydrothermal one-pot method involving an aqueous solution with hexadecylamine as a capping agent. The catalytic performance in the same reduction was improved by removing the surfactant organic layer with lactic acid giving PdCu BNPs 5±3 nm size.

Domingos and co-workers[148] evaluted PdM (M = Ag, Ni, Cu) BNPs supported on ion exchange resin not only for the semihydrogenation of phenylacetylene but also in the reduction of 4-nitrophenol to 4-aminophenol with $NaBH_4$.

4. Electrocatalytic reductions

Palladium-based nanomaterials for electrochemical purposes[173] such as oxygen reduction reactions, reduction to CO_2 to CO, methanol, formic acid and hydrocarbons and other reductions using PdCu BNPs would be considered in this section.

4.1. Oxygen reduction reaction

Bimetallic PdM Nps have been investigated in the last decade as a potential alternative electrocatalyst to Pt@C towards the cathodic oxygen reduction reaction (ORR). These types of catalysts are crucial for the development of fuel-cell technologies for providing sustainable, clean and efficient energy supply.[174] ORR in aqueous solutions occurred mainly through two pathways: a direct four-electron reduction pathway and the two-electron reduction pathway. In fuel-cell processes the first pathway is highly preferred due to its enhance power generation. Depending on the aqueous electrolyte (acidic or alkaline), the ORR mechanisms occur as described in Scheme 18.

acidic aqueous solution

$$O_2 + 4H^+ + 4e^- \longrightarrow 2H_2O$$
$$O_2 + 2H^+ + 2e^- \longrightarrow H_2O_2$$

alkaline aqueous solution

$$O_2 + 2H_2O + 4e^- \longrightarrow 4OH^-$$
$$O_2 + H_2O + 2e^- \longrightarrow HO_2^- + OH^-$$

Scheme 18 Oxygen reduction reaction mechanisms.

Martínez-Casillas and Solorza-Feria[175] used PdCu BNPs as electrocatalyst in ORR under acidic media. The electrochemical current-potential behavior was compared with Pd and Pt showing higher activity for ORR than Pd pure and less active than Pt NPs. The same group[176] used PdCu dispersed on a carbon black support as cathode electrode in a membrane-electrode assembly. The onset potential for ORR was shifted by *ca*. 30 mV to more positive values and enhanced catalytic current densities than pure Pd catalyst. Monodisperse PdCu BNPs supported on high surface area carbon have been prepared by Kariuki and co-workers.[177] This high surface area PdCu@C showed high activity for ORR in acidic electrolyte. Shao and co-workers[178] synthesized a core/shell catalyst consisting of a Pt monolayer as the shell and porous-hollow PdCu alloy BNPs as the core. This material exhibits 3.5 times higher activity than the Pt monolayer deposited on Pd and 14 times higher than commercial Pt@C.

Henkelman and coworkers[179] have studied the activity of PdCu bimetallic random alloy BNPs as catalysts in ORR by using calculations of oxygen binding of atomic oxygen for a range of compositions. Indeed, this group offered a simple model of the average binding energy that could generally predict activity trends in random alloys. Results illustrated that bimetallic PdCu catalyst (with 1:1 Pd/Cu ratio) had high activity in ORR

in comparison with monometallic Pd and other PdCu alloy BNPs. Generally, PdCu alloy BNPs with 50% of Cu was the most active catalyst in ORR. Calculations indicated that Cu, decrease the Pd-O binding energy and Pd ratio enhances the Cu-O binding energy. Considering that binding of oxygen was an indicator of ORR activity, experimental data demonstrated that random alloy BNPs could had higher activity than those of pure Pd. Results revealed that a charge transfer from Cu to Pd increases the d-band of Cu and decreased of d-band of Pd, indicating sturdier oxygen binding to Cu and weaker oxygen binding to Pd.

By means of chemical protocols different PdCu nanocrystals with a variety of nonspherical shapes have been prepared by Tan and co-workers.[180] The ORR activity is shape dependent and it has been found a catalytic enhancement of PdCu (100) nanocubes compared with Pt@C catalyst. Three-dimensional porous structure bimetallic PdCu nanodendrites have been evaluated as ORR catalysts by H.-Q. Yu and co-workers.[181] This material was prepared by supporting Pd on a 3D porous Cu via a galvanic replacement method,[182] and showed a better long-term stability than Pt@C catalyst. Monodisperse PdCu nanocubes prepared from a 1:1 molar ratio of $PdCl_2$ and $Cu(acac)_2$ in oleylamine (OAm) as solvent and reductant in the presence of trioctylphosphine (TOP) as stabilizer was reported by S.-H. Yu and co-workers.[183] These carbon-supported PdCu nanocubes displayed enhance ORR activity compared to spherical PdCu or Pd NPs and of commercial Pt@C catalyst.

In 2014, Goddard III and co-workers[184] have prepared five PdCu alloy surface structures, B2, $L1_2$, $L1_0$, $L1_1$-nonlayered, and $L1_1$-layered (Figure 10). They investigated the structural preference and ORR activity of catalysts by using DFT calculations. Results showed that layered L11 surface structure catalyst had higher ORR kinetics than pure Pd. The RDS (rate determining step) for ORR on the layered PdCu-$L1_1$, nonlayered PdCu-L11, andPdCu-L10 surfaces in solution was the H_2O formation reaction with a barrier of 0.45, 0.59, and 0.60 eV, respectively.

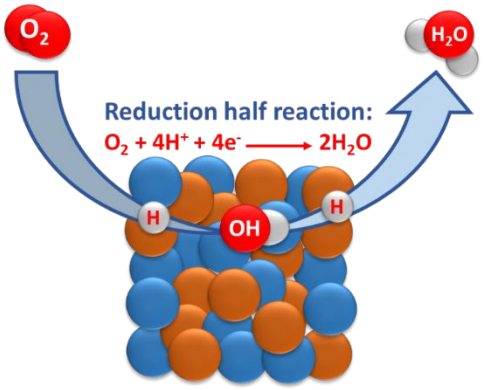

Figure 10 Representation of ORR catalyzed by PdCu alloy.

Monodisperse bimetallic alloyed PdCu nanocrystals (NCs) modified by reduced graphene oxide nanosheets (RGOs) with a one-pot solvothermal strategy method were prepared by Chen and co-workers.[185] HRTEM image of the PdCu NCs showed that the average size was around 6.81 nm and the lattice spacing is about 0.22 nm in different positions, which was related to the planes of the face-centered cubic (fcc) PdCu.

Generally, the synthesized nanocomposites had high electrocatalytic activity, significant methanol-tolerance ability for ORR in less corrosive alkaline media and long-term stability. This catalyst showed higher catalytic activity for oxygen reduction in alkaline media than the commercial Pd black and RGOs. Lu, Sun and co-workers[186] synthesized monodisperse PdCu alloy as shell in the core of Ag or Au Nps. Based on DFT calculations they predicted that core/shell M/PdCuNPs with a 0.8 or 1.2 nm Pd_2Cu shell have similar but optimal surface strain and composition to surpass Pt catalytic activity in ORR. Experimental results indicated that with controlled shell thicknesses of 0.4, 0.75 and 1.1 nm PdCu compositions were formed. Evaluation of the activity in 0.1 M KOH solution indicated that $Ag/Pd_{61}Cu_{37}$ and $Au/Pd_{60}Cu_{40}$ catalysts with 0.75 and 1.1 nm shells were 3 times more efficient than commercial Pt catalyst.

The synthesis of hollow PdCu nanospheres supported on carbon (Pd_2Cu@C, Pd_1Cu_1@C, $PdCu_{1.5}$@C and $PdCu_2$@C) via vesicle-assisted chemical reduction method by using tetrabutylphosphonium bromide (Bu_4PBr) as a surfactant in aqueous environments have performed by Zhu and co-workers.[189] TEM and HAADF STEM image of PdCu@C catalysts indicated hollow spherical shapes of PdCu nanospheres and uniform distribution of PdCu particles on carbon support. The hollow PdCu@C composites have used as catalysts in the ORR showing that Pd_1Cu_1@C catalyst have the most electrochemical activity than the other PdCu@C catalysts. Also, PdCu@C nanostructure have the highest electrocatalytic activity and long-range stability in the ORR in alkaline media than the Pd/C or Pt/C catalysts.

Chan and coworkers[188] applied a facile and one-pot wet chemical method for the synthesis of PdCu nanosponges (NSs) via the reduction of Cu^{2+} and Pd^{2+} ions by using L-ascorbic acid in the presence of sodium dodecyl sulfate (SDS). SDS concentration displayed an important role in controlling the growth and type of morphology of PdCu NSs. The PdCu NSs have been synthesized in the presence of 12.5, 25, and 37.5 mM SDS which have sizes of 46.0 ± 4.3, 36.8 ± 4.5, and 37.2 ± 2.6 nm, respectively. The PdCu NSs were utilized as efficient catalysts for glucose oxidation at −0.01 V vs. Ag/AgCl and oxygen reduction reaction (Figure 11). The catalytic activity of Cu NPs electrode (0.31 mA cm^{-2}), Pd NPs electrode (0.33 mA cm^{-2}), Pt@C electrode (0.66 mA cm^{-2}), Pd/C electrode (0.34 mA cm^{-2}) and PdCu NSs-modified electrodes were compared in ORR under alkaline conditions which results showed the PdCu NSs-modified catalysts have high current density (1.93 mA cm^{-2}) and mass activity for oxygen reduction. Also, PdCu NSs have advantages such as excellent electrocatalytic activity, high stability, sensitivity (1560 μA mM^{-1} cm^{-2}), high selectivity and high potential to be used in fuel cells using ethanol or methanol as fuel (see, Section 6.1) and applied as an electrochemical sensor for the detection of glucose in 0.1 M NaOH in blood samples (see, Section 8).

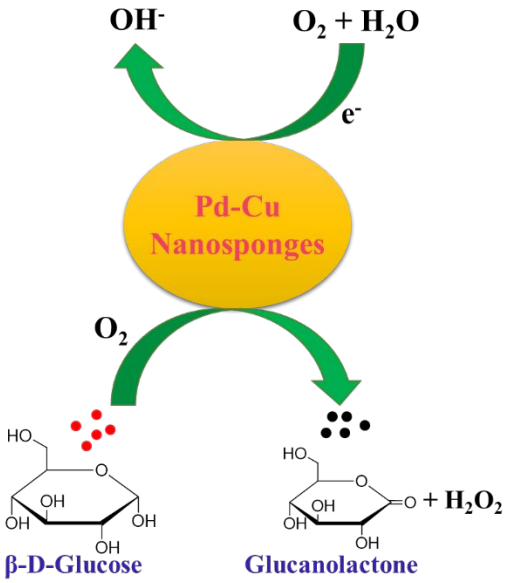

Figure 11 Representation of the electrocatalysis ORR catalyzed PdCu nanosponges.

Guo, Huang and co-workers[189] have reported structurally ordered PdCu, PdCuNi and PdCuCo NPs using a colloidal chemistry technique. From all of them the later material is the best efficient catalyst for ORR showing excellent electrocatalytic activity and durability. DFT calculations revealed that the improved ORR activity on the PdCuM NPs stems from the catalytically active hollow sites arising from the ligand effect and the compressive strain on the Pd surface owing to the smaller atomic size of Cu, Co and Ni.

Carbon-supported PdCu BNPs have been prepared using a copper metal-organic framework (MOF) as sacrificial precursor by Alonso-Vante and co-workers.[190] These nanorod-like particles exhibit in ORR higher catalytic activity than other PdCu@C catalysts. Mustain and co-workers[191] have performed the ORR in alkaline exchange membrane fuel cells by using bimetallic PdCu supported on VulcanXC-7R carbon (PdCu@Vulcan) which was prepared through a solvothermal method. TEM image of PdCu@Vulcan catalyst showed a uniform coverage of PdCu NPs on the Vulcan and analysis of XRD and XPS demonstrated primarily a B_2-type highly metallic alloy. The catalytic activity of PdCu@Vulcan catalyst was compared with commercial Pt@C catalyst showing that PdCu@Vulcan has a special activity of 1.27 mA/cm^2 and a mass activity of 0.59 A/mgPd at 0.9 V, which were higher than the Pt@C catalyst for the ORR. Also, PdCu@Vulcan catalyst revealed higher *in situ* alkaline exchange membrane fuel cell (AEMFC) activity, with operating power densities of 1100 MW/cm^2 operating on H_2/O_2 and 700 MW/cm^2 operating on H_2/Air (CO_2-free) than the commercial Pt@C catalyst. Recently performed comparison studies of the activity of carbon-supported 7.5% wt Pd-2.5% wt M of PdM (M = Ag, Co, Cu, Fe, Ni, Zn) as electrocatalysts for ORR have been carried out by Bebelis and co-workers.[192] These materials were prepared by wet impregnation and compared with 10% wt Pd@C and Pt@C. The activity followed the descending order: PdZn@C > PdNi@C > PdAg@C > PdCo@C > PdFe@C > PdCu@C.

Recently, Liu, Cheng and co-workers[193] have studied the effect of size on ORR of PdCu BNPs. Using the simple ligand-assisted method (OAm as solvent and triphenylphosphine as stabilizer), four different sizes of PdCu BNPs (9.3 nm, 7.1 nm, 6.3 nm and 5.8 nm) were synthesized. As a general trend, ORR activity decreases as BNPs

size increases. The smallest 5.8 nm PdCu@C catalyst exceded the activity of Pt@C. DFT calculations showed that with the increase of bimetallic particle size the edges and corners become less and the adsorption energies of oxygenatoms and charge distribution of the particle are closer to the bulk phase leading to a decrease of ORR catalytic activity.

In conclusion PdCu@C with small particle size prepared by ligand-assisted method is the most simple and active catalyst in ORR so far.

4.2. CO_2 reduction reactions

The electrochemical reduction of CO_2 (CO_2ER) is an important strategy for the synthesis of different raw chemicals such as CO, methanol, hydrocarbons and formate. Therefore, the development of metal catalysts for CO_2ER is of important industrial interest and also plays an additional role to decrease CO_2 emissions. Copper is the unique metal electrochemical catalyst able to reduce CO_2 to a series of organic compounds with comparative Faradaic efficiency (FE).[194] However, there are some drawbacks using copper electrodes for CO_2ER, mainly high overpotential, formation of several products and a competing reaction of hydrogen evolution. On the other hand, palladium has low overpotential for CO_2 reduction but CO or formate are usually the major products.[195]

4.2.1. Reduction of CO_2 to CO

Production of CO from CO_2 is an important industrial transformation because reduction of CO_2 plays an essential role in removing CO_2 from the atmosphere and because CO is a raw material to produce chemicals and synthetic fuels through the Fischer-Tropsch process. However, only gold-base nanostructured electrocatalysts were selective in converting CO_2 to CO with >90% FE.[196-198] In order to reduce material cost alloying Pd with inexpensive Cu is a promising strategy. Umezawa, Ye and co-workers[199] have reported the selective aqueous electrochemical reduction of CO_2 to CO using a PdCu catalyst. The prepared mesoporous PdCu bimetalic material with a high density of mesopores has been carried out via a facile electrodeposition approach.[200] Various ratios of mesoporous PdCu electrocatalysts were prepared and the highest selectivity into CO product obtained with the optimal ratio at Pd_7Cu_3 with FE_{CO} more than 80% at -0.8 V. The TEM image demonstrated a parallel cauliflower-like mesoporous structure of Pd_7Cu_3 electrocatalyst. First-principles and DFT calculations developed by the same group[201] showed that Pd atoms in the catalyst surface serve as reactive centers and the highly selective CO formation was due to the geometric and electronic effects in the alloy. The formation of CO_2H* intermediates, adsorption ability and the CO desorption ability on Pd atoms were enhaced by the presence of Cu.

Palladium-copper NPs supported on carbon with different compositions ($Pd_{56}Cu_{44}$@C and $Pd_{85}Cu_{15}$@C) have been synthesized by Wang, Ma and co-workers.[202] The catalytic activity of PdCu@C composites has been examined in the CO_2 reduction into CO. TEM images of PdCu@C showed that the sizes of PdCu BNPs are in about 3.3 ± 0.3 nm for $Pd_{85}Cu_{15}$ and 2.1 ± 0.2 nm for $Pd_{56}Cu_{44}$. These composites have better catalytic activity with high CO selectivity than the Pd-based or Cu-based catalysts (Pd@C and Cu@C), which is related to synergistic effects between Cu and Pd (Figure 12). Also, $Pd_{85}Cu_{15}$@C catalyst has the highest catalytic activity 86% FE_{CO}, selective CO production, mass activity and current density for CO_2 reduction into CO than the

$Pd_{56}Cu_{44}$@C and Pd@C catalyst due to optimum ratio of the copper element and low-coordination sites.

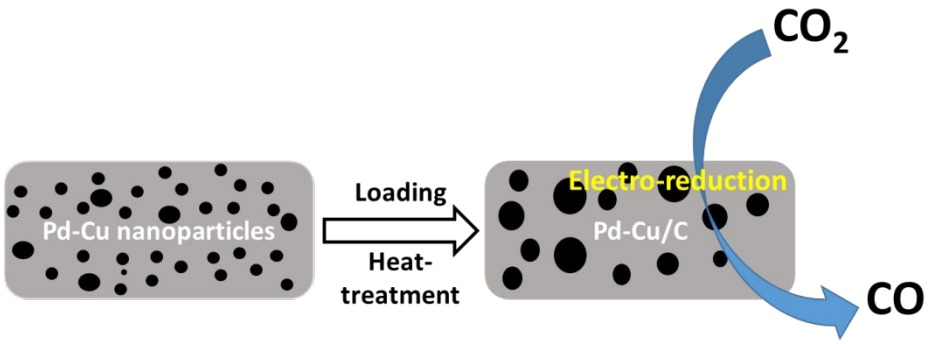

Figure 12 Representation of the electroreduction of CO_2 to CO catalyzed $Pd_{85}Cu_{15}$@C.

Wang, Bian and co-workers[203] have prepared different supported PdCu on graphene catalysts by changing the Pd/Cu ratio (1 wt% Pd-1 wt% Cu, 1 wt% Pd-2 wt% Cu and 1 wt% Pd-3 wt% Cu) by using sodium borohydride co-reduction in a graphite oxide suspension and applied it in the electrochemical reduction of CO_2. The PdCu@GR catalyst was characterized by TEM, SEM, XRD, XPS, cyclic voltammetry (CV), linear sweep voltammetry (LSV), and current-time (I-t) scans technologies. SEM, TEM, and XPS analyses indicated uniform dispersion of metal particles on the graphene support surface and metal nanoparticle sizes of $PdCu_2$@GR, Pd@GR and Cu@GR on the support were obtained in about 7.5 ± 0.25 nm, 6.5 ± 0.25 nm and 5.4 ± 0.10 nm size, respectively. The best catalytic performance of the metal@GR catalyst was achieved on 1% wt. Pd-2% wt. Cu@GR, which has a relative positive peak potential and reduction current were -1.3 V and -2,8 mA, respectively. A possible CO_2 redution mechanism has been proposed in Scheme 19. In the reaction sequence, eq (1) was presumably the rate determining step. Catalytic current value for CO_2 reduction increased essentially linearly with the concentrations of HCO_3^-. These kinetics were consistent with electron transfer and adsorption of $CO_2^{\cdot-}$ [eq (2)] followed by rate limiting proton transfer from HCO_3^-. Proton transfer could trigger a second electron transfer from the electrode to give the adsorbed formate [eq (3)]. CO_3^{2-} would take a chemical reaction with CO_2 to produce bicarbonate for supplying and supporting the formate formation [eq (5)].

$$CO_2\ (solution) \longrightarrow CO_2\ (ads) \quad (1)$$

$$CO_2\ (ads) + e^- \longrightarrow CO_2^{\cdot-} \quad (2)$$

$$CO_2^{\cdot-}\ (ads) + HCO_3^- + e^- \longrightarrow HCO_2^-\ (ads) + CO_3^{2-} \quad (3)$$

$$HCO_2^-\ (ads) \longrightarrow HCO_2^-\ (solution) \quad (4)$$

$$CO_3^{2-} + CO_2 + H_2O \longrightarrow 2HCO_3^- \quad (5)$$

Scheme 19 CO_2 electroreduction reaction mechanism.

A series of shape-controlled PdCu nanocatalysts, obtained by a wet-chemical reduction method,[204] have been employed by Gong and co-workers[205] in CO_2 reduction to CO. PdCu bimetallic NCs were synthetized by using Na_2PdCl_4 and $CuCl_2{\cdot}2H_2O$ and glucose as reductant in the presence of hexadecylamine (HDA). By simply varying the Pd/Cu precursor ratio, six types of PdCu NCs with different morphologies were obtained. The flower-like Pd_3Cu catalyst exhibit high FE_{CO} and reaches a fourfold CO current

density at -1.3 V compared to commercial Pd black. Tafel plots and DFT calculations suggested that the alloy effect is responsible for the observed high CO selectivity. Xie, Yang and co-workers[206] have applied also PdCu BNPs with different morphologies and compositions as efficient electrocatalysts for the reduction of CO_2 to CO. They used a two-step method based on galvanic replacement reaction[182] between Cu seeds and Pd^{2+} precursors. Spherical $Pd_{0.3}Cu_1$ NPs showed the highest FE for CO conversion (93%) at -0.87 V potential.

4.2.2. Reduction of CO_2 to alcohols

Conversion of CO_2 to alcohols has been achieved recently by Wang, Lu and co-workers.[207] They have designed an organic doped bimetallic PdCu catalyst derived from a pyridine. 4-[3-Phenoxy-2,2-bis(phenoxymethyl)propoxy]pyridine (PYD) was entrapped within a PdCu alloy to produce a PYD@PdCu composite. This ccomposite was applied as an efficient catalyst for the electrochemical reduction of CO_2 to alcohols in aqueous media. Using this catalyst, methanol and ethanol were obtained in 26% and 12% FE at -0.04 V and -0.64 V, respectively. Also, the catalytic activity of Pd NPs, PYD@Pd, Cu NPs, PYD@Cu and PdCu alloy were compared with PYD@PdCu in CO_2ER to alcohols under the same reaction conditions. It was found that PYD was favorable for methanol generation and Cu component was favorable for ethanol production. Generally, ethanol was not produced using PYD@Pd or Pd NPs cathode, whereas by using Cu NPs, PYD@Cu and PdCu alloy and PYD@PdCu ethanol was the major product. Catalysts containing copper were favorable for production of ethanol, while only less than 1% FE ethanol was obtained by using pure Cu NPs, and 11% FE for ethanol obtained by PdCu alloy which increased the catalytic activity than pure Cu in CO_2ER. In addition, the PYD@PdCu cathode possesses heterogeneous properties and high stability. Recycling experiments demonstrated that the PYD@PdCu electrocatalyst can be reused during fifteen times with slight decreased in catalytic activity.

Taking into account that aerogels have enormous porosity, Sun, Han and co-workers[208] have recently prepared several Pd_xCu_y aerogels by *in situ* reduction of metal precursors and supercritical CO_2 ($scCO_2$). The elecrocatalytic performances of Pd_xCu_y aerogels were carried out in CO_2 saturated $[Bmim]BF_4$ aqueous solution with 25 mol% of the ionic liquid $[Bmim]BF_4$ and 75 mol% of H_2O by using a H-type cell.[209] It was founs that $Pd_{83}Cu_{17}$ aerogel is very efficient and stable electrocatalyst with a FE of MeOH production up to 80% with a current density of 31.8 mA cm^{-2}. The efficient adsorption and stabilization of CO_2 radical anion, high Pd^0/Pd^{II} and $Cu^I + Cu^0/Cu^{II}$ ratio in the aerogel structure are responsible for the superior performance and selectivity of this electrocatalyst. This work provides a promising method for electrolytic synthesis of CH_3OH from CO_2.

4.2.3. Reduction of CO_2 to hydrocarbons

As mentioned above, metallic Cu is a very good catalyst for CO_2 reduction to hydrocarbons by electrochemical methods.[210] However, Cu foils and single crystals suffer from low surface areas, low catalytic densities and rapid deactivation.[211] Meyer and co-workers[212] reported a novel electrodeposition strategy for preparing highly dispersed ultrafine metal NPs catalysts on an electroactive polymeric film. This film derived from electropolymerization of a vinyl-2,2'-bipyridine complex of Fe(II) followed by treatment

with cyanide to display the bpy ligand by cyanide. The Fe-CN moiety can bind metal ions, which after electroreduction to the corresponding metal, migration occurs to film surfaces where NPs are formed with size control (Scheme 20). The authors compared Cu-loaded films with nanoCu (the best catalyst for CO_2 reduction to hydrocarbons)[213] and PdCu alloy. Bimetallic catalyst exhibits twofold enhancement of FE for CO_2ER to methane in both aqueous and organic solutions. They suggested that the origin of this improvement arised from a synergistic mechanism involving Pd-H reduction of adsorbed CO from CO_2 reduction on Cu. The polymer also appears to provide a basis for the local concentration of CO_2 resulting in the enhancement of catalytic current densities by threefold.

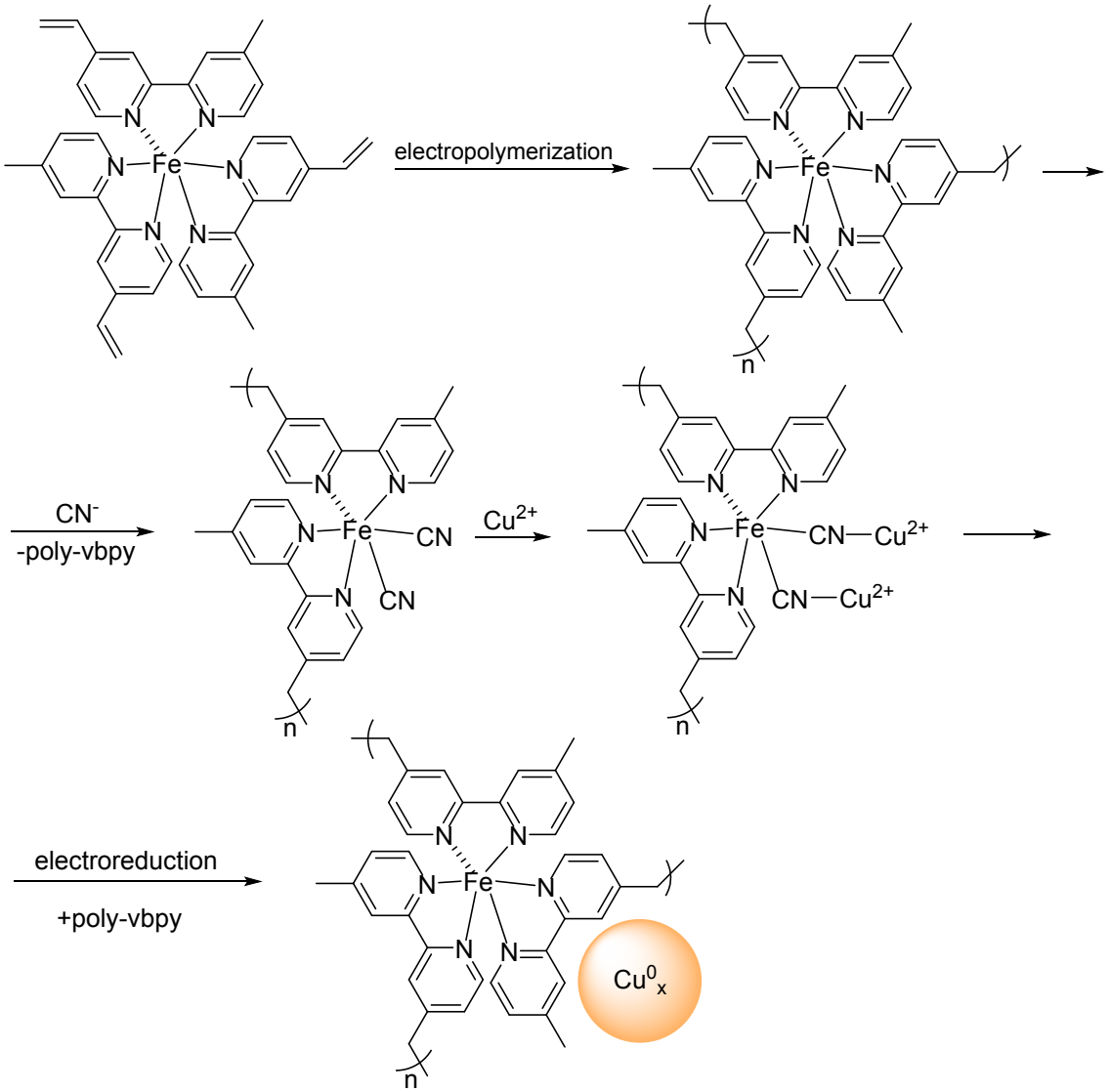

Scheme 20 Stepwise synthesis of nanoCu@polymer.

Bimetallic PdCu catalysts with ordered, disordered and phase-separated atomic arrangements (Pd/Cu 1:1 ratio) as well as two additional disordered arrangements $PdCu_3$ and Pd_3Cu, have been used by Yamauchi, Kenis and co-workers[214] for CO_2ER to C1 and C2 compounds. The ordered PdCu catalyst with alternating PdCu arrangement exhibits higher selectivity for methane production (>80%) than the phase-separated catalyst. On the other hand, the phase-separated PdCu and $PdCu_3$ achieved higher selectivity (>60%)

for ethylene and ethanol. These results suggested that neighbor Cu atoms favored dimerization of C1 intermediates.

During CO_2ER studies using PdCu bimetallic catalysts with different structures by Gong and co-workers[205] it was found out that the concave rhombic dodecahedral $PdCu_3$ favors the formation of methane. This catalyst decreases the onset potential for methane by 200 mV and showed a sevenfold methane current density at -1.2 V compared to Cu foil. DFT calculations suggested that both the introduction of high-index facets and alloying contribute to the enhanced methane current. On the other hand, the alloy effect in flower-like Pd_2Cu catalyst is responsible for high CO selectivity.

4.2.4. Reduction of CO_2 to formate

Electroreduction of CO_2 to formate has been used as a fuel indirect formic acid fuel cells (for direct formic acid fuel cells see, Section 6.2) and as a chemical feedstock for the synthesis of fine chemicals. Pd NPs have shown high activity towards the CO_2ER to formate. However, these Pd NPs are deactivated during the electrocatalysis due to surface poisoning by CO. On the other hand, Cu mitigates the CO poisoning of Pd. Takashima and co-workers[215] have prepared Pd NPs covered with Cu atomic layers using underpotential deposition (UPD). These Cu layers induced charge transfer from Pd to Cu and a downward shift of the average d-band center of the catalyst relative to the Fermi level. These bimetallic catalysts showed an increase in FE (84%) for formate production higher than the original Pd catalyst.

4.3. Hydrogen generation

Hydrogen generation from water splitting is an important potential strategy to develop sustainable and clean energy.[216] Pt-based electrocatalyst is the mostly used material for hydrogen evolution reaction (HER). Due to economical reasons, recently other Pt-free alternatives have been studied. A non-Pt-based catalyst, $PdCu_3$ NPs was developed by Peter and co-workers.[217] They employed oleylamine as solvent, stabilizer and reducing agent to synthesize these BNPs in the presence of cetyltriethylammonium bromide (CTAB). Upon electrochemical cyclic these NPs were transformed into a Cu-deficient $PdCu_3$ alloy by electrochemical dissolution of Cu. This catalyst showed high stability and enhancement of the catalytic activity in the HER attributed to the formation of active Pd site with low coordination number.

Zhang, Ma and co-workers[218] have designed a novel core@shell PdCu@Pd nanocubes to optimize the binding energy for *H and maximize the number of active sites on the surface of the catalyst for highly efficient HER. This highly monodispersed PdCu@Pd nanocubes with an average size of 11.7 nm have been prepared by a modified described procedure.[183] They showed enhanced HER activity than PdCu nanocubes, spherical PdCu NPs and Pd nanocubes[219] reported by the same group. These PdCu@Pd nanocubes exhibit onset potential of -0.5 mV *vs.* RHE and Tafel slope of 35 mV dec^{-1}, which are close to that obtained with the commercial Pt but showing higher stability than Pt catalyst.

Monodisperse carbon-supported bimetallic Pd_xCu_{100-x} NPs, with smaller average size about 4.7 nm, have been prepared by Cheng and co-workers.[220] Among these electrocatalysts $Pd_{71}Cu_{29}$@C exhibits the best activity with onset potential of 75 mV vs

RHE, exchange current density of 0.38 mA cm^{-2} and Tafel slope of 48 mV dec^{-1} in 0.1 M H_2SO_4. In addition, it shows superior electrocatalytic stability than commercial Pt@C during more than 1000 CV cycles.

Xie, Yang and co-workers[206] during electrocatalytic reduction studies of CO_2 to CO, using PdCu BNPs with different morphologies, found that dendritic PdCu nanoalloys have the highest FE for hydrogen production (65%) via RHE at a polarized potential of -0.87 V.

In conclusion, small size PdCu BNPs display better catalytic performance than BNPs with a larger size for HER and exhibit higher stability than commercial Pt-based catalysts.

4.4. Reductive dehalogenation

Reductive dehalogenation of organic halides to the corresponding hydrocarbons is an important transformation specially for the degradation of waste hazardous halogenated compounds.[221] Simonet and co-workers[222,223] described a disordered PdCu alloy as a cathode material for the first catalytic cleavage of carbon-halide bonds. A PdCu interface of well-defined structure has been prepared by injection of copper metal in solutions of palladium sulphate in 0.1 N H_2SO_4. The copper surface is instantly covered with a PdCu deposit. The simultaneous presence of copper and palladium at the interface could cause a synergistic effect in the catalytic cleavage of carbon-halide bonds in alkyl halides. In this work, the potential shift of PdCu alloy used as cathode is much larger than the conventional smooth palladium and palladated surfaces, which promote efficient one-electron cleavage of C-I and C-Br bonds even in wet organic polar solvents. PdCu electrode could be reused for in large numbers of experiments without any change in activity. The same group performed dehalogenation of long chain α,ω-dibromoalkanes $Br(CH_2)_nBr$ ($n > 3$) using PdCu and PdAg systems as cathode materials.[224]

PdCu NPs supported on glassy carbon have been prepared by Gennaro and co-workers[225] and applied in the electrochemical reduction of organic cholorides in *N*,*N*-dimethylformamide (DMF) and DMF/H_2O (3:1 v/v) as solvents. This catalyst was prepared through electrolytic deposition of Cu followed by galvanic displacement of Cu with Pd. XPS and energy-dispersive X-ray spectroscopy studies demonstrated that the composition of the NPs is dependent on the deposition time of Pd. Cu is always the main component, whereas Pd is preferentially limited to the upper layer of the nanoparticle surface. SEM image of the prepared electrode in DMF containing 0.1M Et_4NBF_4 showed average size of PdCu NPs in about 45-50 nm beside small NPs (10–15 nm). Generally, results showed good electrocatalytic activities for the reduction of both aliphatic and aromatic chlorides in DMF/H_2O (3:1 v/v) by using nanostructured electrodes. Indeed, addition of H_2O as co-solvent significantly increases electrocatalytic activity towardss the reductive cleavage of C-Cl bonds of aromatic aryl chlorides not only of PdCu NPs but also Cu NPs which were reduced at Cu. In general, the reduction activity of aromatic and aliphatic chlorides with PdCu are comparable with bulk metals Cu and Pd. Therefore, no appreciable synergetic effect on the catalyst is observed. However, the prepared electrode has a small loading of Pd giving a higher stability and preserving their catalytic activity.

5. Oxidation reactions

In this section, oxidation reactions of CO, alcohols such as benzylic alcohols and ethanol to aldehydes and methanol to methyl formate, cyclopentene to cyclopentanone, cyclohexane to cyclohexanone and ethylene to vinyl acetate catalyzed by PdCu BNPs will be considered.

5.1. Oxidation of CO

Catalytic oxidation of CO with oxygen at low temperature is an important environmental issue since small exposure (ppm) to this odorless invisible gas can be letal. CO oxidation is also important for high pure hydrogen generation, CO removal from vehicle exhaust, end-pipe gases and feed gas for fuel cells, air purification, gas mask and other industrial applications. Noble metal catalysts (Pt, Pd, Au, etc.) show high catalytic activity and good stability. Non-noble metal oxide and mixed oxide catalysts show high catalytic activity at low temperature but they deactivate in the presence of trace amount of moisture. Supported Wacker catalysts, $PdCl_2$ and $CuCl_2$ in Al_2O_3, also exhibit good stability and activity for CO oxidation even in the presence of halogen impurities and water vapor in the feed gas.[226-237] However, low temperature and high humidity rendered the system instable. The presence of water facilitates Cu transfer from the surface to the pores, which inhibits the contact between Pd and Cu species and the reoxidation of Pd^0 species. Several groups have studied the catalytic activity of PdCu BNPs in CO oxidation.

Catalytic systems based on Pd and Cu-containing zeolites (HZSM-5) with different metal loadings have been prepared by ion-exchange HZSM-5 zeolite with metal-amine complex cations. Oleksenko and co-workers[238] studied the catalytic activity of these materials in CO oxidation using various gas mixtures (0.5-2% CO, 20% O_2 and 78-79.5% He). Complete decomposition of the metal-amine complexes in the zeolite structure increase the catalytic activity. PdCu@HZSM-5 exhibits equal activity than 2.7 wt% Pd@HZSM-5, which contains five-times more palladium.

A series of PdCu BNPs supported on Ce-Zr mixed oxides or on $(Ce,Zr)O_x@Al_2O_3$ mixed supports have been examined and compared to monometallic systems for the oxidation of CO. Hungria and co-workers[239] studied the effect of Cu on this catalytic oxidation with these materials. The beneficial effect of Cu on the alumina-containing samples are related to the formation of an active PdCu alloy in contact with the Ce-Zr mixed oxide component. A preferential interaction between Cu and Al_2O_3 was proposed to optimize the properties of the alloy phase by decreasing de Cu concentration in the latter.

El-Shall and co-workers[240] have used microwave irradiation (MWI) to prepare pure monometallic (Au, Ag, Pt, Pd, Ru, Rh, Cu and Ni) and bimetallic (PdCu, CuRh, AuPd,AuRh, PtRh, PdRh and AuPt) NPs with controlled size and shape. The BNPs were supported on ceria NPs and used for CO oxidation. Experimental results reveal that $PdCu@CeO_2$ exhibits the highest activity for CO oxidation at low temperature such as 86 ºC gave 94% conversion.

Effects of different Cu precursors for the preparation of PdCu BNPs supported on Al_2O_3 on CO oxidation have been reported by Wang and Lu.[241] From the Cu salts used [$Cu(NO_3)_2$, $CuSO_4$ and $Cu(OAc)_2$] Cu and Pd nitrates gave well dispersed Cu and Pd species in Cu-rich PdCu alloy. However, the use of $CuCl_2$ and $PdCl_2$ as precursors provided the lowest catalytic activity due to the observed agglomeration of CuO.

Sonochemically synthesized PdCu@Al_2O_3 catalysts have been used for hydrogen purification by Haghighi and co-workers.[242] Fewer agglomerations were observed by increasing ultrasonic irradiation (UI) time and the Pd loading has no significant effect on the surface area. Material with 1.5% Pd and 20% Cu with 95 min UI had the best activity over the course of reaction at the best low temperature activity.

Wang and co-workers[243-246] have prepared PdCu catalyst supported on different inorganic materials. Wacker catalyst, $PdCl_2$ and $CuCl_2$, was supported on attapulgite clay by the wet impregnation method followed by calcination at 300 ºC and by evaporation ammonia method and then calcinated as well.[243,244] However, no PdCu alloy was detected and Cu species exist as $Cu_2Cl(OH)_3$ nanoplatelets. In the case of palygorskite support, also a hydrated magnesium aluminum silicate, the Cu species exist as a CuCl(OH) phase,[245] whereas after UI more Cu species exist as $Cu_2Cl(OH)_3$.[246]

Nikolaev and co-workers[247] synthesized the PdCu@Al_2O_3, Cu@Al_2O_3, and Pd@Al_2O_3 catalysts containing 0.37 wt.% Cu and 0.64 wt.% Pd via deposition-precipitation and impregnation methods. The effect of hydrogen treatment at different temperatures on the activity and structure of these catalysts in low-temperature CO oxidation was investigated. PdCu bimetallic catalyst (reduced at 423 K) has higher reactivity than the Pd and Cu monometallics in CO oxidation, due to a synergy between the metal species in the bimetallic catalyst. Characterization of PdCu@Al_2O_3 showed the formation of 5 nm alloy particles and a relatively high content of Pd^0 and MO_x species (M = Pd, Cu). TEM-EDS measurements of PdCu prepared at 423 K showed about 95% of particles in the bimetallic form and the average Pd and Cu contents in these particles were about 48% and 52%, respectively.

Di and co-workers[248] have designed bimetallic PdCu catalyst supported on alumina prepared by simple incipient wetness impregnation using $Pd(NO_3)_2$ and $Cu(NO_3)_2$, as Pd and Cu precursors, followed by the process of cold plasma reduction at atmospheric pressure. The influence of reduction sequence and Pd/Cu ratios on the structure and performance of PdCu@Al_2O_3–Plama was studied. The highest CO oxidation activity was obtained with the catalyst with a Pd/Cu atomic ratio of 1:1. In addition, the catalytic activity of PdCu@Al_2O_3–Plasma was compared with bimetallic PdCu@Al_2O_3–C, catalyst prepared by co-impregnation of $Pd(NO_3)_2$ and $Cu(NO_3)_2$ method by thermal reduction at 300 °C in H_2 atmosphere. PdCu@Al_2O_3–Plama has higher catalytic activity for CO oxidation than PdCu@Al_2O_3–C and Pd@Al_2O_3–C catalysts (Figure 13).

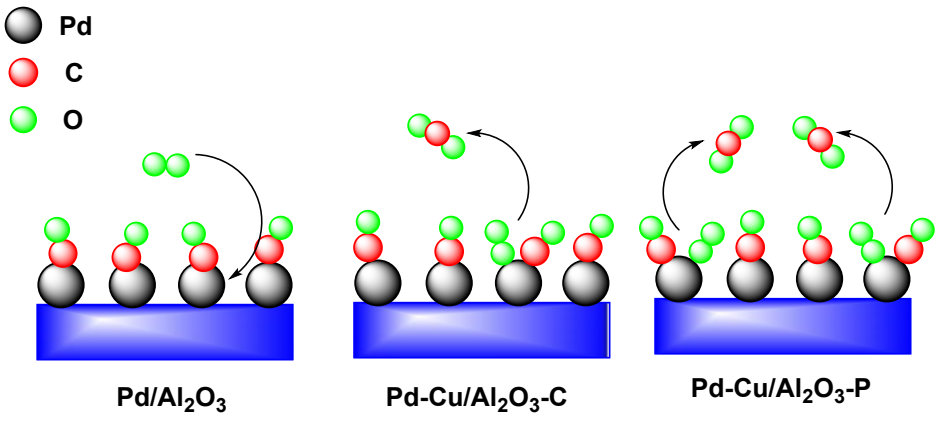

Figure 13 Mechanistic representation for CO oxidation by supported catalysts PdCu@Al_2O_3 prepared by different methods and monometallic Pd@Al_2O_3–C.

5.2. Oxidation of alcohols

Selective oxidation of primary alcohols to aldehydes is a fundamental transformation in organic chemistry. This oxidation has been performed traditionally with stoichiometric inorganic oxidants and more recently by aerobic oxidation under transition metal catalysis. The use of heterogeneous PdCu bimetallic catalysts is a recent useful methodology. Radivoy and co-workers[249] used PdCu BNPs supported on bio-silica (celite) and 2,2,6,6-tetramethylpiperidine-*N*-oxyl (TEMPO) as co-catalyst for the aerobic oxidation of primary benzylic alcohols to aromatic aldehydes. Supported monometallic Cu and Pd and bimetallic PdCu on different materials were tested in the oxidation of benzyl alcohol to benzaldehyde in toluene under an oxygen balloon and 6 mol% of TEMPO. These catalysts have been prepared in THF at room temperature by reduction of anhydrous metal chlorides with lithium powder and a catalytic amount of 4,4'-di-tert-butylbiphenyl (DTBB)[250] in the presence of the solid support. The best results were obtained with 18 mol% loading of supported $PdCu_5$@bio-SiO_2 in a Pd/Cu 1:5 ratio on celite giving benzaldehyde in 97% yield and 100% selectivity. This methodology was applied to the oxidation of different benzylic alcohols to the corresponding aldehydes (Scheme 21). It has been proposed that TEMPO could be acting as reoxidant for reduced Cu species in the catalyst. This $PdCu_5$@bio-SiO_2 was recovered and reused in three consecutive cycles giving in the case of benzaldehyde yields in the range of 97 to 90%.

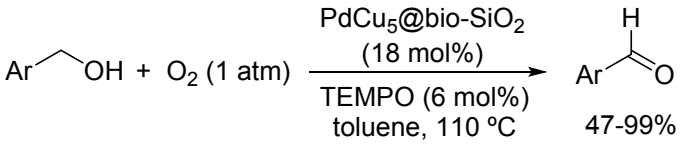

Ar = Ph, 2-ClC_6H_4, 4-ClC_6H_4, 2-$MeOC_6H_4$, 4-$MeOC_6H_4$, 2-HOC_6H_4, 3-HOC_6H_4, 4-$Me_2NC_6H_4$, 4-MeC_6H_4, 1-Nphth, styryl, 2-thienyl

Scheme 21 Oxidation of benzylic alcohols catalyzed by $PdCu_5$@bio-SiO_2 and TEMPO.

King and Personick[251] used low micromolecular concentrations of iodide ions to control the relative reduction of Cu leading to the generation of unique terraced PdCu BNPs, which exhibited increased selectivity in the oxidation of ethanol to acetaldehyde. The catalytic performance of the catalyst was compared to the monometallic Pd NPs synthesized in the presence and absence of iodide showing that the BNPs gave higher selectivity to acetaldehyde (93%), whereas Pd NPs with and without iodide yielded acetic acid in addition to acetaldehyde and ethyl acetate. They suggested that the submonolayer coverage of Cu at the surface of the terraced PdCu NPs is passivating a portion of the active surface site decreasing the production of ethyl acetate and acetic acid. The equation for this iodide-assisted reduction is indicated in Scheme 22. The iodide can be reduced by ascorbic acid and re-adsorbed to the Pd surface to continue the cycle.

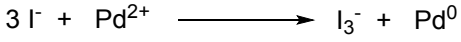

Scheme 22 Oxidation of Pd^{2+} by iodide ion.

Gas phase methanol can be oxidized to methyl formate using a bimetallic PdCu@TiO_2 photocatalyst. Colmenares and co-workers[252] prepared this photocatalyst using sonication and light. The bimetallic system with 1wt% Pd and 1 wt% Cu on TiO_2 P90 prepared at rt and atmospheric pressure provide >80% selectivity to methyl formate and slow deactivation with time. Conversion decreased slowly after 2 h of illumination.

5.3. Other oxidation reactions

Alkenes are transformed into carbonyl compounds by Wacker-type oxidation using $PdCl_2$ and $CuCl_2$ as catalysts. Feng, Xu and co-workers[253] applied PdCu@Al_2O_3, prepared by the impregnation method, as catalysts for the oxidation of cyclopentene to cyclopentanone. They reported that the best catalyst has a Pd/Cu in 5:1 ratio working at 100 ºC, 1 MPa initial oxygen pressure in ethanol as solvent to provide cyclopentanone with >95% selectivity and >85% conversion (Scheme 23).

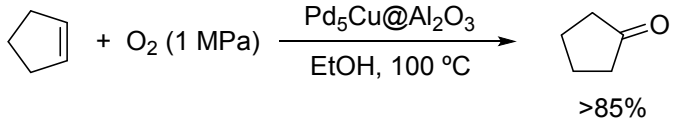

Scheme 23 Oxidation of cyclopentene to cyclopentanone catalyzed by $Pd_5Cu@Al_2O_3$.

PdCu bimetallic multipods have been prepared by reduction of $CuCl_2$ and H_2PdCl_4 with glucose and octadecylamine (ODA) as capping agent by Zeng and co-workers.[254] These multipods were 19.2 ± 1.2 nm in size with 42.7% of Pd and 57.3% of Cu according to ICP-AES analysis and were supported on TiO_2. Oxidation of cyclohexane to cyclohexanone and cyclohexanol was carried out with 30% aqueous H_2O_2 in acetonitrile at 50 ºC with monometallic Cu@TiO_2 and bimetallic multipod, and sphere-like nanocrystals (SNCs) using 10% mass loading. Multipods PdC@TiO_2 catalyst exhibited the highest selective oxidation to cyclohexanone with 78% conversion and 74% and 26% selectivity towardss cyclohexanone and cyclohexanol, respectively (Scheme 24). This catalytic activity has been attributed to the large surface area and to the exposure of high-index facets of the PdCu multipods@TiO_2.

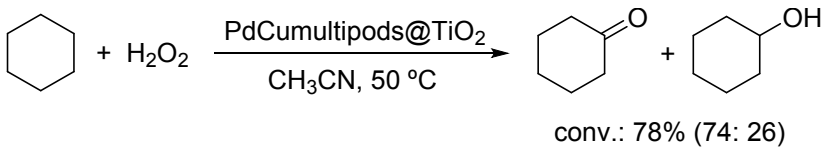

Scheme 24 Oxidation of cyclohexane with H_2O_2 to cyclohexanone and cyclohexanol catalyzed by multipods PdCu@TiO_2.

Nowadays, catalytic oxidation is used as a convenient route for the preparation of oxygenated compounds from lignocellulose biomass, producing ethylene and AcOH. These subproducts will be converted to vinyl acetate monomer (VAM), styrene and methyl methacrylate. VAM is an important polymeric precursor utilized in polyvinyl

alcohol and polyvinylbutyral polymerization systems and have applications in membrane science, medical research, 3D Print, and adhesives industries. In the past, the vinyl acetate monomer (VAM) was achieved from non-renewable sources, but renewable sources like biomass is more promising and eco-friendly. For example, Schmal and coworkers[255] have reported the use of nanostructured PdCu catalysts supported on ZrO_2 mixed oxides, incorporating Al^{3+} and Ti^{4+} like promoters, in the synthesis of vinyl acetate from ethylene, acetic acid and oxygen (Figure 14). The statistical analysis of the catalytic synthesis of VAM by using this PdCu@ZrO_2 catalyst was conducted by experimental planning design, varying the O_2 flow in feed and the catalyst nature. The experimental results of the catalytic tests revealed the amount of O_2 effects on the conversion, selectivity and the turnover frequency. Indeed, increasing of O_2 concentration, enhanced the molar fraction of VAM. This nanostructured PdCu@ZrO_2 catalyst was characterized by BET, XRD, HRTEM and H_2 chemisorption. XRD diffraction demonstrated that the PdCu catalyst has tetragonal/orthorhombic nature with differences in the lattice position. Also, XPS analysis illustrated ionic oxides and metallic particles of the PdCu (111), PdCu (200), and Zr (111) phases, which played role as electron donor of Zr-OH and Zr-H species. The presence of Cu^{2+} in the lattice explains the initial formation of acetaldehyde, acetic acid hydrogenation and posterior hydrogen spillover, releasing the hydroxyl group during VAM hydrogenation from the active site.

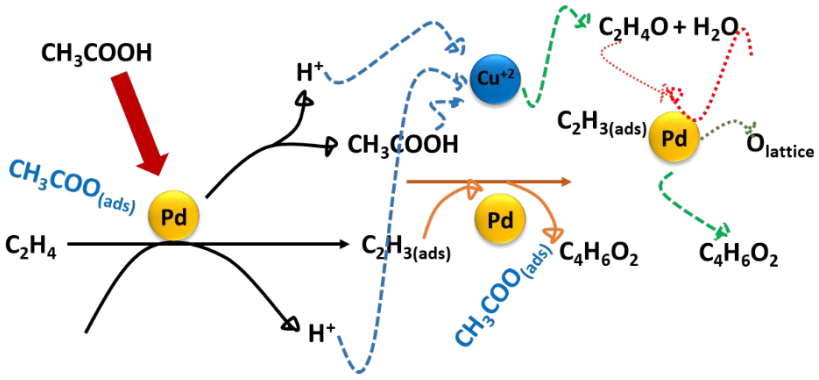

Figure 14 Representation of the syntesis of VAM from ethylene, acetic acid and oxygen catalyzed by PdCu@ZrO_2.

Hydroxylation of benzene to phenol is a challenging task in oxidation catalysis. In 1991, Li-Fen and co-workers[256] have reported the oxidation of benzene to phenol using PdCu@SiO_2 as supported catalyst. Phenol was obtained as a major product at the temperature of 150 ^oC and benzoquinone as a minor byproduct when lower temperatures (100 ^oC) were used. The presence of both Pd and Cu plays an essential role in the efficiency of the reaction because each of the metals alone had no catalytic activity. Study of the reaction in the liquid phase using Pd-single component catalyst afforded highest yield of phenol, whereas reaction in gas phase phenol was achieved in low yield. More recently, Cho and Lee[257] have studied gas phase oxidation of benzene to phenol using a mixture of hydrogen and oxygen as feeding gas and Cu supported on aluminosilycate zeolite ZSM-5 as catalyst modified with palladium. The catalyst was prepared by incipient wetness impregnation of dried Cu@ZSM-5 with a solution of $Pd(NO_3)_2$.

Catalytic performance of both Cu@ZSM-5 and PdCu@ZSM-5 catalysts showed that the former gave a 60% of benzene conversion and a phenol selectivity of 5.8%, whereas PdCu@ZSM-5 increased the conversion to 99.9% giving a selectivity of 32.2%. The presence of Pd prevents the agglomeration of Cu ions to form dimmers with the active Cu^{+} species being maintained.

6. Electrocatalytic oxidation reactions

Electrochemical applications of PdCu bimetallic catalysts will be considered in this section. Application of different alcohols as direct alcohol fuel cells (DAFCs) such as methanol, ethanol, isopropanol and polyols such as glycol and glycerol will be covered. Other electrochemical oxidation reactions such as formic acid oxidation (FAO), formaldehyde oxidation and styrene epoxidation will be also included.

6.1. Alcohol oxidation

DAFCs have gained much attention for their use as power sources for portable applications, such as electronic devices and electric cars. Alcohols have high energy density, ease transportation and storage in contrast to hydrogen fueled polymer electrolyte membrane fuel cells (PEMFCs). The high cost of Pt-based electrodes in the oxidation of alcohols have encorauged the developmentof Pd-based nanomaterials as active, robust and low-cost electrocatalyst for DAFCs.[173]

6.1.1. Electrochemical oxidation of methanol

Direct methanol fuel cells (DMFCs) are the most common DAFCs due to high energy conversion efficiencies, system simplicity, low pollution and environmental compatibility. Palladium is completely inactive for methanol oxidation reaction (MOR) in acidic solution but very active in alkaline media. However, palladium exhibits lower activity compare to platinum. This MOR activity can be enhanced by the presence of a second metal such as copper. Ma, Bao and co-workers[258] prepared monodisperse PdCu BNPs with controllable size and composition using an improved one-step multiphase synthesis.[259] These BNPs were loaded on a Vulcan XC-72 carbon support. In particular, supported BNPs with a composition $Pd_{85}Cu_{15}$ exhibited the highest activity for the electrochemical MOR in alkaline media with values close to those of Pt@C catalyst.

Porous PdCu BNPs with high surface areas have been prepared through a surfactant-assisted growth process at 95 ºC for 30 min in the presence of dodecyltrimethylammonium chloride (DTAC) and using ascorbate for the reduction of H_2PdCl_4 and $CuSO_4$ by Chang and co-workers.[260] This porous PdCu BNPs with 1:3 metal ratio was employed as anodes under alkaline conditions in DMFCs. The porous PdCu electrodes showed a higher mass activity in the MOR than the commercial Pd@C electrodes due to the advantages of larger electroactive surface area (EASA) values, a greater number of active sites, and bimetallic synergistic effects. Problems associated with CO poisoning, degradation of the membrane and corrosion were minimized.

Bhattacharya, Dasgupta and co-workers[261] described the electrocatalytic activity of Pd_3Cu BNPs for MOR. They PdCu BNPs by a facile room temperature soft chemical method by co-reduction of Pd^{2+} and Cu^{2+} using ethylenediaminetetraacetic acid disodium

salt (EDTA) and hydrazine at room temperature. TEM image of Pd_3Cu nanoalloy showed the BNPs sizes between 17 to 25 nm and XRD indicated that the alloy structure existed for the BNPs. With enhancement of amount of Cu in the PdCu nanoalloy, the catalytic activity increased in MOR, being Pd_3Cu nanoalloy the best electrocatalyst.

Supported PdCu BNPs on graphene oxide (GO) have been prepared by Chen, Xing, Gao and co-workers.[262] They used a two-step method (Scheme 25) with various Pd/Cu ratios and studied its electrochemical activities and stabilities by cyclic voltammetry and chronoamperometry in the electrooxidation of methanol and ethanol in alkaline media. The high catalytic activity of PdCu@GO was related to the existence of small PdCu core restricted by a thin Pd-rich shell. TEM images of PdCu@GO catalyst indicated a good dispersion of PdCu BNPs on the GO layers with narrow size distribution.

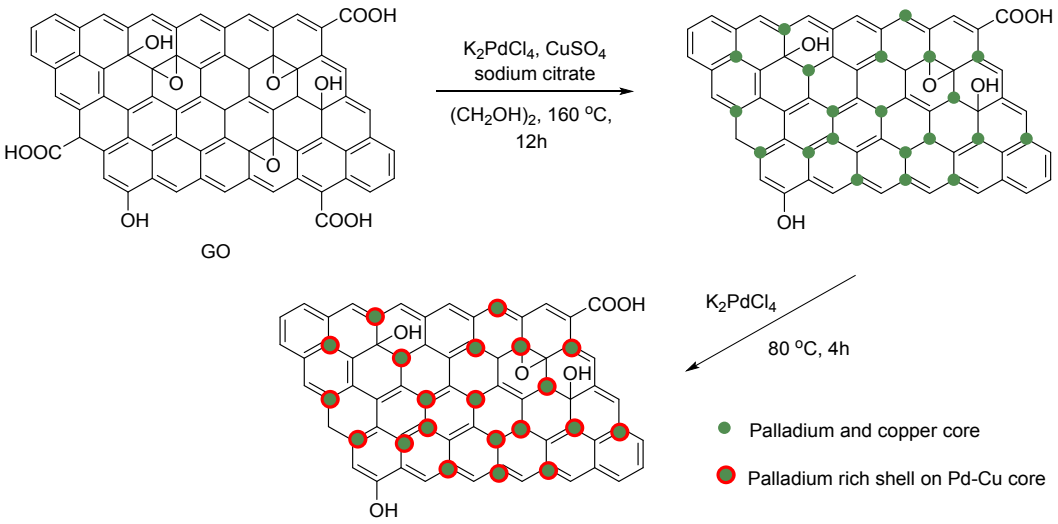

Scheme 25 Synthesis of PdCu@GO via a two-step method.

Liu, Tang, Luo and co-workers[263] synthesized supported PdCu BNPs on vertically oriented reduced graphene oxide (VRGO) and used it the methanol oxidation reaction (Figure 15). This catalyst was prepared by using a facile cyclic voltammetric electrodeposition method of graphene oxide. The structure and composition of PdCu@VRGO catalyst were characterized by XRD, TEM, SEM, Raman spectroscopy, and XPS. Cyclic voltammetry and chronoamperometry were used for investigation of electrochemical properties. Excellent electrocatalytic activity of catalyst in MOR was related to the unique vertical orientation of the sandwich-like PdCu@VRGO nanoflakes on the electrode. Also, SEM images of the PdCu@VRGO catalyst demonstrated that the VRGO sheets sandwiched between the PdCu BNPs are nearly perpendicular to the electrode substrate. Study of CO poison resistance of the catalysts PdCu@VRGO showed an excellent resistance and stability.

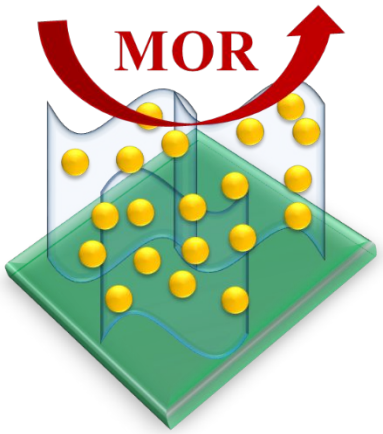

Figure 15 Representation of MOR using PdCu@VRGO as catalyst.

A bottom-up processing technique has been used by Kordas and co-wokers[264] for the preparation of multiwalled carbon nanotubes (MWCNTs) decorated with PdCu BNPs. Copper particles were deposited on the surface of Pd decorated buckypaper (a thin sheet made from an aggregate of MWCNTs) by chemical plating in which the Pd NPS act as catalyst for initiating the reduction of Cu^{2+} ions in the presence of formaldehyde. In a subsequent step, the Cu particles were partially exchanged with Pd to obtain PdCu@MWCNTs, by appling galvanic replacement reactions in aqueous solution of Pd^{2+} ions. The electrochemical properties of the different electrode materials were evaluated in the MOR. Copper seems to be mainly responsible for the oxidation, while palladium is protecting copper from being oxidized.

Wu, Anandan and co-workers[265] have prepared the nanoalloy of PdCu by using Triton X-100 as surface modifier with three various stoichiometry ratio (3:1, 1:1, 1:3) by simple co-reduction process at 5 °C (Figure 16) and their electrocatalytic activity in the methanol oxidation was investigated. Morphology and composition of the prepared catalysts were examined by XPS, XRD, TEM, SEM and EDAX with selected area electron diffraction (SAED) techniques showed that peak position in XRD analysis mean pure Pd and Cu NPs, which indicated the formation of PdCu nanoalloy. Also, the SEM images displayed that Pd and Cu are decided as a unified network in the PdCu nanoalloy. PdCu nanoalloy catalyst (3:1) and demonstrated better catalytic activity and stability than the other prepared catalysts. The high catalytic activity of the alloying of Pd with Cu is related to the synergetic effect in MOR.

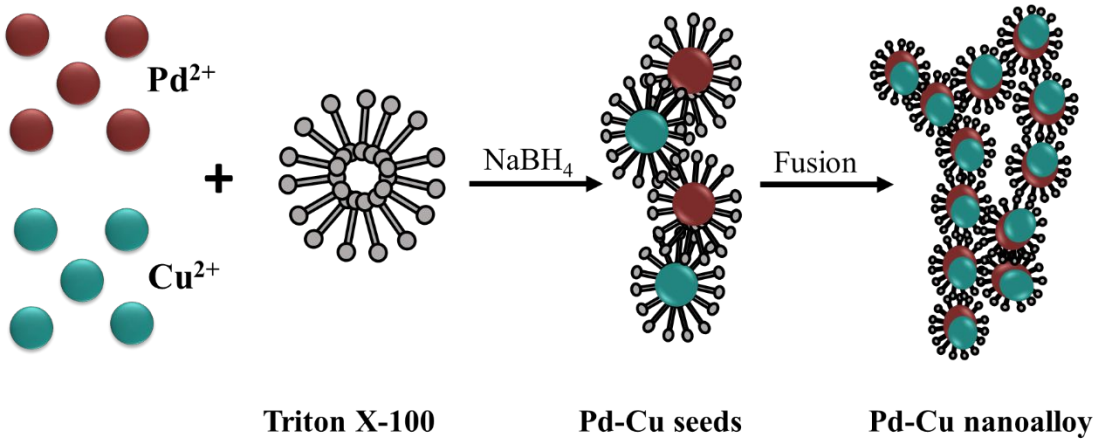

Figure 16 Representation of the preparation of Pd_3Cu nanoalloy.

Porous bimetallic PdCu nanofinger suppoted on graphene oxide have been described by Wang and co-workers.[266] Several PdCu@GO catalysts with different Pd/Cu ratios were synthesized by reaction of graphene oxide with an aqueous dispersion of $CuCl_2$ and H_2PdCl_4 under sonication. TEM and STEM images indicated the dispersed decoration of spherical BNPs on graphene nanosheets. This monofinger-like architecture exhibited large surface area and the Pd_7Cu_3@GO catalyst showed an enhanced electrocatalytic activity and stability than Pd@C for MOR.

6.1.2. Electrochemical oxidation of ethanol

Ethanol has some advantages compared to methanol such as less toxicity, low permeability, higher theoretical energy density and its production from biomass is less dependent on fossil fuels. For these reasons, ethanol can be applied as an alternative fuel source in direct alkaline alcohol fuel cells (DAAFCs). In direct ethanol fuel cells (DEFCs), ethanol is converted into acetate on a Pd-based electrocatalysts involving a 4-electron transfer giving acetaldehyde and then acetate.[267] The selectivity on ethanol oxidation reaction (EOR) takes place at strong alkaline media higher than 0.5 M NaOH. This behavior contrast with Pt-based oxidation in acidic media, which gave acetic acid, acetaldehyde and CO_2.

Due to the Pd tendency to cleave C-C bonds, alloyed Pd-based materials have been investigated in the last decade. The use of a PdCu bimetallic catalyst was described by Wang and co-workers[268] as electrocatalyst towards EOR. This PdCu@C was prepared by CO treatment at 470 K enhanced the catalytic activity about 190% due to the formation of perfect alloy core@PdO shell structure. Zhang and co-workers[269] dealloyed a ternary MgPdCu alloys to form ultrafine nanoporous PdCu alloys by treatment with a HCl solution. These nanostructures were obtained with ligaments/channels of less than 10 nm. These ultrafine nanoporous PdCu alloys exhibited high specific surface areas and superior electrocatalytic performance towards electro-oxidation not only of ethanol but also of methanol in alkaline media to be applied in DAAFCs.

Multiwalled carbon nanotubes (MWCNTs) supported Pd, PdCu (1:1 ratio) PdSn (1:1 ratio) and PdCuSn (1:1:1) catalysts have been prepared by chemical reduction with $NaBH_4$ of the precursor salts by Wang and co-workers.[270] PdCuSn@MWCNTs provided the best catalytic activity enhancement in MOR and EOR as compared with the binary PdCu@MWCNTs, PdSn@MWCNTs and the monometallic Pd@MWCNTs.

Guo and co-workers[271] synthesized a Cu@PdCu@C catalyst with the core shell structure by galvanic replacement between Pd^{2+} ions and Cu particles. These NPs are composed of the Cu core and PdCu alloying shell with a thickness of *ca*. 0.5 nm. The peak current density of ethanol oxidation on Cu@PdCu@C is 166.0 mA cm^{-2} which is *ca*. three times higher than that on Pd@C catalyst. In addition, durability and poisoning tolerance of this catalyst are also significantly improved.

PdCu nanocrystals supported on reduced graphene oxide (RGO) have been prepared by Wang, Feng and co-workers.[272] They used a solvothermal strategy to prepare this catalyst by adding $PdCl_2$ and $Cu(NO_3)_2$ to a solution of CTAB in ethylene glycol followed by Na_2CO_3 addition to reach pH = 6 and then GO. Final heating at 160 ºC in an autoclave gave the corresponding PdCu@RGO catalyst. This nanocomposite exhibited a enlarged surface area of Pd showing improved electrocatalytic activity and stability towards EOR. Graphene nanosheets have been used as support for PdCu BNPs by Zhao and co-workers.[273] This catalyst has been prepared by a electroless deposition route to anchor Cu nanoseeds on graphene nonosheets followed by deposition of Pd. A significant enhanced tolerance to poisoning was observed on EOR in alkaline media.

Haan and co-workers[274] have prepared Pd_3Cu@C and Pd@C *via* a metal salt reduction method (NaH_2PO_2) in the presence of activated carbon (Vulcan XC-72). The bimetallic catalyst revealed higher catalytic activity in EOR in alkaline medium when compared to monometallic catalyst. These results demonstrate that the addition of Cu induces and electronic effect on the Pd surface contributing to the increase in the oxidation rate.

Monodisperse PdCu nanocrystals with tunable compositions and controlled sizes have been prepared by Wang and co-workers[275] using ODA. In the case of EOR, PdCu with a 1:1 ratio exhibited the highest mass activity which is about four times higher than Pd black and 1.7 times higher than Pd_7Cu_3. Submicrometer-sized PdCu networks have been easily prepared using $NaBH_4$ as reducing agent at rt in aqueous medium by Liu, Chen and co-workers.[276] The composition-optimized $Pd_{73}Cu_{27}$ was compared with a commercial available Pd@C catalyst showing superior electrocatalytic performance with a 178% enhancement in Pd-based mass activity for EOR.

Supported PdCu BNPs prepared by one-pot reduction and co-reduction of respective metal precursors at rt have been reported by Dasgupta, Bhattacharya and co-workers.[277] Spectroscopic and microscopic studies revealed that the BNPs are agglomerated and interconverted spherical shaped nanoalloy with a radius in the range of 17 to 25 nm. Electrochemical experiments on anodic oxidation of ethanol in alkaline media showed that Pd_9Cu@C was the best catalyst for EOR and was highly stable at rt. The authors proposed the mechanism depited on Scheme 26.

$$Pd + EtOH \rightleftharpoons Pd\text{-}(EtOH)_{ads}$$

$$Pd\text{-}(EtOH)_{ads} + 3\,OH^- \longrightarrow Pd\text{-}(CH_3CO)_{ads} + 3H_2O + 3e^-$$

$$Pd\text{-}(CH_3CO)_{ads} + M\text{-}OH_{ads} \longrightarrow Pd\text{-}CH_3CO_2H$$

$$Pd\text{-}CH_3CO_2H + OH^- \longrightarrow Pd\text{-}CH_3CO_2^- + H_2O$$

$$PdCO + Cu(OH)_2 \equiv Pd + Cu + 2H^+ + CO_2^{2-}$$

$$PdHCO + Cu(OH)_2 \equiv Pd + Cu + 3H^+ + CO_2^{2-} + e^-$$

Scheme 26 Mechanism proposed for the electrooxidation of ethanol with PdCu BNPs.

Dong and co-workers[278] have prepared porous bimetallic PdCu alloy nanosponges (BANs). These well-defined three-dimensional (3D) PdCu-BANs with highly porous structure were synthesized by reduction of the corresponding salts H_2PdCl_4, $CuCl_2$ and also $Al(NO_3)_3$ with $NaBH_4$ with different compositions. The best catalyst was PdCu (1:1 ratio), which presented higher catalytic activity and stability than Pd@C towards EOR. The use of aluminum plays a critical role in facilitating the final morphology of the highly porous BANs.

In section 4.1.1 about ORR it has been described that ordered trimetallic PdCuCo NPs exhibit higher activity than Pt@C and Pd@C.[189] The same catalyst showed enhanced activity and stability also in EOR.

Mao, Huang and Yu[279] used a surface rich Pd_xCu_y@C catalyst for methanol and ethanol oxidation in alkaline medium. They used wet chemical reaction conditions using ethylene glycol as solvent and soluble (polyvinyl)pyrrolidone (PVP) K-30 polymer for the preparation of BNPs on active carbon (Vulcan XC-72) and final calcination at 200 ºC for 3 h. The values of x and y, determined by ICP-AES, were PdCu, $Pd_{1.5}Cu$, Pd_2Cu and $Pd_{2.5}Cu$. Catalyst with a Pd/Cu 2:1 ratio showed the highest activity in MOR and EOR.

Using a surfactant free strategy, Han and co-workers[280] synthesized a 3D nanochain PdCu alloy for EOR. The composition-optimized Pd_4Cu 3D nanochain catalyst exihited an increased electrochemically active surface area and mass activity over a commercially available Pd@C catalyst.

Carbon supported oxide-rich PdCu BNPs, prepared by the $NaBH_4$ reduction method, with different compositions have been reported by Li and co-workers.[281] Among them, oxide-rich Pd_9Cu@C exhibited the highest electrocatalytic activity on EOR. About 74% of Cu atoms are in their oxide form, either as CuO or Cu_2O. The decreased Pd 3d electron density disclosed by XPS was ascribed to the formation of CuO_x, which decreased the adsorption of CH_3CO_{ads} intermediates enhancing the activity.

Recently, Li, Du and co-workers[282] described ternary PdCu-SnO_2 nanowires (NWs) for efficient EOR. PdCu alloy and PdCu-SnO_2 NWs were prepared by using a galvanic displacement method. They have a one-dimensional structure, rough surfaces with non-homogeneous edges. Electrochemical measurements revealed that PdCu-SnO_2 NWs exhibited a 7-fold higher mass activity than Pd@C and that SnO_2 was introduced in the interface which promoted the oxidation of ethanol.

The mentioned recent findings in Section 6.1.1 and 6.1.2 on MOR and EOR with different PdCu based-catalysts will contribute to the development of efficient DMFCs and DEFCs.

6.1.3. Electrochemical oxidation of isopropanol

The electrooxidation of isopropanol has been mainly performed on PtPt and PdPd alloys. Isopropanol can be used as an alternative fuel to methanol and ethanol due to its high volumetric power density. However, only one example has been described using PdCu alloys as catalysts. Atanassov and co-workers[283] introduced the palladium–copper catalysts by sacrificial support method (SSM) in combination with a chemical reduction method. The sacrificial support method is based on the implementation of silica or alumina materials instead of conventional carbon supports (Figure 17). They prepared three atomic ratio of PdCu including 1:3, 1:1 and 3:1 by chemical reduction ($NaBH_4$) of Pd(II) and Cu(II) nitrates to provide highly dispersed NPs with high surface area. They

were characterized by XRD, SEM, TEM and BET analyses. The surface area of all materials was around 50 $m^2 g^{-1}$. SEM images showed well developed 3D porous structure and TEM images well distributed nanoparticles. The best catalyst Pd_3Cu exhibited the highest mass activity and was more tolerant to acetone compared to PdNi.[284]

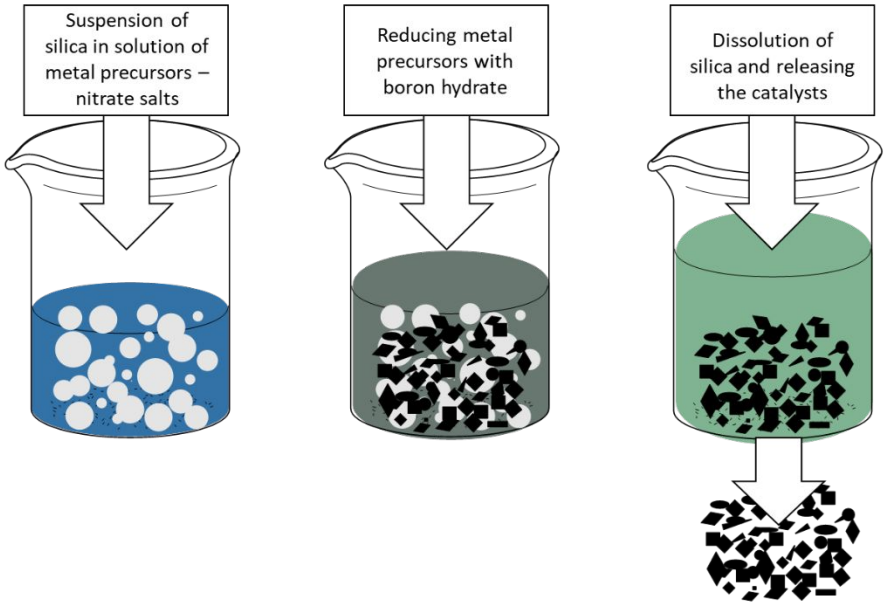

Figure 17 Schematic representation of PdCu BNPs by a sacrificial support method.

6.1.3. Electrochemical oxidation of polyalcohols

Three polyalcohols have been the focus of recent work, ethylene glycol, propylene glycol and glycerol. All of them can be obtained from renewable sources, ethylene and propylene glycols from cellulosic feedstock and glycerin is a byproduct of biodiesel production. However, they produce less power density in DAAFCs than the other alcohols and therefore more efficient catalysts than Pd should be developed.

Arriaga and co-workers[285] prepared PdCu@C (Vulcan XC-72) by a previously described chemical method using ethylene glycol as reaction medium, PVP as surfactant and $NaBH_4$ as reducing agent.[286] This material is formed by semi-spherical BNPs with a particle distribution around 6 nm and with a mass composition of 92% of Pd and 8% of Cu. Its electrocatalytic activity was evaluated by cyclic voltammetry experiments towards ethylene glycol and glycerin oxidation in 0.3M KOH as electrolyte. This catalyst showed superior performance compared to commercial Pd, maintaining 3- and 2-fold higher current density.

Other carbon-supported catalyst $Pd_{87}Cu_{13}$@C, previously used in EOR,[274] was also used by Haan and co-workers[287] for the electrochemical oxidation of ethylene and propylene glycols. This catalyst showed electrochemical oxidation rates 4 times higher than Pd@C and 3 times higher for glycerin. Indeed, the combination of the bifunctional and electronic effects led to enhancement in oxidation rate. The maximum power densities of glycerin and ethylene glycol fuel cells increased by 75% and 32%, respectively. However, oxidation rates of polyalcohols were weaker than the monoalcohols such as ethanol. The same group[288] synthesized PdCu@C catalysts with

different compositions such as $Pd_{63}Cu_{37}$@C, $Pd_{46}Cu_{54}$@C, $Pd_{28}Cu_{72}$@C and $Pd_{11}Cu_{89}$@C and compared with Pd@C in the electrochemical oxidation of polyols. The greatest activity for ethylene glycol oxidation was observed on $Pd_{28}Cu_{72}$@C, 7 times faster than Pd@C. For propylene glycol, $Pd_{11}Cu_{89}$@C was 12 times faster, and for glycerin $Pd_{63}Cu_{37}$@C was 14 times faster than Pd@C.

6.2. Formic acid oxidation

Formic acid has been used as an alternative fuel source in polymer electrolyte membrane (PEM)-based fuel cells, which are referred to as direct formic acid fule cells (DFAFCs). In comparison with DAFCs, some advantages of formic acid oxidation reaction (FAOR) over MOR and EOR include decrease crossover effects through the proton exchange membrane and also increase eletrooxidation rates, low toxicity and low-temperature operation. However, DFAFCs exhibit low volumetric energy density.[173] The mechanism involved in FAOR occurs via a direct oxidation (eq 1) or by an indirect pathway (eq 2) (Scheme 27).

$$HCO_2H \longrightarrow CO_2 + 2H^+ + 2e^- \quad (1)$$

$$HCO_2H \longrightarrow CO_{ads} + H_2O \longrightarrow CO_2 + 2H^+ + 2e^- \quad (2)$$

Scheme 27 Mechanisms proposed for the electro-oxidation of formic acid.

Palladium-based catalysts have superior performance than Pt catalysts but exhibit significant decay subsequent to discharging for several hours. Dai and Zou[287] reported that PdCu BNPs, formed through a galvanic replacement process, enhanced FAOR. They showed much higher FAOR activities than pure Pd and are much more resistant to the surface CO poisoning. This behavior has been attributed by the formation of more active sites by dissolution of Cu from the particle surfaces. Layered PdCu BNPs, prepared by a vapor deposition method, with different thickness of Pd supported on glassy carbon have been used in FAOR by Hu, Scudiero, Ha and co-workers.[290-292] By XPS a charge transfer from Pd to Cu produces a positive binding energy shift for the overlayer Pd 3d and an opposite shift for Cu 2p. This electronic perturbation of the PdCu material produces a drastic increase in current density and an improved stability for FAOR.

Carbon-supported PdCu catalysts with different compositions have been applied by Lu and co-workers[293] for FAOR. Among all catalysts Pd_3Cu@C gave the best electrocatalytic performance. On the other hand, Pd_3Cu@C, used by Haan and co-workers[274] for EOR, has been showed high activity towards FAOR than monometallic Pd@C.

Xu, Qiu and co-workers[294] have reported the preparation of nanoporous PdCu alloys by selective dealloying of PdCuAl alloys in an alkaline solution.[295] These materials were synthesized with different Pd/Cu compositions, 1:1 and 3:7 with a ligament size of 6 nm and 15 nm, respectively. The presence of Cu enhances the activity and stability of these nanoporous materials towards FAOR specially Pd/Cu with a 1:1 ratio. When the Cu contents is lower than 50%, FAOR occurs mainly through the direct pathway (Scheme 27, eq 1) and when the contents reaches 70% the CO pathway increases (Scheme 27, eq 2).

As mentioned in Sections 6.1.1 and 6.1.2, Wang and co-workers[270] concluded that PdCuSn@MWCNTs was the best catalyst compared to bimetallic PdCu@MWCNTs and

PdSn@MWCNTs for MOR and EOR. They also reported that specially for ethanol and formic acid oxidation the promotion effect of Sn is very important. The excellent activity of this trimetallic catalyst was attributed to the bifunctional and electronic mechanism of action based upon the depletion of surface Cu atoms as well as widely-embedded PdSn(0) nanoclusters on the surface. The adsorption of oxygen or hydroxyl radicals on Sn sites adjacent to the reacting species enhances the oxidation reaction of either the fuel or the poisoning intermediate.

Wan and co-workers[296] have described PdCu BNPs prepared by potentiostatic electrodeposition from a mixture electrolyte formed by H_2PdCl_4 and $CuSO_4$. This material was used to fabricate a glass carbon electrode (GCE) PdCu@GCE, which exhibited higher activity towards FAOR than Pd@GCE. They concluded that increasing the Cu contents the formic acid oxidation peak decreases.

A facile synthesis of PdCu tripods with purity higher than 90% was carried out by adding $CuCl_2$ and KBr to Na_2PdCl_4 in aqueous medium by Xia and co-workers.[297] The bromide ions could strongly bind to the three (100) side faces of a triangular seed forcing the Pd atoms to grow from the three corners of a seed to generate a tripod. When compared with commercial Pd black, this PdCu tripòds showed enhanced activity (almost eight folds) towards the FAOR.

Carbon-supported Au-decorated PdCu NPS have been reported as catalyst towards FAOR by Zhang and co-workers.[298] This material was prepared by a two-step process, firstly the PdCu alloy was synthesized by co-reduction of Pd and Cu ions in ethylene glycol using sodium citrate as reducing and stabilizing agent. Gold was decorated on the surface of the PdCu alloy through spontaneous replacement of Pd and Cu by Au. This PdCu@Au-C exhibited higher activity than PdCu@C and Pd@C. Nanostructured PdCu alloy decorated Cu nanotubes (NTs) have been described by Gao, Cheng and co-workers.[299] This new catalyst PdCu@CuNTs showed also improved activity and durability towards FAOR compared with PdCu@C and Pd@C.

Hosseni and co-workers[300] performed an efficient FAOR using PdCu supported on porous poly(2-methoxyaniline) film, prepared in the presence of sodium docecyl sulfate (P2MA-SDS). In this case, the PdCu alloy was synthesized trough a galvanic replacement reaction between Pd(II) ions and Cu particles.

Bimetallic PdCu multipods have been described by Yang and co-workers[301] towards FAOR and ORR. They prepared these multipods mainly consisting of tripods, tetrapods, pentapos and hexapods by synthesizing first Cu NPs as sacrificial templates. Then, galvanic replacement reaction between Pd^{2+} ions and Cu NPs together with the reduction of the generated Cu^{2+} ions by oleylamine took place.These multipod structure contains abundant active edges/corner atoms showing a remarkable improvementof the electrocatalytic performance not only for FAOR but also for ORR compared with PdCu alloy nanospheres and commercial Pd@C catalysts. Recently, Yazdan-Abad, Noroozifar and co-workers[302] reported a PdCu@RGO modified electrode towards FAOR. They used also a galvanic reduction method for the preparation of PdCu alloy by Zn/2% HCl. Electrochemical measurements revealed that the catalytic current density of this catalyst was 4.7 fold higher than commercial Pd@C.

6.3. Other oxidation reactions

Formaldehyde oxidation has been studied mainly to understand methanol oxidation because it is produced by its partial oxidation. Due to its toxicity formaldehyde is not suitable for fuel cells. However, formaldehyde oxidation is used in electroless copper plating and textile industry. Raoof, Aghajani and co-workers[303] have prepared bimetallic PdCu particles deposited at the surface of carbon nanotube paste electrodebypartial galvanic replacement process for the oxidation of formaldehyde in 0.1M NaOH solution. The same group[304] have described the same oxidation in 0.5M H_2SO_4 using spherical bimetallic PdCu BNPs deposited on poly(2-methoxyaniline) film modified electrochemically pretreated carbon paste electrode.

Wang and co-workers[275] applied PdCu nanocrystals with different compositions and controlled sizes in the EOR (Section 6.1.2) and styrene epoxidation. Styrene oxide is being applied extensively in the synthesis of fine chemicals and pharmaceuticals and industrial important organic intermediates. Generally, in the styrene epoxidation process, three products are obtained in which styrene oxide is main product and benzaldehyde and benzoic acid are produced as byproducts. This material was prepared in an octadecylamine with different compositions ($Pd_{0.2}Cu_{0.8}$, $Pd_{0.3}Cu_{0.7}$, $Pd_{0.5}Cu_{0.5}$, $Pd_{0.7}Cu_{0.3}$ and $Pd_{0.8}Cu_{0.2}$) and controlled sizes (5.2 nm, 6.8 nm, 8.1 nm, 16.4 nm). The $Pd_{0.3}Cu_{0.7}$ catalyst with 16.4 nm size demonstrated the best activity with a significant increasing in both styrene conversion (75%) and styrene oxide selectivity (70%) during 8 h better than other PdCu NCs with other Cu/Pd molar ratios. Indeed, the styrene conversion increased continually by increasing the reaction time and could attain as high as 93% for 16 h. The selectivity to styrene oxide enhanced from 51% to 70%.

7. Oxygen-assisted water gas shift reaction

The development of catalysts for water gas shift (WGS) reaction is an important issue for hydrogen production as a future fuel.[173] The presence of CO in the feed gas causes irreversible poisoning of the catalyst in the electrode and consequently the WGS reaction (Scheme 28) contributes to CO clean-up. Sekizawa and co-workers[305,306] reported that the addition of less than 1 mol% of oxygen enhances the removal of trace CO from reformed fuels without consuming significant amount of hydrogen. This oxygen-assisted water gas shift (OWGS) reaction (Scheme 28) has been efficiently performed using high surface area ceria-supported PdCu bimetallic catalysts by Song and co-workers.[307] They prepared PdCu@CeO_2 with different compositions and found out that the catalyst containing 1 wt% Pd and 30 wt% Cu exhibited a maximum CO conversion, close to 100%. Results indicated that Pd and Cu loaded by incipient wetness impregnation revealed better catalytic performance than that prepared by the deposition-precipitation method. A direct relation between BET surface area of ceria support and CO conversion was also observed. The nanocrystalline ceria was synthesized by the urea gelation method.

$$CO + H_2O \longrightarrow CO_2 + H_2 \quad \textbf{WGS reaction}$$

$$(1+x)\,CO + H_2O + x/2\,O_2 \longrightarrow (1+x)\,CO_2 + H_2 \quad \textbf{OWGS reaction}$$

Scheme 28 WGS and OWGS reactions.

The same group studied the catalytic activity of this PdCu@CeO_2 in comparison to Pd@CeO_2 and Cu@CeO_2 in the OWGS reaction under hydrogen rich conditions.[308] A higher activity and stability of the bimetallic catalyst was attributed to the existence of a synergistic interaction between Pd and Cu in the ceria support. Extended X-ray absorption fine structure (EXAFS) analysis indicated that a PdCu alloy was formed at the Pd edge, which explained the stability and durability over the monometallic counterparts. EXAFS, TPR and XPS analyses suggested that Pd addition helps to keep the Cu in reduced state improving the catalystic activity. In a subsequent study, the effect of oxygen addition to WGS reaction at various temperatures and contact time was studied.[309] Small amounts of oxygen enhanced WGS reaction on PdCu@CeO_2 and PtCu@CeO_2 catalysts at 200 to 300 ºC during short contact time (less than 10 min) where unreacted oxygen exists. It was proposed that the addition of oxygen partially oxidizes chemisorbed CO leading to vacant sites for H_2O adsorption and reaction. TPR and oxygen storage capacity (OSC) measurements revealed strong interactions between Cu and Pd or Pt, which makes the bimetallic catalysts less pyrophoric than nanometallic Cu catalyst. This is due to the high dispersion of the noble metals in Cu. The presence of Cu in PdCu@CeO_2 facilitates CO_2 desorption decreasing the carbonatation of the ceria surface. The role of the metal components in PdCu@CeO_2 and PtCu@CeO_2 catalysts for OWGS was also analyzed.[310] Among the monometallic, bimetallic and trimetallic catalysts examined, the PdCu combination showed uniquely high activity in OWGS and the suitable composition was 2 wt% Pd and 5-10 wt% Cu. The higher activity of PdCu@CeO_2 was probably due to the synergistic interaction between Pd and Cu evidenced by TPR, OSC and EXAFS. According to EXAFS analysis, bimetallic PdCu and PtCu form alloy BNPs where the noble metal is surrounded by Cu atoms. OSC meausrements point to higher resistance of PdCu to oxidation showing that Pd keeped Cu in reduced state in air pulse conditions. Form kinetic studies, Pd was found to promote CO shift, rather than CO oxidation by increasing the number of active sites and by suppressing hydrogen activation. Transitient response technique showed that Cu enhanced desorption of strongly chemisorbed CO_2 on the catalyst surface in contrast to very slow desorption from the surface of monometallic Pd. The excellent OWGS activity of PdCu@CeO_2 can be due to the complementary role of the two metals.

The role of the solid supports CeO_2 and Al_2O_3 in OWGS reaction was also investigated by Song group.[311] Better performance of CeO_2 than Al_2O_3 as well as enhancement of WGS upon oxygen addition were observed. Kinetic studies revealed that ceria can readily activate H_2O upon oxygen addition to OWGS reaction. FTIR spectra indicated that surface species in CO atmosphere were contrasted between alumina and ceria-supported catalysts, which suggested strong interaction at metal-ceria interface. Ceria properties influence both dispersion of PdCu species and reducibility (metal-support interaction) to control H_2O activation.

8. Sensors

Transition metals are employed in sensing electrodes for oxidation or reduction of a target molecule. Palladium has been used in the detection of hydrogen as well as hydrocarbons and volative organic conpounds.[173]

For security reasons, the use of hydrogen fuel requires reliable hydrogen sensing devices such as conductometric hydrogen sensors based on the change of electric

conductivity upon exposure to hydrogen gas. Ayesh[312] reported hydrogen gas sensors based on bimetallic PdCu nanoclusters. These materials were prepared by sputtering and inert gas condensations inside an ultrahigh vacuum compatible system. This method enabled the self-assembly of nanoclusters on SiO_2/Si substrates with preformed electrical electrodes. These sensors were sensitive at low hydrogen concentrations, work at room temperature with high sensitivity, capable of detecting concentrations of hydrogen as low as 0.5% in air and exhibit short response time much greater than conventional sensors.

Singh and co-workers[313] have developed bimetallic PdCu nanostructures by a sequential synthesis technique with trisodium citrate as a complexing agent and PVP as a protecting agent giving nanorods with around 3 nm diameter (Scheme 29). These nanorods showed improving sensitivity for liquefied petroleum gas (LPG). They prepared films, via a spin-coating method, which sensitivity and sensor response towards LPG are better in comparison to humidity and highly sensitive at room temperature.

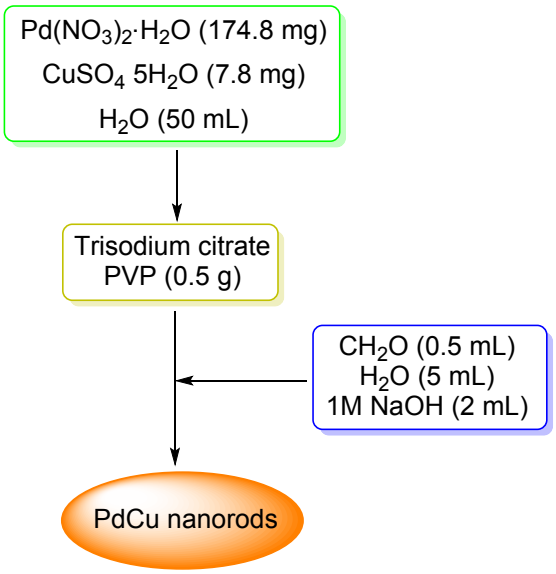

Scheme 29 Sequential technique for the synthesis of PdCu nanorods.

Nanoporous silica-based support SBA-16, prepared from tetraethoxysilane and a ternary combination of surfactants, has been used to fabricate PdCu@SBA-16 by Azizi and co-workers.[314] The corresponding electrochemical sensor was prepared using the galvanic replacement method to provide a highly sensitive sensor for formaldehyde determination by oxidation in alkaline solution. The nanoporosity of the support favoured the formation of PdCu BNPs and more active sites for formaldehyde oxidation. The electrochemical performance of this sensor was very efficient including wide linear range, low detection limit, rapis response and high sensitivity and selectivity for formaldehyde determination.

Glucose sensing is required for the controlled monitoring of glucose levels specially in blood. Bimetallic-based catalysts have been developed to enhance the sensitivity and selectivity of sensors and as alternative to glucose oxydases biosensors.[173] Liu and co-workers[315] described PdCu BNPs decorated three-dimensional graphene hydrogel (PdCu@GE) for non-enzymatic amperometric glucose sensors. For the preparation, Pd(II) and Cu(II) salts, with different mass ratios, glutamate, graphene oxide and ethylene glycol were mixed and the resulting aqueous dispersion was sealed on an autoclave and

heated at 100 ºC for 3 h. The PdCu BNPs were dispersed and encapsulated within the GE layers. This material showed significant electrocatalytic activity towards glucose oxidation in alkaline solution containing chloride ions compared to the monometallic Pd@GE. In addition, the PdCu@GE modified electrode exhibited resistance against poisoning by commonly interfering species such as dopamine, ascorbic acid, uric acid, 4-acetamidophenol and some monosaccharides.

Coral-structurated bimetallic PdCu nanozyme has been reported by Niu, Lan, Zhang and co-workers.[316] This material exhibited enhanced peroxidase activity and efficiency. It was prepared by a microwave-assisted wet-chemical method composed of assembled PdCu branches and showed better ability than Pd to catalyze the reaction of colorless tetramethylbenzidine to its blue oxide in the presence of H_2O_2. It was further found that thiocyanate could exhibit the color reaction by decreasing their activity of PdCu selectivity. On the basis of this principle, thiocyanate anion could be detected in the range of 0.001 to 100 μM.

Biosensors based on enzymes exhibit highly sensitive performance. However, these systems have some drawbacks including complex enzyme immobilization and stabilization, easy activity degradation and high cost.[173] For these reasons, Pd-based nanomaterials have been selected for the modification of biosensor electrodes. Phenolic compounds are widespread contaminant compounds due to theis toxicity and possible accumulation in the environment. A phenol sensor based on laccase immobilized on reduced graphene oxide supported PdCu nanocages has been prepared by Wang and co-workers.[317] This material PdCu@RGO was synthesized by a one-pot solvothermal method and used as electrode material for laccase. The biosensor allowed rapid detection of catechol with high selectivity, low detection time, good reproducibility and high anti-interference ability.

9. Other applications

During the last decades several catalysts based on transition metals have been developed for alkynes hydrosilylation to provide vinylsilanes, which are valuable building blocks.[318] Cai and co-workers[319] reported an efficient, recyclable $PdCu_2@SiO_2$ catalyst for the regio-and steroselective *syn*-hydrosilylation of terminal and internal alkynes. The reaction was carried out with triethylsilane using 0.4 mol% of catalyst loading, 1 equiv of NaI and THF as solvent at room temperature giving the corresponding silane in good yield and dr (Scheme 30). Comparative studies with pure Pd or Ni and bimetallic catalysts (PdCu, PdNi) with different compositions revealed that $PdCu_2@SiO_2$ showed the best activity and selectivity. In addition, this catalyst can be reused at least during 5 cycles. The enhanced catalytic activity may be originated from the ultrasound size and homogeneous distribution of the supported BNPs.

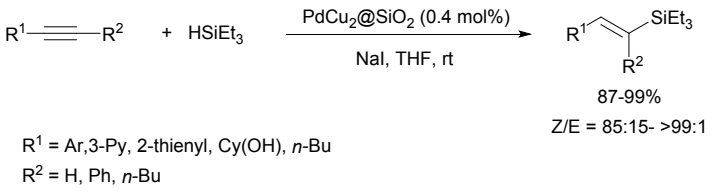

Scheme 30 Hydrosilylation of alkynes catalyzed by $PdCu_2@SiO_2$.

In addition to chemical and electrochemical applications PdCu BNPs have shown antimicrobial activity. Jaiswall and co-workers[320] prepared a series of PdCu bimetallic nanostructure-based nanofluids with the aim of investigating their antimicrobial activity. They used different molar ratios such as 20:1, 1:1 and 1:20 following a similar method described in Scheme 29.[313] Results of antimicrobial activity revealed that the prepared nanofluids possessed a good antibacterial and antimicrobial activity.

Using the same methodology Ullah and co-workers[321] prepared monometallic Pd and Cu and bimetallic PdCu NPs. The bimetallic PdCu material showed the highest activity for the reduction of nitrophenol in the presence of $NaBH_4$. Concerning their physiological activity towards different microorganism strains, the PdCu BNPs showed the maximum antibacterial activities as compared to monometallic Cu and Pd NPs even higher than the standard drug offoxacin.

10. Conclusions

Synergic and cooperative interactions between Pd and Cu affords superior catalytic performance than monometallic catalysts, because of the reduction in size and increase surface area. In addition, using these types of bimetallic catalysts the noble metal loading can be reduced. Given the electronegativy of Pd (2.20) is higher than Cu (1.90) both electron-rich site and charge site exist on the catalyst surface explaining the excellent redox properties. Unsupported highly active PdCu BNPs can be prepared with different shape, size and structure, for instance nonocrystals can be prepared using long chain aliphatic amines as coordinating ligands, which allowed to control the co-reduction of Pd and Cu salts giving different morphologies as well as by galvanic replacement of Cu by Pd. Supported PdCu BNPs can be mainly prepared by sequential impregnation of by co-impregnation methods.

Synthetic applications as catalysts in C-C bond forming reactions has been mainly performed with PdCu nanowires, which allowed to perform the S-M reaction of arylboronic acids with aryl chlorides. For the S-H reaction supported PdCu@MgO-PVI composites and PdCu@GQD@Fe_3O_4 allowed the alkynylation with aryl chlorides with high recyclability. In the case of the H-M alkenylation reaction, PdCu@MMT-K10 is an excellent catalyst for the arylation of acrylates and styrenes with aryl iodides and bromides as well as of acrylates with anilines. For the Guerbert reaction of alcohols for producing fuels and chemicals, Pd_3Cu@HT is the catalyst of choice. In the case of the three-component A^3-coupling (aldehyde, amine and alkyne), PdCu nanowires showed high efficiencyand recyclability for the synthesis of propargylamines.

Among chemical reduction reactions, nitrates elimination for water purification has became an extremely important application of PdCu BNPs as catalysts. Several supported catalysts such as PdCu@Al_2O_3, PdCu@TiO_2-Al_2O_3, PdCu@C, PdCu@ZSM-15 and PdCu@hematite revealed efficiency under hydrogenation conditions, whereas the resin supported catalyst PdCu@WA30 has a remarkable activity allowing its simultaneous regeneration. Iron is an alternative reductant to hydrogen using PdCu@GR as catalyst. For hydrodechlorination hydrogenation reactions, PdCu BNPs supported on silica or hydrotalcite and active carbon are very efficient and selective catalysts. Hydrogenation of CO_2 to methanol can be performed with PdCu BNPs supported in silica or titania,

whereas to ethanol $Pd_2Cu@TiO_2$ has shown excellent selectivity. Semihydrogenation of alkynes to alkenes can be performed with $PdCu@Al_2O_3$ and with PdCu@CNTs with higher selectivity than Lindlar catalyst. Hydrogenation of 1,3-butadiene to purify butene has been selectively carried out with $PdCu@Mn_2O_3$ prepared by sol-immobilization. Selective hydrogenation of furfural to furfuryl alcohol can be achieved using $PdCu@SiO_2$ or PdCu@MgO as catalysts. Hydrogenolysis of glycerol to 1,2-propanediol has been accomplished with supported $PdCu@MgAl_2O$ or $PdCu@TiO_2$ as recyclable catalysts, whereas sorbitol was hydrogenated to ethylene glycol and propylene glycol under $PdCu@ZrO_2$ catalysis. Other hydrogenations such as levulinic acid to γ-valerolactone and succinic acid to γ-butyrolactone has been carried out with PdCu BNPs supported on zirconia and alumina, respectively. In the case of styrene oxide hydrogenation to 2-phenylethanol, PdCu encapsulated with polyurea in supercritical CO_2 has been employed. Nitroaromatics have been reduced to aromatic amines under hydrogenation conditions using PdCu BNPs stabilized by poly(*N*,*N*)-diethylacrylamide grafted poly(acrylonitrile-styrene) polymeric microspheres.

Electrocatalytic reductions can be accomplished with bimetallic PdCu catalysts with comparable and even better results than Pt@C. In the case of oxygen reduction reactions PdCu@C in alkaline media as well as unsupported PdCu nanocrystals and nanosponges and supported PdCu nanocrystals on graphene oxide nanosheets can be used as catalysts. Electrochemical reduction of CO_2 to CO has been mainly carried out with PdCu@C or graphene but the best catalytic activity has been found with spherical $Pd_{0.3}Cu_1$ BNPs. For electroreduction of CO_2 to ethanol PdCu BNPs dopped with a pyridine derivative gave high activity and recyclability. However, for methanol $Pd_{83}Cu_{17}$ aerogel is the best selective catalyst better than Cu. Transformation of CO_2 to hydrocarbons has been performed with concave rhombic dodecahedral $PdCu_3$ catalyst which favours the formation of methane. For CO_2 electroreduction to formate Pd NPs covered with Cu atomic layers has shown higher activity than Pd NPs. Several PdCu BNPs have revealed higher activity than Pt-based electrocatalysts for hydrogen generation from water splitting. This is the case of PdCu@Pd nanocubes as well as monodispersed $Pd_{71}Cu_{29}$@Cwith an averagesize about 4,7 nm. Cu metal covered by a PdCu deposit has been used as a cathode with higher activity than Pd for reductive dehalogenation of organic halides to the corresponding hydrocarbons. Reduction of aryl and alkyl chlorides has been successfully carried out with PdCu BNPs supported on glassy carbon.

Catalytic oxidation of CO by oxygen at low temperature, usually carried out with Wacker catalysts, has been performed efficiently with supported PdCu BNPs at ceria and alumina prepared avowing to start from $PdCl_2$ and $CuCl_2$ as precursors. In the case of the oxidation of benzylic alcohols to aromatic aldehydes $PdCu_5$@celite and TEMPO can be used as catalysts and PdCu BNPs in the presence of iodide ions for the oxidation of ethanol to acetaldehyde. Cyclopentanone can be prepared from cyclopentene by means of oxygen in the presence of 1 wt% of PdCu@C as catalyst. The oxidation of cyclohexane to cyclohexanone and cyclohexanol takes place with H_2O_2 using multipods $PdCu@TiO_2$ as catalyst. Vinyl acetate can be prepared from ethylene, acetic acid and oxygen under $PdCu@ZrO_2$ catalysis. Benzene can be transformed into phenolby using a mixture of hydrogen and oxygen with Cu supported on an aluminosilicate zeolite modified by Pd, PdCu@ZSM-5.

Electrocatalytic oxidation reaction of alcohols used for direct alkaline alcohol fuel cells can be accomplished with PdCu BNPs as an alternative to Pt@C catalyst. In the case of methanol, mainly supported PdCu materials on active carbon graphene oxide and vertically oriented reduced graphene oxide. For ethanol fuel cells, PdCu supported on carbon, multiwalled carbon nanotubes (MWCNTs) and reduced graphene oxide showed enhanced activity compare to Pt@C. Pd_3Cu BNPs on silica or alumina as sacrificial supports catalyzed the electrooxidation of isopropanol. For polyalcohols PdCu@C catalyzed the oxidation of glycerol and ethylene glycol fuel cells. For direct formic acid fuel cells PdCu BNPs supported on carbon or MWCNTs, but also PdCu tripods and multipods with catalytic current density higher than Pd@C. Formaldehyde oxidation has been efficiently carried out with PdCu nanoparticles deposited on the surface of carbon nanotube paste. For styrene epoxidation Pd_3Cu_7 nanocrystal gave the highest selectivity and conversion values.

Oxygen-assisted water gas shift reaction, used for hydrogen production, can be performed with supported PdCu BNPs on ceria with a composition of 2 wt% Pd and 5-10 wt% Cu.

Concerning applications of PdCu BNPs as sensors for low concentration of hydrogen, PdCu nanoclusters work at room temperature with high sensitivity and PdCu nanorods for liquefied petroleum gas. In the case of formaldehyde detection nanoporous silica-based support SBA-16 has been used to fabricate the PdCu@SBA-16 sensor. Glucose sensors based on PdCu BNPs decorated 3D graphene hydrogel showed significant electrocatalytic activity in alkaline solution containing chloride ions. For thiocyanate sensing, coral-structurated bimetallic PdCu material has been reported. A phenol biosensor based on laccase immobilized on reduced graphene oxide supported PdCu nanocages has shown rapid detection of catechol.

Other applications such as hydrosilylation of acetylene can be performed using $PdCu_2@SiO_2$ as catalyst to furnish regio- and seroselectively vinylsilanes. It has been also found that PdCu BNPs showed better antimicrobial activity than the monometallic Pd and Cu NPs.

Acknowledgements

The authors are grateful to Institute for Advanced Studies in Basic Sciences (IASBS) Research Council and Iran National Science Foundation (INSF-Grant number of 97021804) for support of this work. We also thank to the the Spanish Ministerio de Economía, Industria y Competitividad, Agencia Estatal de Investigación (AEI) and Fondo Europeo de Desarrollo Regional (FEDER, EU) (projects CTQ2016-76782-P, CTQ2016-81797-REDC, and CTQ2017-85093-P), the Generalitat Valenciana (PROMETEOII/ 2014/017) and the University of Alicante for financial support.

Abbreviations

AAS: Atomic absorption spectrometry
acac: Acetylacetonate
ads: Adsorbed

AES: Atomic emission spectroscopy
AR: Adsorption-reduction
ARF: Cationic microporous amberlite resin with formate as counteranion
AX: Alumina xerogel
BANs: Bimetallic alloy nanosponges
BET: Brunauer-Emmett-Teller surface area analysis
BINAM: 1,1'-Binaphthyl-2,2'-diamine
BNPs: Bimetallic nanoparticles
Bpy: 2,2'-Bipyridine
cat.: Catalyst
CNTs: Carbon nanotubes
CI: Co-impregnation
CO_2ER: CO_2 electrochemical reduction
CS: Chitosan
CV: Cyclic voltametry
CTAB: Cetyltrimethylammonium bromide
3D: Tridimensional
DAAFCs: Direct alkaline alcohol fuel cells
DABCO: 1,4-Diazabicyclo[2.2.2]octane
DAAFCs: Direct alkaline alcohol fuel cells
DAFCs: Direct alcohol fuel cells
DCPVP: Deposition of colloids stabilized with poly(vinylpyrrolidone
DEFCs: Direct ethanol fuel cells
DFAFCs: Direct formic acid fuel cells
DFT: Density functional theory
DIPEA: Diisopropylethylamine
DMA: *N*,*N*-Dimetylacetamide
DMFCs: Direct methanol fuel cells
DPU: Deposition-precipitation with urea
DRIFTS: Diffuse reflectance infrared Fourier transform spectra
DTBB: 4,4'-Di-*tert*-butylbiphenyl
EASA: Electroactive surface area
EDTA: Ethylenediaminetetracetic acid disodium salt
EDAX: Energy dispersed spectroscopy
EDX: Energy-dispersed X-ray
EnCat: Encapsulated catalyst
EOR: Ethanol oxidation reaction
EPMA: Electron probe microanalysis
EXAFS: Extended X-ray absorption fine structure
FAO: Formic acid oxidation
fcc: face-centered cubic
FE: Faradaic efficiency
FTIR: Fourier transformation infrared spectroscopy
GCE: Glass carbon electrode
GE: Graphene hydrogel
GQD: Graphene quantum dots
GR: Graphene

GRO: Graphene oxide
HAADF: High angle annular dark field
HAD: Hexadecylamine
HER: Hydrogen evolution reaction
HERFD: High-energy resolution fluorescence detection
H-M: Heck-Mizoroki
HRTEM: High-resolution transmission electron microscopy
HT: Hydrotalcite
ICP: Inductively coupled plasma
IE-R: Ion exchange-regenation
IPA: Isopropanol
lit.: Literature
LPG: Liquefied petroleum gas
LSV: Linear sweep voltammetry
ML: Monolayer
MMT: Montmorillonite
MOF: Metal organic framework
MOR: Methanol oxidation reaction
MS: Molecular sieves
MSI: Metal-support interaction
MW: Microwave
MWCNTs: Multiwalled carbon nanotubes
NCs: Nanocrystals
NHC: N-Heterocyclic carbene
NPs: Nanoparticles
NSs: Nanosponges
NTs: Nanotubes
NWs: Nanowires
NZVI: Nanoscale zerovalent iron
OAm: Oleylamine
ODA: Octadecylamine
ORR: Oxygen reduction reaction
OSC: Oxygen storage capacity
OWGS: Oxygen-assisted water gas shift
PAN: Polyacrylonitrile
P2MA: Poly(2-methoxyaniline)
PDEAm: Poly(*N*,*N*-diethylacrylamide)
PEMFCs: Polymer electrolyte membrane fuel cells
PS: Polystyrene
PVI: (Polyvinyl)imidazole
PVP: (Polyvinyl)pyrrolidone
PVPy: (Polyvinyl)pyridine
PXRD: Powder X-ray diffraction
PYD: 4-[3-Phenyl-2,2-bis(phenoxymethyl)propoxy]pyridine
R: Amberlite resin
RDS: Rate determining step
RIE-R: Reaction ion exchange-regeneration

SAA: Single atom alloy
SBET: Specific surface area
SC: Supercritical
SDS: Sodium dodecyl sulfate
S-DVB: Polystyrene divinyl benzene matrix
SEM: Scanning electron microscopy
SI: Sol immobilization
SIMS-Tof: Time of flight secondary ion mass spectrometry
S-H: Sonogashira-Hagihara
S-M: Suzuki-Miyaura
SNCs: Sphere like nanocrystals
SSITKA: Steady state isotopic transient kinetic analysis
STEM: Scanning transmission electron microscopy
STY: Space-time yields
TEM: Transmission electron microscopy
TEMPO: 2,2,6,6-Tetramethylpiperidine *N*-oxide
TOAF: Tetraoctylammonium formate
TOF: Turnover frecuency
TOP: Trioctylphosphine
TPD: Temperature-programmed desorption
TPR: Transient response technique
TSI: Two-step impregnation
UI: Ultrasonic irradiation
UPD: Underpotential deposition
VAM: Vinyl acetate monomer
Vp: Pore volume
VRGO: Vertically oriented reduced graphene oxide
WGS: Water gas shift
XAS: X-Ray absorption spectroscopy
XPS: X-Ray photoelectron spectroscopy
XRD: X-Ray diffraction

References

1 M. H. Pérez-Temprano, J. A. Casares and P. Espinet, *Chem. – Eur. J.*, 2012, **18**, 1864–1884.
2 W. Yu, M. D. Porosoff and J. G. Chen, *Chem. Rev.*, 2012, **112**, 5780–5817.
3 Z. Wei, S. Sun, Y. Li, A. K. Datye and Y. Wang, *Chem. Soc. Rev.*, 2012, **41**, 7994–8008.
4 M. Sankar, N. Dimitratos, P. J. Miedziak, P. P. Wells, C. J. Kielye and G. J. Hutchings, *Chem. Soc. Rev.*, 2012, **41**, 8099–8139.

5 J. Shi, *Chem. Rev.*, 2013, **113**, 2139–2181.
6 A. K. Singh and Q. Xu, *ChemCatChem*, 2013, **5**, 652–676.
7 A. Aijaz and Q. Xu, *J. Phys. Chem. Lett.*, 2014, **5**, 1400–1411.
8 N. Miyaura and A. Suzuki, *Chem. Rev.*, 1995, **95**, 2457–2483.
9 S. Kotha, K. Lahiri and D. Kashinath, *Tetrahedron*, 2002, **58**, 9633–9695.
10 R. Rossi, F. Bellina and M. Lessi, *Tetrahedron*, 2011, **67**, 6969–7025.
11 A. Fihri, M. Bouhara, B. Nekoueishahraki, J.-M. Basset and V. Polshettiwar, *Chem. Soc. Rev.*, 2011, **40**, 5181–5203.
12 A. Molnar, *Chem. Rev.*, 2011, **111**, 2251–2320.
13 C. C. C. J. Seechurn, M. O. Kitching, T. J. Colacot and V. Snieckus, *Angew. Chem., Int. Ed.*, 2012, **51**, 5062–5085.
14 H. Li, J. Seechurn and T. J. Colacot, *ACS Catal.*, 2012, **2**, 1147–1164.
15 I. Maluenda and O. Navarro, *Molecules*, 2015, **20**, 7528–7557.
16 M. B. Thathagar, J. Beckers and G. Rothenberg, *J. Am. Chem. Soc.*, 2002, **124**, 11858–11859.
17 M. B. Thathagar, J. Beckers and G. Rothenberg, *Adv. Synth. Catal.*, 2003, **347**, 979–985.
18 A. Fodor, Z. Hell and L. Pirault-Roy, *Appl. Catal. A*, 2014, **484**, 39–50.
19 A. Fodor, A. Magyar, D. Barczikai, L. Pirault-Roy and Z. Hell, *Catal. Lett*., 2015, **145**, 834–839.
20 A. Fodor, Z. Hell and L. Pirault-Roy, *Catal. Lett.*, 2016, **146**, 596–608.
21 M. Nasrollahzadeh, B. Jaleh and A. Ehsani, *New J. Chem.*, 2015, **39**, 1148–1153.
22 J.-J. Lv, Z.-J. Wang, J.-J. Feng, R. Qiu, A.-J. Wang and X. Xu, *Appl. Catal. A*, 2016, **522**, 188–193.
23 W. Xi, X. Chen, S. Xu, J. Cui and L. Wang, *Nano Res.*, 2016, **9**, 2912–2920.
24 A. Dhankhar, R. K. Rai, D. Tyagi, X. Yao and S. K. Singh, *ChemistrySelect*, 2016, **1**, 3223–3227.
25 K. Lamei, H. Eshghi, M. Bakavoli and S. Rostamnia, *Appl. Organomet. Chem.*, 2017, **31**, e3743.
26 K. Sonogashira, *J. Organomet. Chem.*, 2002, **653**, 46–49.
27 R. Chinchilla and C. Nájera, *Chem. Rev.*, 2007, **107**, 874–922.
28 R. Chinchilla and C. Nájera, *Chem. Soc. Rev.*, 2011, **40**, 5084–5121.
29 S. Chouzier, M. Gruber and L. Djakovitch, *J. Mol. Catal. A Chem.*, 2004, **212**, 43–52.
30 L. Djakovitch, H. Heise and K. Koehler, *J. Organomet. Chem.*, 1999, **584**, 16–26.
31 A. Corma, H. García and A. Primo, *J. Catal.*, 2006, **241**, 123–131.
32 L.-M. Tan, Z.-Y. Sem, W.-Y. Zhong, X. Liu, Hendra, W. L. Kwan and C.-L. Lee, *Org. Lett.*, 2013, **15**, 65–67.
33 C. Rossy, E. Fouquet and F.-X. Felpin, *Beilstein J. Org. Chem.*, 2013, **9**, 1426–1431.
34 C. Rossy, J. Majimel, M. Trégner Delapierre, E. Fouquet and F.-X. Felpin, *J. Organomet. Chem.*, 2014, **755**, 78–85.
35 D. Sengupta, J. Saha, G. De and B. Basu, *J. Mater. Chem. A*, 2014, **2**, 3986–3992.
36 W. Xu, H. Sun, B. Yu, G. Zhang and Z. Gao, *ACS Appl. Mater. Inter.*, 2014, **6**, 20261–20268.
37 M. Gholinejad, N. Jeddi and B. Pullithadathil, *Tetrahedron*, 2016, **72**, 2491–2500.
38 C. Evangelish, A. Balerna, R. Psaro, G. Fusini, A. Carpita and M. Benfatto, *ChemPhysChem*, 2017, **18**, 2151–2156.

39 M. Gholinejad, J. Ahmadi, C. Nájera, M. Seyedhamzed, F. Zareh and M. Kompany-Zarch, *ChemCatChem*, 2017, **9**, 1422–1449.
40 Q. Liu, M. Xu, J. Zhao, Z. Yang, C. Qi, M. Zeng, R. Xia, X. Cao and B. Wang, *Int. J. Biol. Macromol.*, 2018, **113**, 1308–1315.
41 M. Gholinejad, M. Bahrami, C. Nájera and B. Pullithadathil, *J. Catal.*, 2018, **363**, 81–91.
42 A. V. Rassolov, G. N. Baeva, I. S. Mashkovsky and A. Y. Stakheev, *Mendelev. Commun.*, 2018, **28**, 538–540.
43 R. F. Heck, *J. Am. Chem. Soc.*, 1968, **90**, 5518–5526.
44 T. Mizoroki, K. Mori and A. Ozaki, *Bull. Chem. Soc. Jpn.*, 1971, **44**, 581.
45 I. P. Beletskaya and A. V. Cheprakov, *Chem.Rev.*, 2000, **100**, 3009–3066.
46 K. Köhler, S. S. Prockl and W. Kleist, *Curr. Org. Chem.*, 2006, **10**, 1585–1601.
47 V. Polshettivar and A. Molnar, *Tetrahedron*, 2007, **63**, 6949–6978.
48 R. K. Ramchandani, B. S. Uphade, M. P. Vinod, R. D. Wakharkar, V. R. Choudhary and A. Sudalai, *Chem. Commun.*, 1997, 2071–2072.
49 C. Waterlot, D. Couturier and B. Rigo, *Tetrahedron Lett.*, 2000, **41**, 317–319.
50 F. Akiyama, H. Miyazaki, K. Kaneda and S. Teranishi, *J. Org. Chem.*, 1980, **45**, 2359–2361.
51 P. He, Y. Wang, X. Wang, F. Pei, H. Wang, L. Liu and L. Yi, *J. Power Sources*, 2011, **196**, 1042–1047.
52 F. Heshmatpour, R. Abazari and S. Balalaie, *Tetrahedron*, 2012, **68**, 3001-3011.
53 J. T. Kozlowski and R. J. Davis, *ACS Catal.*, 2013, **3**, 1588–1600.
54 K. A. Goulas, S. Sreekumar, Y. Song, P. Kharidehal, G. Gunbas, P. J. Dietrich, G. R. Johnson, Y. C. Wang, A. M. Grippo, L. C. Grabow, A. A. Gokhale and F. D. Toste, *J. Am. Chem. Soc.*, 2016, **138**, 6805–6812.
55 R. Saha, D. Arunprasath and G. Sekar, *J. Catal.*, 2019, **377**, 673–683.
56 Z. Qureshi, J. Y. Kim, T. Bruun, H. Lam and M. Lautens, *ACS Catal.*, 2016, **6**, 4946–4952.
57 V. A. Peshkov, O. P. Pereshivko and E. V. van der Eycken, *Chem. Soc. Rev.*, 2012, **41**, 3790–3807.
58 R. Yi, Z.-J. Wang, Z. Liang, M. Xiao, X. Xu and N. Li, *Appl. Organometal. Chem.*, 2019, e4917.
59 N. Barrabés and J. Sá, *Appl. Catal. B Environ.*, 2011, **104**, 1–5.
60 K. D. Vorlop and T. Tacke, *Chem. Ing. Tech.*, 1989, **61**, 836–837.
61 S. Horold, K. D. Vorlop, T. Tacke and M. Sell, *Catal. Today*, 1993, **17**, 21–30.
62 F. Gauthard, F. Epron and J. Barbier, *J. Catal.*, 2003, **220**, 182–191.
63 N. Barrabés, J. Just, A. Dafinov, F. Medina, J. L. G. Fierro, J. E. Sueiras, P. Salagre and Y. Cesteros, *Appl. Catal. B. Environ.*, 2006, **62**, 77–85.
64 O. S. G. P. Soares, J. J. M. Órfão and M. F. R. Pereira, *Appl. Catal. B Environ.*, 2009, **91**, 441–448.
65 O. S. G. P. Soares, J. J. M. Órfão and M. F. R. Pereira, *Ind. Eng. Chem. Res.*, 2010, **49**, 7183–7192.
66 F. Deganello, L. F. Liotta, A. Macaluso, A. M. Venezia and G. Deganello, *Appl. Catal. B Environ.*, 2000, **24**, 265–273.
67 J. Batista, A. Pintar and M. Ceh, *Catal. Lett.*, 1997, **43**, 79–84.
68 J. Batista, A. Pintar, J. P. Gomilsek, A. Kodre and F. Bornette, *Appl. Catal. A Gen.*, 2001, **217**, 55–68.

69 J. Batista, A. Pintar, D. Mandrino, M. Jenko and V. Martin, *Appl. Catal. A Gen.*, 2001, **206**, 113–124.
70 A. Pintar, J. Batista and J. Levec, *Chem. Eng. Sci.*, 2001, **56**, 1551–1559.
71 W. Gao, N. Guan, J. Chen, X. Guan, R. Jin, H. Zheng, Z. Liu and F. Zhang, *Appl. Catal. B Environ.*, 2003, **46**, 341–351.
72 F. Zhang, S. Miao, Y. Yang, X. Zhang, J. Chen and N. Guan, *J. Phis. Chem. C*, 2008, **112**, 7665–7671.
73 W. Gao, J. Chen, X. Guan, R. Jin, F. Zhang and N. Guan, *Catal. Today*, 2004, **93-95**, 333–339.
74 N. Wehbe, M. Jaafar, C. Guillard, J. M. Herrmann, S. Miachon, E. Puzenat and N. Guilhaume, *Appl. Catal. A Gen.*, 2009, **368**, 1–8.
75 G. Strukul, R. Gavagnin, F. Pinna, E. Modaferri, S. Perathoner, G. Centi, M. Marella and M. Tomaselli, *Catal. Today*, 2000, **55**, 139–149.
76 M. P. Maia, M. A. Rodriguz and F. B. Passos, *Catal. Today*, 2007, **123**, 171–176.
77 L. Lemaignen, C. Tong, V. Begon, R. Burch and D. Chadwick, *Catal. Today*, 2002, **75**, 43–48.
78 U. Matatov-Meytal and M. Sheintuch, *Catal. Commun.*, 2009, **10**, 1137–1141.
79 Y. Yoshinaga, T. Akita, I. Mikami and T. Okuhara, *J. Catal.*, 2002, **207**, 37–45.
80 O. S. G. P. Soares, J. J. M. Órfão and M. F. R. Pereira, *Catal. Lett.*, 2010, **139**, 97–104.
81 C. Pfaff, L. Melo and P. Betancourt, *React. Kinet. Catal. Lett.*, 2002, **77**, 263–266.
82 K. Nakamura, Y. Yoshida, I. Mikami and T. Okuhara, *Chem. Lett.*, 2005, **34**, 678–679.
83 K. Nakamura, Y. Yoshida, I. Mikami and T. Okuhara, *Appl. Catal. B Environ.*, 2006, **65**, 31–36.
84 A. E. Palomares, J. G. Prato, F. Marquez and A. Corma, *Appl. Catal. B Environ.*, 2003, **46**, 3–13.
85 A. E. Palomares, J. G. Prato, F. Rey and A. Corma, *J. Catal.*, 2004, **221**, 62–66.
86 Y. Wang, J. H. Qu, H. J. Liu, *J. Mol. Catal. A Chem.*, 2007, **272**, 31–37.
87 D. Gasparovicova, M. Kralik, M. Hronec, A. Biffis, M. Zecca and B. Corain, *J. Mol. Catal. A Chem.*, 2006, **244**, 258–266.
88 D. Gasparovicova, M. Kralik and M. Hronec, *Collect. Czech. Chem. C*, 1999, **64**, 502–514.
89 U. Matatov-Meytal and M. Sheintuch, *Catal. Today*, 2005, **102**, 121–127.
90 Y. Wang, T. Kasuga, I. Mikami and T. Okuhara, *Chem. Lett.*, 2007, **36**, 994–995.
91 J. Sá, N. Barrabés, E. Kleymenov, C. Lin, K. Föttinger, O. V. Safonova, J. Szlachetko, J. A. van Bokhoven, M. Nachtegaal, A. Urakawa, G. A. Crespo and G. Rupprechter, *Catal. Sci. Technol.*, 2012, **2**, 794–799.
92 C. P. Theologides, G. G. Olympiou, P. G. Savva, K. Kapnisis, A. Anayiotos and C. N. Costa, *Appl. Catal. B Environ.*, 2017, **205**, 443–454.
93 K. Wada, T. Hirata, S. Hosokawa, S. Iwamoto and M. Inoue, *Catal. Today*, 2012, **185**, 81–87.
94 H. Kadowaki and Y. Meguro, *J. Nucl. Sci. Technol.*, 2012, **49**, 881–887.
95 M. Al Bahri, L. Calvo, M. A. Gilarranz, J. J. Rodriguez and F. Epron, *Appl. Catal. B Environ.*, 2013, **138-139**, 143–148.
96 T. Ye, D. P. Durkin, N. A. Banek, M. J. Wagner and D. Shuai, *ACS Appl. Mater. Interf.*, 2017, **9**, 27421–27426.
97 W. Gao and F. Li, *Adv. Mater. Res.*, 2011, **197-198**, 967–971.

98 J. Jung, S. Bae and W. Lee, *Appl. Catal. B Environ.*, 2012, **127**, 148–158.
99 S. Jung, S. Bae and W. Lee, *Environ. Sci. Technol.*, 2014, **48**, 9651–9658.
100 S. Hamid, S. Bae, W. Lee, M. T. Amin and A. A. Alazba, *Ing. Eng. Chem. Res.*, 2015, **54**, 6247–6257.
101 Y. Yun, Z. Li, Y.-H. Chen, M. Saino, S. Cheng and L. Zheng, *Water Air Soil Pollut.*, 2016, **227**, 111.
102 Y. Yun, Z. Li, Y.-H. Chen, M. Saino, S. Cheng and L. Zheng, *Water Sci. Techn.*, 2016, **73**, 2697–2703.
103 G. Mendow, A. Sánchez, C. Grosso and C. A. Querini, *J. Envir. Chem. Engin.*, 2017, **5**, 1404–1414.
104 C. Bradu, C. Căpăt, F. Papa, L. Frunza, E.-A. Olaru, G. Crini, N. Morin-Crini, E. Euvrard, I. Balint, I. Zgură and C. Munteanu, *Appl. Catal. A Gen.*, 2019, **570**, 120–129.
105 F. Alonso, I. P. Beletskaya and M. Yus, *Chem. Rev.*, 2002, **102**, 4009–4091.
106 M. A. Keane, *ChemCatChem*, 2011, **3**, 800–821.
107 S. Lambert, B. Heinrichs, A. Brasseur, A. Rulmont and J.-P. Pirard, *Appl. Catal. A Gen.*, 2004, **270**, 201–208.
108 S. Lambert, F. Ferauche, A. Brasseur, J.-P. Pirard and B. Heinrichs, *Catal. Today*, 2005, **100**, 283–289.
109 A. Śrębowata, W. Lisowski, J. M. Sobczak and Z. Karpiński, *Catal. Today*, 2011, **175**, 576–584.
110 N. Barrabés, D. Cornado, K. Föttinger, A. Dafinov, J. Llorca, F. Medina and G. Rupprechter, *J. Catal.*, 2009, **263**, 239–246.
111 B. T. Meshesha, N. Barrabés, J. Llorca, A. Dafinov, F. Medina and K. Föttinger, *Appl. Catal. A Gen.*, 2013, **453**, 130–143.
112 M. Bonarowska, O. Machynskyy, D. Lomot, E. Kemnitz and Z. Karpiński, *Catal. Today*, 2014, **235**, 144–151.
113 Y. I. Yermakov, V. F. Surovikin, G. V. Plaksin, V. A. Semikolenov, V. A. Likholobov, A. L. Chuvilin and S. V. Bogdanov, *React. Kinet. Catal. Lett.*, 1987, **33**, 435–440.
114 R. Hina, I. Arafa and F. Al-Khateeb, *Prog. React. Kinet. Mech.*, 2016, **41**, 29–38.
115 M. Gregori, P. Benito, G. Fornasari, M. Migani, S. Millefanti, F. Ospitali and S. Albonetti, *Micropor. Mesopor. Mat.*, 2014, **190**, 1–9.
116 P. Benito, M. Gregori, S. Andreoli, G. Fornasari, S. Millefanti, F. Ospitali and S. Albonetti, *Catal. Today*, 2015, **246**, 108–115.
117 X. Fang, J. Zhao and D. Fang, *Desalin. Water Treat.*, 2018, **101**, 142.
118 W. Wang, S. Wang, X. Ma and J. Gong, *Chem. Soc. Rev.*, 2011, **40**, 3703–3727.
119 X. Jiang, N. Koizumi, X. Guo and C. Song, *Appl. Catal. B Environ.*, 2015, **170**, 173–183.
120 L. Liu, F. Fan, Z. Jiang, X. Gao, J. Wei and T. Fang, *J. Phys. Chem. C*, 2017, **121**, 26287–26299.
121 X. Jiang, X. Wang, X. Nie, N. Koizumi, X. Guo and C. Song, *Catal. Today*, 2018, **316**, 62–70.
122 X. Nie, X. Jiang, H. Wang, W. Luo, M. J. Janik, Y. Chen, X. Guo and C. Song, *ACS Catal.*, 2018, **8**, 4873–4892.
123 X. Jiang, Y. Jiao, C. Moran, X. Nie, Y. Gong, X. Guo, K. S. Walton and C. Song, *Catal. Commun.*, 2019, **118**, 10–14.
124 F. Lin, X. Jiang, N. Boreriboon, Z. Wang, C. Song and K. Cen, *Appl. Catal. A Gen.*, 2019, **585**, 117210.

125 X. Jiang, X. Nie, X. Wang, H. Wang, N. Koizumi, Y. Chen, X. Guo and C. Song, *J. Catal.*, 2019, **369**, 21–32.
126 P. Mierczynsky, R. Ciesielski, A. Kedziora, W. Maniukiewicz and T. P. Maniecki, *Catal. Ind.*, 2017, **9**, 99–103.
127 S. Bai, Q. Shao, P. Wang, Q. Dai, X. Wang and X. Huang, *J. Am. Chem. Soc.*, 2017, **139**, 6827–6830.
128 P. Mierczynski, R. Ciesielski, A. Kedziora, M. Zaborowski, W. Maniukiewicz, M. Nowosielska, M. I. Szynkowska and T. P. Maniecki, *Catal. Lett.*, 2014, **144**, 723–735.
129 P. Mierczynski, W. Maniukiewicz, M. Zaborowski, R. Ciesielski, A. Kedziora, and T. P. Maniecki, *Reac. Kinet. Mech. Cat.*, 2015, **114**, 211–228.
130 L. Guczi, Z. Schay, G. Stefler, L. F. Liotta, G. Deganello and A. M. Venezia, *J. Catal.*, 1999, **182**, 456–462.
131 M. P. R. Spee, J. Boersma, M. D. Meijer, G. van Koten and J. W. Geus, *J. Org. Chem.*, 2001, **66**, 1647–1656.
132 S. K. Kim, J. H. Lee, I. Y. Ahn, W.-J. Kim and S. H. Moon, *Appl. Catal. A Gen.*, 2011, **401**, 12–19.
133 G. Kyriakou, M. B. Boucher, A.D. Jewell, E. A. Lewis, A. E. Baber, H. L. Tierney, M. Flytzani-Stephanopoulos and E. C. H. Sykes, *Science*, 2012, **335**, 1209–1212.
134 Q. Fu and Y. Luo, *ACS Catal.*, 2013, **3**, 1245–1252.
135 M. B. Boucher, B. Zugic, G. Cladaras, J. Kammert, M. D. Marcinkowski, T. J. Lawton, E. C. H. Sykes and M. Flytzani-Stephanopoulos, *Phys. Chem. Chem.Phys.*, 2013, **15**, 12187–12196.
136 A. Murugadoss, E. Sorek and M. Asscher, *Top. Catal.*, 2014, **57**, 1007–1014.
137 P. V. Markov, G. O. Bragina, G. N. Baeva, O. P. Tkachenko, I. S. Mashkovsky, I. A. Yakushev, N. Y. Kozitsyna, M. N. Vargaftik and A. Y. Stakheev, *Kinet. Catal.*, 2015, **56**, 591–597.
138 A. J. McCue, A. M. Shepherd and J. A. Anderson, *Catal. Sci. Technol.*, 2015, **5**, 2880–2890.
139 X. Cao, A. Mirjalili, J. Wheeler, W. Xie and B. W.-L. Jang, *Front. Chem. Sci. Eng.*, 2015, **9**, 442–449.
140 P. V. Markov, G. O. Bragina, A. V. Rassolov, G. N. Baeva, I. S. Mashkovsky, V. Yu. Murzin, Y. V. Zubavichus and A. Y. Stakheev, *Mendeleev. Commun.*, 2016, **26**, 502–504.
141 I. S. Mashkovsky, P. V. Markov, G. O. Bragina, O. P. Tkachenko, I. A. Yakushev, N. Y. Kozitsyna, M. N. Vargaftik and A. Y. Stakheev, *Russ. Chem. Bull., Int. Ed.*, 2016, **65**, 425–431.
142 Z. Wang, L. Yang, R. Zhang, L. Li, Z. Cheng and Z. Zhou, *Catal. Today*, 2016, **264**, 37–43.
143 P. Insorn and B. Kitiyanan, *Catalysts*, 2016, **6**, 199.
144 Y. Lui, Y. He, D. Zhou, J. Feng and D. Li, *Catal. Sci. Technol.*, 2016, **6**, 3027–3037.
145 P. V. Markov, G. O. Bragina, G. N. Baeva, A. V. Rassolov, I. S. Mashkovsky and A. Y. Stakheev, *Kinet. Catal.*, 2018, **59**, 601–609.
146 R. Zhang, B. Zhao, L. Ling, A. Wang, C. K. Russell, B. Wang and M. Fan, *ChemCatChem*, 2018, **10**, 2424–2432.
147 E. Buxaderas, M. A. Volpe and G. Radivoy, *Synthesis*, 2019, **51**, 1466–1472.
148 T. R. Silva, D. C. de Oliveira, T. Pal and J. B. Domingos, *New J. Chem.*, 2019, **43**, 7083–7092.

149 D. A. Lomelí-Rosales, J. A. Delgado, M. Diaz de los Bernardos, S. Pérez-Rodríguez, A. Gual, C. Claver and C. Godard, *Chem.– Eur. J.*, 2019, **25**, 8321–8331.
150 R. Mélendrez, G. Del Angel, V. Bertin, M. A. Valenzuela and J. Barbier, *J. Mol. Catal. A Chem.*, 2000, **157**, 143–149.
151 L. Zhang, H. Su, M. Sun, Y. Wang, W. Wu, T. Yu and J. Zeng, *Nano Res.*, 2015, **8**, 2415–2430.
152 M. M. Pereira, F. B. Noronha and M. Schmal, *Catal. Today*, 1993, **16**, 407–415.
153 A. Cooper, B. Bachiller-Baeza, J. A. Anderson, I. Rodríguez-Ramos and A. Guerrero-Ruiz, *Catal. Sci. Technol.*, 2014, **4**, 1446–1455.
154 T. Odoom-Wubah, Q. Li, M. Chen, H. Fang, B. B. Asare Bediako, I. Adilov, J. Huang and Q. Li, *ACS Omega*, 2019, **4**, 1300–1310.
155 S. Sitthisa, T. Pham, T. Prasomsi, T. Sooknoi, R. G. Mallinson and D. E. Resasco, *J. Catal.*, 2011, **280**, 17–27.
156 M. Lesiak, M. Binczarski, S. Karski, W. Maniukiewicz, J. Rogowski, E. Szubiakiewicz, J. Berlowska, P. Dziugan and I. Witońska, *J. Mol. Catal. A Chem.*, 2014, **395**, 337–348.
157 K. Fulajtárova, T. Soták, H. Hronec, I. Vávra, E. Dobročka and M. Omastová, *Appl. Catal. A Gen.*, 2015, **502**, 78–85.
158 H. Hronec, K. Fulajtárova, I. Vávra, T. Soták, E. Dobročka and M. Mičušik, *Appl. Catal. B Environ.*, 2016, **181**, 210–219.
159 Q. Deng, X. Wen and P. Zhang, *Catal. Commun.*, 2019, **126**, 5–9.
160 P. Liu, W. Qiu, C. Zhang, Q. Tan, C. Zhang, W. Zhang, Y. Song, H. Wang and C. Liu, *ChemCatChem*, 2019, **11**, 3296–3306.
161 X. Chang, A.-F. Liu, B. Cai, J.-Y. Luo, H. Pan and Y.-B. Huang, *ChemSusChem*, 2016, **9**, 3330–3337.
162 S. Xia, Z. Yuan, L. Wang, P. Chen and Z. Hou, *Appl. Catal. A Gen.*, 2011, **403**, 173–182.
163 A. N. Ardila, M. A. Sánchez-Castillo, T. A. Zepeda, A. L. Villa and G. A. Fuentes, *Appl. Catal. B Environ.*, 2017, **219**, 658–671.
164 Y. Jia and H. Liu, *Chin. J. Catal.*, 2015, **36**, 1552–1559.
165 S. C. Patankar and G. D. Yadav, *ACS Sustain. Chem. Eng.*, 2015, **3**, 2619–2630.
166 S. C. Patankar, A. G. Sharma and G. D. Yadav, *Clean Technol. Envir.*, 2018, **20**, 683–693.
167 G. D. Yadav and Y. S. Lawate, *J. Supercrit. Fluids*, 2011, **59**, 78–86.
168 B.-S. Wan, S.-J. Liao, Y. Xu and D.-R. Yu, *React. Kinet. Catal. Lett.*, 1998, **63**, 397–401.
169 Y. Gao, F. Wang, S. Liao and D. Yu, *React. Kinet. Catal. Lett.*, 1998, **64**, 351–357.
170 S. Dongjian, S. Jing, D. Fang, C. Mingqing and H. Bingxiao, *React. Funct. Polym.*, 2013, **73**, 1015–1021.
171 S. Chen, S. V. Jenkins, J. Tao, Y. Zhu and J. Chen, *J. Phys. Chem. C,* 2013, **117**, 8924–8932.
172 K. Mallikarjuna and H. Kim, *Colloids Surfarce A*, 2017, **535**, 194–200.
173 A. Chen and C. Ostrom, *Chem. Rev*., 2015, **115**, 11999–12044.
174 W. Yu, M. D. Porosoff and J. G. Chen, *Chem. Rev*., 2012, **112**, 5780–5817.
175 D. C. Martínez-Casillas and O. Solorza-Feria, *ECS Trans.*, 2009, **20**, 275–280.
176 D. C. Martínez-Casillas, G. Vázquez-Huerta, J. F. Pérez-Robles and O. Solorza-Feria, *J. Power Sources*, 2011, **196**, 4468–4474.

177 N. N. Kariuki, X. Wang, J. R. Mawdsley, M. S. Ferrandon, S. G. Niyogi, J. T. Waugley and D. J. Myers, *Chem. Mater*., 2010, **22**, 4144–4152.
178 M. Shao, K. Shoemaker, A. Peles, K. Kaneko and L. Protsailo, *J. Am. Chem. Soc*., 2010, **132**, 9235–9255.
179 W. Tang, L. Zhang and G. Henkelman, *J. Phys. Chem. Lett.*, 2011, **2**, 1328–1331.
180 L. Zhang, F. Hou and Y. Tan, *Chem. Commun*., 2012, **48**, 7152–7154.
181 L. Xiong, Y.-X. Huang, X.-W. Liu, G.-P. Seng, W.-W. Li and H.-Q. Yu, *Electrochimica Acta*, 2013, **89**, 24–28.
182 X. Lu, M. Mckiernan, Z. Peng, E. P. Lee, H. Yang and Y. Yia, *Sci. Adv. Mater.*, 2010, **2**, 413–420.
183 Q. Gao, Y.-M. Ju, D. An, M.-R. Gao, C.-H. Cui, J.-W. Liu, H.-P, Cong and S.-H. Yu, *ChemSusChem*, 2013, **6**, 1878–1882.
184 Y. Sha, T. H. Yu, B. V. Merinov and W. A. Goddard III, *ACS Catal*., 2014, **4**, 1189–1197.
185 J.-J. Lv, S.-S. Li, A.-J. Wang, L.-P. Mei, J.-J. Feng, J.-R. Chen and Z. Chen, *J. Power Sources*, 2014, **269**, 104–110.
186 S. Guo, X. Zhang, W. Zhu, K. He, D. Su, A. Mendoza-Garcia, S. F. Ho, G. Lu and S. Sun, *J. Am. Chem. Soc*., 2014, **136**, 15026–15033.
187 L. An, M. Zhu, B. Dai and F. Yu, *Electrochimica Acta*, 2015, **176**, 222–229.
188 W.-P. Wu, A. P. Periasamy, G.-L. Lin, Z.-Y. Shihand H.-T. Chang, *J. Mater. Chem. A*, 2015, **3**, 9675–9681.
189 K. Jiang, P. Wang, S. Guo, X. Zhang, X. Shen, G. Lu, D. Su and X. Huang, *Angew. Chem., Int. Ed*., 2016, **55**, 9030–9035.
190 Y. Luo, L. A. Estudillo-Wong, L. Cavillo, G. Granozzi and N. Alonso-Vante, *J. Catal*., 2016, **338**, 135–142.
191 X. Peng, T. J. Omasta, J. M. Roller and W. E. Mustain, *Front. Energy*, 2017, **11**, 299–309.
192 G. Bampos, S. Bebelis, D. I. Kondarides and X. Verykios, *Top. Catal*., 2017, **60**, 1260–1273.
193 Y. Yang, C. Dai, D. Wu, Z. Liu and D. Cheng, *ChemElectroChem*, 2018, **5**, 2571–2575.
194 T. N. Huan, N. Ranjbar, G. Rousse, M. Sougrati, A. Zitolo, V. Mougel, F. Jaouen and M. Fontecave, *ACS Catal*., 2017, **7**, 1520–1525.
195 X. Min and M. W. Kanan, *J. Am. Chem. Soc*., 2015, **137**, 4701–4708.
196 Y. Chen, C. W. Li and M. W. Kanan, *J. Am. Chem. Soc*., 2012, **134**, 19969–19972.
197 W. Zhu, R. Michalsky, Ö. Metin, H. Lv, S. Guo, C. J. Wright, X. Sun, A. A. Peterson and S. Sun, *J. Am. Chem. Soc*., 2013, **135**, 16833–16836.
198 H. Mistry, P. Reske, Z. Zeng, Z.-J. Zhao, J. Greeley, P. Strasser and B. R. Cuenya, *J. Am. Chem. Soc*., 2014, **136**, 16473–16476.
199 M. Li, J. Wang, P. Li, K. Chang, C. Li, T. Wang, B. Jiang, H. Zhang, H. Liu, Y. Yamauchi, N. Umezawa and J. Ye, *J. Mater. Chem. A*, 2016, **4**, 4776–4782.
200 C. Li and Y. Yamauchi, *Chem. – Eur. J*., 2014, **20**, 729–733.
201 M. Li, P. Li, K. Chang, H. Liu, X. Hai, H. Zang and J. Ye, *Chem. Commun*., 2016, **52**, 8235–8238.
202 Z. Yin, D. Gao, S. Yao, B. Zhao, F. Cai, L. L. Liu, P. Tang, P. Zhai, G. Wang, D. Ma and X. Bao, *Nano Energy*, 2016, **27**, 35–43.
203 X. Liu, L. Zhu, H. Wang, G. Heand Z. Bian, *RSC Adv*., 2016, **6**, 38380–38387.

204 Z. Q. Zhang, J. Huang, L. Zhang, M. Sun, Y. C. Wang, Y. Lin and J. Zeng, *Nanotechnology*, 2014, **25**, 435602.
205 W. Zhu, L. Zhang, P. Yang, X. Chang, H. Dong, A. Li, C. Hu, Z. Huang, Z.-J. Zhao and J. Gong, *Small*, 2017, 1703314.
206 D. Chen, Q. Yao, P: Cui, H. Liu, J. Xie and J. Yang, *ACS Appl. Energy Mater*., 2018, **1**, 883−890.
207 H.-P. Yang, S. Qin, Y.-N. Yue, L. Liu, H. Wang and J.-X. Lu, *Cat. Sci. Technol*., 2016, **6**, 6490−6494.
208 L. Lu, X. Sun, J. Ma, D. Yang, H. Wu, B. Zhang, J. Zhang and B. Han, *Angew. Chem., Int. Ed*., 2018, **57**, 14149−14152.
209 X. Sun, L. Lu, Q. Zhu, C. Wu, D. Yang, C. Chen and B. Han, *Angew. Chem., Int. Ed*., 2018, **57**, 2427−2431.
210 A. Peterson and J. K. Nørskov, *J. Phys. Chem. Lett*., 2013, **3**, 251−258.
211 Y. Hori, H. Konishi, T. Futamura, A. Murata, O. Koga, H. Sakurai and K. Oguma, *Electrochimica Acta*, 2005, **50**, 5354−5369.
212 S. Zhang, P. Kang, M. Bakir, A. M. Lapides, C. J. Dares and T. J. Meyer, *PNAS*, 2015, **112**, 15809−15814.
213 R. Reske, H. Mistry, F. Behafard, B. Roldan Cuenya and P. Strasser, *J. Am. Chem. Soc*., 2014, **136**, 6978−6986.
214 S. Ma, M. Sadakiyo, M. Heima, R. Luo, R. T. Haasch, J. I. Gold, M. Yamauchi and P. J. A. Kenis, *J. Am. Chem. Soc*., 2017, **139**, 47−50.
215 T. Takashima, T. Suzuki and H. Irie, *Electrochimica Acta*, 2017, **229**, 415−421.
216 A. Kudo and Y. Miseki, *Chem. Soc. Rev*., 2009, **38**, 253−278.
217 R. Jana, A. Bhim, P. Bothra, S. K. Pati and S. C. Peter, *ChemSusChem*, 2016, **9**, 2922−2927.
218 J. Li, F. Li, S.-X. Guo, J. Zhang and J. Ma, *ACS Appl. Mater. Inter*., 2017, **9**, 8151−8160.
219 J. Li, P. Zhou, F. Li, J. Ma, Y. Liu, X. Zhang, H. Huo, J. Jin and J. Ma, *J. Power Sources*, 2016, **302**, 343−351.
220 X. Zhang, D. Wu and D. Cheng, *Electrochimica Acta*, 2017, **246**, 572−579.
221 F. Alonso, I. P. Beletskaya and M. Yus, *Chem. Rev*., 2002, **102**, 4009−4091.
222 J. Simonet, P. Poizot and L. Laffont, *J. Electroanal. Chem*., 2006, **591**, 19−26.
223 P. Poizot, L. Laffont-Dantras and J. Simonet, *Platinum Metals Rev*., 2008, **52**, 84−95.
224 V. Jouikov, P. Poizot and J. Simonet, *J. Electrochem. Soc*., 2009, **156**, E171−E178.
225 C. Durante, V. Perazzolo, A. A. Isse, M. Favaro, G. Granozzi and A. Gennaro, *ChemElectroChem*, 2014, **1**, 1370−1381.
226 K. I. Choi and M. A. Vannice, *J. Catal*., 1991, **127**, 489−511.
227 E. D. Park and J. S. Lee, *J. Catal*., 1998, **180**, 123−131.
228 J. S. Lee, E. D. Park and B. J. Song, *Catal. Today*, 1999, **54**, 57−64.
229 E. D. Park and J. S. Lee, *J. Catal*., 2000, **193**, 5−15.
230 L.Wang, Y. Zhou, Q. Liu, Y. Guo and G. Lu, *Catal. Today*, 2010, **153**, 184−188.
231 Y. Shen, G. Z. Lu, Y. Guo and Y. Wang, *Chem. Commun*., 2010, **46**, 8433−8435.
232 Y. Shen, Y. Guo, L. Wang, Y. Wang, X. Gong and G. Lu, *Catal. Sci. Technol*., 2011, **1**, 1202−1207.
233 Y. Shen, G. Lu, Y. Guo, Y. Wang, Y. Guo and X. Gong, *Catal. Today*, 2011, **175**, 558−567.
234 F. Wang, H. Zhang and D. He, *Environ. Technol*. 2014, **35**, 347−354.

235 X. Du, H.-Y. Li, J. Yu, X. Xiao, Z. Shi, D. Mao and G. Lu, *Catal. Sci. Technol*., 2015, **5**, 3970–3979.
236 F. Zhou, X. Du, J. Yu, D. Mao and G. Lu, *RSC Adv*., 2016, **6**, 66553–66563.
237 L. Wang, X. Lu, W. Wang, W. Zhan, Y. Guo and Y. Guo, *Chinese J. Catal*., 2018, **39**, 1560–1567.
238 L. P. Oleksenko, G. M. Telbiz, V. K. Yatsimirsky and I. V. Kurmich, *Adsorp. Sci. Technol*., 1999, **17**, 545–555.
239 A. B. Hungria, A. Iglesias-Juez, A. Martínez-Arias, M. Fernández-García, J. A. Anderson, J. C. Conesa and J. Soria, *J. Catal*., 2002, **206**, 281–294.
240 V. Abdelsayed, A. Aljarash, M. S. El-Shall, Z. A. Al Othman and A. H. Alghamdi, *Chem. Mater*., 2009, **21**, 2825–2834.
241 F. Wang and G. Lu, *Int. J. Hydrogen Energ*., 2010, **35**, 7253–7260.
242 P. Estiface, M. Haghighi, N. Mohammadi and F. Rahmani, *Ultrason. Sonochem*., 2014, **21**, 1155–1165.
243 Y. Wang, L. Fan, J. Shi, X. Li and Y. Zhao, *Catal. Lett*., 2015, **145**, 1429–1435.
244 Y. Wang, X. Li, T. Lv, R. Wu and Y. Zhao, *Reac. Kinet. Mech. Cat*., 2018, **124**, 203–216.
245 Y. Wang, J. Shi, R. Wu, X. Li and Y. Zhao, *Appl. Clay Sci*., 2015, **119**, 126–131.
246 Y. Wang, Y. Wang, X. Li, Z. Liu and Y. Zhao, *Environ. Technol*., 2018, **39**, 780–786.
247 S. Nikolaev, E. V. Golubina and M. J. Shilina, *Appl. Catal. B: Environ*., 2017, **208**, 116–127.
248 L. B. Di, D. Z. Duan, D.-W. Park, W.-S. Ahn, B.-J. Lee and X. L. Zhang, *Top. Catal.*, 2017, **60**, 925–933.
249 E. Buxaderas, M. Graziano-Mayer, M. A. Volpe and G. Radivoy, *Synthesis*, 2017, **49**, 1387–1393.
250 F. Alonso, Y. Moglie, G. Radivoy and M. Yus, *J. Org. Chem*., 2013, **78**, 5031–5037.
251 M. E. King and M. L. Personick, *J. Mater. Chem. A*, 2018, **6**, 22179–22188.
252 P. Lisowski, J. C. Colmenares, D. Lomot, O. Chernyayeva and D. Lisovytskiy, *J. Mol. Catal. A Chem.*, 2016, **411**, 247–256.
253 W.-W. Liu, Y.-S. Feng, G.-Y. Wang, W.-W. Jiang and H.-J. Xu, *Chinese Chem. Lett*., 2016, **27**, 905–909.
254 Z.-Q. Zhang, J. Huang, L. Zhang, M. Sun, Y.-C. Wang, Y. Lin and J. Zheng, *Nanotechnolgy*, 2014, **25**, 435602.
255 A.R. G. Caranton, J. C. da Silva Pinto, F. Stavale, J. Barreto and M. Schmal, *Catal. Today*, 2020, *in press*; doi: 10.1016/j.cattod.2018.10.034.
256 T. Kitano, T. Wani, T. Ohnishi, J. Li-Fen, Y. Kuroda, A. Kunai and K. Sasaki, *Catal. Lett*., 1991, **11**, 11–18.
257 K.-S. Cho and Y.-K. Lee, *J. Korean Phys. Soc*., 2012, **61**, 293–296.
258 Z. Yin, W. Zhou, Y. Gao, D. Ma, C. J. Kiely and X. Bao, *Chem. – Eur. J*., 2012, **18**, 4887–4893.
259 Z. Yin, D. Ma and X. H. Bao, *Chem. Commun*., 2010, **46**, 1344–1346.
260 Z.-Y. Shih, C.-W. Wang, G. Xu and H.-T. Chang, *J. Mater. Chem. A*, 2013. **1**, 4773–4778.
261 K. Mandal, D, Bhattacharjee, P. S. Roy, S. K. Bhattacharya and S. Dasgupta, *Appl. Catal. A Gen.*, 2015, **492**, 100–106.

262 H. Y. Na, L. Zhang, H. X. Qiu, T. Wu, M. X. Chen, N. Yang, L. Z. Li, F. B. Xing and J. P. Gao, *J. Power Sources*, 2015, **288**, 160–167.
263 L. Yang, D. Yan, C. Liu, H. Song, Y. Tang, S. Luo and M. Liu, *J. Power Sources*, 2015, **278**, 725–732.
264 J.-F. Lin, M. Mohl, G. Toth, R. Puskás, A. Kukovecz and K. Kordas, *Top. Catal*., 2015, **58**, 1119–1126.
265 S. Arulmani, S. Krishnamoorthy, J. J. Wu and S. Anandan, *Electroanal*., 2017, **29**, 433–440.
266 X. Cui, X. Wang, X. Xu, S. Yang and Y. Wang, *Electrochim. Acta*, 2018, **260**, 47–54.
267 C. Bianchini, V. Bambagioni, J. Filippi, A. Marchionni, F. Vizza, P. Bert and A. Tampucci, *Electrochem. Commun*., 2009, **11**, 1077–1080.
268 W.-D. Kang, Y.-C. Wei, C.-W. Liu and K.-W. Wang, *Electrochem. Commun*., 2011, **13**, 162–165.
269 Z. Zhang, C. Zhang, J. Sun, T. Kuo and C. Zhao, *RSC Adv*., 2012, **2**, 11820–11828.
270 F. Zhu, G. Ma, Z. Bai, R. Hang, B. Tang, Z. Zhang and X. Wang, *J. Power Sources*, 2013, **242**, 610–620.
271 J. Cai, Y. Zeng and Y. Guo, *J. Power Sources*, 2014, **270**, 257–261.
272 Q.-L. Zhang, J.-N. Zheng, T.-Q. Xu, A.-J. Wang, J. Wei, J.-R. Chen and J.-J. Feng, *Electrochim. Acta*, 2014, **132**, 551–560.
273 Q. Dong, Y. Zhao, X. Han, Y. Wang, M. Liu and Y. Li, *Int. J. Hydrogen Energ*., 2014, **39**, 14669–14679.
274 J. Noborikawa, J. Lau, J. Ta, S. Hu, L. Scudiero, S. Derakhshan, S. Ha and J. L. Haan, *Electrochim. Acta*, 2014, **137**, 654–660.
275 J. Mao, Y. Liu, Z. Chen, D. Wang and Y. Li, *Chem. Commun*., 2014, **50**, 4588–4591.
276 X. Zhao, J. Zhang, L. Wang, Z. Liu and W. Chen, *J. Mater. Chem. A*, 2014, **2**, 20933–20938.
277 P. Mukherjee, P. S. Roy, K. Mandal, D. Bhattacharjee, S. Dasgupta and S. K. Bhattacharya, *Electrochim. Acta*, 2015, **154**, 447–455.
278 Y. Zhai, Z. Zhu, W. Hong and S. Dong, *Electroanal*., 2015, **27**, 1871–1875.
279 H. Mao, T. Huang and A. Yu, *Electrochim. Acta*, 2015, **174**, 1–7.
280 J. Liu, Z. Huang, K. Cai, H. Zhang, Z. Lu, T. Li, Y. Zuo and H. Han, *Chem. – Eur. J*., 2015, **21**, 17779–17785.
281 Z. Guo, T. Liu, W. Li, C. Zhang, D. Zhang and Z. Pang, *Catalysts*, 2016, **6**, 62–75.
282 T. Song, F. Gao, L. Jin, Y. Zhang, C. Wang, S. Li, C. Chen and Y. Du, *J. Colloid Interface Sci*., 2020, **560**, 802–810.
283 A. Serov, U. Martinez, A. Falase and P. Atanassov, *Electrochem. Commun*., 2012, **22**, 193–196.
284 Y. Cheng, Y. Liu, D. Cao, G. Wang and Y. Gao, *J. Power Sources*, 2011, **196**, 3124–3128.
285 J. Maya-Cornejo, N. Arjona, M. Guerra-Balcázar, L. Álvarez-Contreras, J. Ledesma-García and L. G. Arriaga, *Procedia Chem*., 2014, **12**, 19–26.
286 N. Arjona, M. Guerra-Balcázar, L. Ortiz-Frade, G. Osorio-Monreal, L. Álvarez-Contreras, J. Ledesma-García and L. G. Arriaga, *J. Mater. Chem. A*, 2013, **1**, 15524–15529.
287 F. Munoz, C. Hua, T. Kwong, L. Tran, T. Q. Nguyen and J. L. Haan, *Appl. Catal. B Environ.,* 2015, **174**, 323–328.

288 O. Muneeb, J. Estrada, L. Tran, K. Nguyen, J. Flores, S. Hu, A. M. Fry-Petit, L. Scudiero, S. Ha and J. L. Haan, *Electrochim. Acta*, 2016, **218**, 133–139.
289 L. Dai and S. Zhou, *J. Power Sources*, 2011, **196**, 9369–9372.
290 S. Hu, L. Scudiero and S. Ha, *Electrochim. Acta*, 2012, **83**, 354–358.
291 S. Hu, S. Ha and L. Scudiero, *Electrochim. Acta*, 2013, **105**, 362–370.
292 S. Hu, H. Gao, S. Dai, L. Scudiero and S. Ha, *ECS Trans*., 2013, **58**, 1015–1022.
293 L. Lu, L. Shen, Y. Shi, T. Chen, G, Jiang, C. Ge, Y. Tang, Y. Chen and T. Lu, *Electrochim. Acta*, 2012, **85**, 187–194.
294 C. Xu, Y. Liu, J. Wang, H. Geng and H. Qiu, *J. Power Sources*, 2012, **199**, 124–131.
295 C. Xu, A. Lu, H. Qiu and Y. Liu, *Electrochem. Commun.*, 2011, **13**, 766–769.
296 W. Wei, Y. Liu, Q. Wan and N. Yang, *Adv. Mat. Res*., 2013, **704**, 264–269.
297 L. Zhang, S.-II Choi, J. Tao, H.-C. Peng, S. Xie, Y. Zhu, Z. Xie and Y. Xia, *Adv. Funct. Mater*., 2014, **24**, 7520–7529.
298 Y. Suo, Z. Zhang, J. He, Z. Zhang and G. Hu, *Ionics*, 2016, **22**, 985–990.
299 D. Wu, H. Xu, D. Cao, A. Fisher, Y. Gao and D. Cheng, *Nanotechnology*, 2016, **27**, 495403.
300 S. R. Hosseini, S. Ghasemi, N. Farzaneh and N. Kamali, *Ionics*, 2017, **23**, 707–716.
301 D. Chen, P. Sun, H. Liu and J. Yang, *J. Mater. Chem. A*, 2017, **5**, 4421–4429.
302 M. Z. Yazdan-Abad, N. Alfi, M. Farsadrooh, K. Kerman and M. Noroozifar, *J. Electroanal. Chem.* 2019, **848**, 113299.
303 J.-B. Raoof, S. R. Hosseini, R. Ojani and S. Aghajani, *J. Mol. Liq*., 2015, **204**, 106–111.
304 S. R. Hosseini, J.-B. Raoof, S. Ghasemi and Z. Gholami, *Mater. Res. Bull*., 2016, **80**, 107–119.
305 T. Utaka, K. Sekizawa and K. Eguchi, *Appl. Catal. A Gen.*, 2000, **194**, 21–26.
306 T. Utaka, T. Takeguchi, R. Kikuchi and K. Eguchi, *Appl. Catal. A Gen.*, 2003, **246**, 117–124.
307 E. S. Bickford, S. Velu and C. Song, *Catal. Today*, 2005, **99**, 347–358.
308 E. B. Fox, S. Velu, M. H. Englhard, Y.-H. Chin, J. T. Miller, J. Kropf and C. Song, *J. Catal*., 2008, **260**, 358–370.
309 J. Kugai, J. T. Miller, N. Guo and C. Song, *J. Catal*., 2011, **277**, 46–53.
310 J. Kugai, J. T. Miller, N. Guo and C. Song, *Appl. Catal. B Environ*., 2011, **105**, 306–316.
311 J. Kugai, E. B. Fox and C. Song, *Appl. Catal. A Gen.*, 2013, **456**, 204–214.
312 A. I. Ayesh, *J. Alloy Compd*., 2016, **689**, 1–5.
313 A. K. Jaismal, S. Singh, A. Singh, R. R. Yadav, P. Tandon and B. C. Yadav, *Mater. Chem. Phys*., 2015, **154**, 16–21.
314 S. Kavian, S. N. Azizi and S. Ghasemi, *J. Electroanal. Chem*., 2017, **799**, 308–314.
315 M. Yuan, A. Liu, M. Zhao, W. Dong, T. Zhao, J. Wang and W. Tang, *Sens. Activators B*, 2014, **190**, 707–714.
316 Y. Fe, X. Niu, L. Li, X. Li, W. Zhang, H. Zhao, M. Lan, J. Pan and X. Zhang, *ACS Appl. Nano Mater*., 2018, **1**, 2397–2405.
317 L.-P. Mei, J.-J. Feng, L. Wu, J.-Y. Zhou, J.-R. Chen and A.-J. Wang, *Biosens. Biolectron*., 2015, **74**, 347–352.
318 *Hydrosilylation: A Comprehensive Review on Recent Advances*, ed. B. Marciniec, Springer, Amsterdam, 2009.
319 J.-w. Zhang, G.-p. Lu and C. Cai, *Green Chem*., 2017, **19**, 2535–2540.

320 A. K. Jaiswall, M. Gangwar, G. Nath and R. R. Yadav, *J. Adv. Chem. Eng*., 2016, **6**, 1000151.
321 I. Ullah, K. Khan, M. Schail, K. Ullah, A. Ullah and S. Shaheen, *Int. J. Nanomedicine*, 2017, **12**, 8735–8745.

GRAPHICAL ABSTRACT

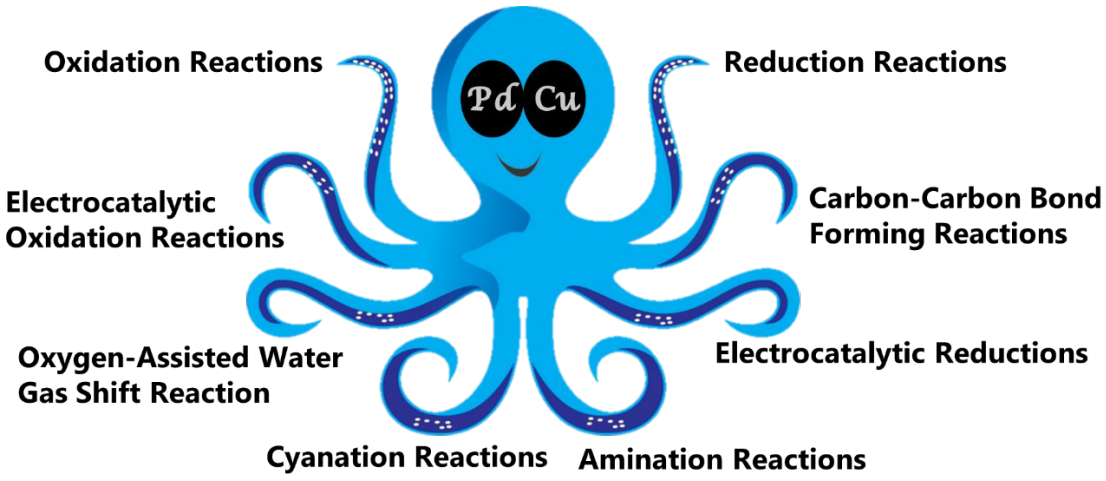

Dear Editor,

Please find attached our manuscript entitled “Applications of bimetallic PdCu catalysts” as a review for Catalysis Science and Technology. We submitted the proposal to Chemical Society Review and the Editor suggested us to send this manuscript to Catalysis Science and Technology. In this review we have highlighted important synthetic applications of PdCu bimetallic catalyst in many area of interest such as carbon-carbon bond forming reactions, chemical and electrochemical reductions, chemical and electrochemical oxidations, oxygen-assisted water gas shift (OWGS) reaction and in sensing electrodes. Synergic and cooperative interactions between Pd and Cu affords superior catalytic performance than monometallic catalysts decreasing cost for industrial applications.

So, we would like you consider this manuscript for publication.

Yours sincerely,

Carmen Nájera

Professor of Organic Chemistry

University of Alicante